CONCENTRATIONS OF NATURAL RADIONUCLIDES IN WATER SOURCES AND ITS SURROUNDING SOIL IN AIZAWL AND KOLASIB DISTRICTS OF MIZORAM

A THESIS SUBMITTED IN PARTIAL FULFILLMENT OF THE REQUIREMENTS FOR THE DEGREE OF DOCTOR OF PHILOSOPHY

VANRAMLAWMA

MZU REGISTRATION NO.: 199 OF 2008 to 2009

Ph.D REGISTRATION NO.: MZU/PH.D./1102 to 24.04.2018

DEPARTMENT OF PHYSICS

SCHOOL OF PHYSICAL SCIENCES

NOVEMBER, 2020

CONCENTRATIONS OF NATURAL RADIONUCLIDES IN WATER SOURCES AND ITS SURROUNDING SOIL IN AIZAWL AND KOLASIB DISTRICTS OF MIZORAM

By

Vanramlawma

Department of Physics

Name of Supervisor: Prof. Zaithanzauva Pachuau

Name of Joint Supervisor: Prof. B. Zoliana

Submitted

in partial fulfillment for the requirement of the Degree of Doctor of Philosophy in Physics of Mizoram University, Aizawl

Prof.Zaithanzauva Pachuau
Phone: 9862770341(M)

Mizoram University
Department of Physics
(A DST-FIST Supported Department)
School of Physical Sciences
Aizawl 796 004 Mizoram
E-mail : zaiapach14@gmail.com, mzut032@mzu.edu.in

Date: 17th September 2021

Certificate

This is to certify that the thesis entitled '*Concentrations of natural radionuclides in water sources and its surrounding soil in Aizawl and Kolasib districts of Mizoram'* submitted by Shri Vanramlawma, for the degree of Doctor of Philosophy of the Mizoram University, Aizawl, embodies the record of original investigations carried out by him under my supervision. The thesis presented is worthy of being considered for the award of the Ph. D. degree. This work has not been submitted for any degree to any other University.

(Prof. ZAITHANZAUVA PACHUAU)

Supervisor

(Prof. B. ZOLIANA)

Jt. Supervisor

Declaration

Mizoram University

November, 2020

*I, **Vanramlawma**, hereby declare that the subject matter of this thesis is the record of work done by me, that the content of this thesis did not form the basis of the award of any previous degree to me or to the best of my knowledge to anybody else, and that the thesis has not been submitted by me for any research degree in any other University or Institute.*

This is being submitted to the Mizoram University for the degree of Doctor of Philosophy in Physics.

(VANRAMLAWMA)
Candidate

(Prof. R.C. TIWARI)
Head

(Prof. ZAITHANZAUVA PACHUAU)
Supervisor

(Prof. B. ZOLIANA)
Jt. Supervisor

Acknowledgment

I would like to express my gratitude to my Supervisor Prof. Zaithanzauva Pachuau, Department of Physics, Mizoram University, for his valuable guidance and supervision throughout the course of my work.

I would also like to express my sincere gratitude to my Joint Supervisor Prof. B. Zoliana, Department of Physics, Govt. Zirtiri Residential Science College, who introduced me to the subject and guide me through every step of my path in the completion of this work.

I express my heartfelt thanks to Prof. Diwakar Tiwari, Dean, School of Physical Sciences for his support in completion of my work. I acknowledged all the support I received from Prof. R.C. Tiwari, Head, Department of Physics and the Teaching and non-Teaching Faculties of the Department of Physics, Mizoram University.

I would also like to thank Dr. B.K. Sahoo and his team from Radiological Physics and Advisory Division, Bhabha Atomic Research Centre, Mumbai, who spare their valuable time in training me and providing me with their valueable knowledge. I extend my gratitude to my Lab-mate Dr. Hmingchungnunga, Department of Physics, Mizoram University, Dr. Lawrence Zonunmawia Chhangte and Dr. Rosangliana, Department of Physics, Govt. Zirtiri Residential Science College; and also Mr. Laldingngheta Ralte and Mr. Remlalsiama, Research Scholars, Department of Physics, Mizoram University, for sharing me their knowledge in the subject.

I am indebted to my parents and family members for their encouragement and moral support during the course of my studies. Above all else, I thank the Lord Almighty for being with me throughout these years and keeping me in good health to complete this work.

Dated: 17th September, 2021

Department of Physics,

Mizoram University, Aizawl. (**VANRAMLAWMA**)

Lists of Figures

Lists of Tables

This Thesis is Dedicated

to

My Father

C. Lalmawipuia

(1965 - 2019)

1

Introduction

1.1. Natural Radioactivity:

Background radioactivity arising from naturally occurring radionuclide is a common occurrence in nature. Natural radioactivity is found to exist almost everywhere in the earth's environment and is concentrated in air, water, soils, rocks and plants. From time to time, naturally occurring radionuclide undergoes radioactive decay process during which they disintegrate into their daughter elements or progenies, thereby releasing ionizing radiations in the form of alpha, beta or gamma radiations. The daughter element or progenies further disintegrate into another radioactive elements until a stable state is reached, thus forming a series of decay chain.

Due to their ionizing nature, this type of radiation can alter the chemical composition or even the biological state of living beings, thus causing adverse effect on the health of an individual. The influence of natural radioactivity on human health is of great concern because radiations arising from natural radioactive sources are considered to be the main contributors of the radiation annual dose received by human beings worldwide according to the United Nations Scientific Committee on the Effects of Atomic Radiation (UNSCEAR, 2000). It has been estimated that 87% of radiation dose received by human beings sourced from naturally occurring radionuclide and the remaining 13% from anthropogenic or man-made sources (UNSCEAR, 1993). Since natural radionuclide dominantly contributes to the radiation dose received by human, the present work will focus solely on the radioactivity which arises from natural radioactive sources rather than those from anthropogenic or man-made sources. Depending upon their source or origin, naturally occurring radionuclide can be broadly classified into terrestrial, i.e., those radionuclide which originates from the surface of the earth and extra-terrestrial, i.e. those radionuclide which originate from the cosmos (Radenkovic *et al*, 2009; Tzortzis *et al*, 2003).

1.2. Ionizing radiation:

Ionizing radiation are those radiations such that, on interaction with an atom or molecule, it can knock off the electrons from the outer shell of the atom and creates positive ions. Ionizing radiations such as alpha, beta and gamma radiation directly ionize atoms and are therefore known as directly ionizing radiations, while interactions of neutrons with atoms of other elements to produce ionizing radiations are classified as indirectly ionizing radiations.

a) Alpha radiation: Alpha radiations are helium nuclei which consist of positively charged particles. Since they have a low penetrating power, radiation caused by alpha decay cannot penetrate the skin of human beings or even a thin sheet of paper, and is therefore considered harmless externally. However, if alpha emitting radionuclide are ingested or inhaled, they can cause damage to the internal organs of the body, especially to the lungs, stomach and kidneys.

b) Beta radiation: Depending upon the mode of decay, beta radiation due to radioactive decay of heavy nuclei involves electron emission, positron emission or electron capture. In electron emission, a nucleus contains an excess neutron and then emits an electron and anti-neutrino. In positron emission, a nucleus contains an excess proton, and then emits a positron and a neutrino. In heavy nuclei, where electron orbits are closely packed and are much closer to the nucleus, the excess positive charge of the nucleus may sometimes be neutralised by the capture of an orbital electron, this process is known as electron capture.

The penetrating power of beta radiation lies between those of alpha and gamma radiations and can be stopped by an aluminium sheet of a few millimeters thickness.

c) Gamma radiation: The emission of alpha or beta particles from naturally occurring radionuclide is invariably followed by the emission of gamma radiation. The emission of alpha or beta particles from a radioactive substance may leave the daughter nucleus in one or more excited states. When the nucleus in the excited state passes to the ground state or to a lower excited state from a higher excited state, it emits high energy photons in the form of gamma radiations.

Gamma radiations have high penetrating power and can easily penetrates the body and cause damage to the body cells, but can be stopped by a lead or concrete block.

d) Neutrons: Although neutrons do not produce ionization directly, they can interact with atoms of other element which could in turn produce ionizing radiations in the form of alpha, beta, gamma radiations as well as X-rays.

Neutrons have a high penetrating power because they are electrically neutral and are not deflected by electric and magnetic fields.

1.3. Extra-terrestrial Radionuclide:

Radionuclide having extra-terrestrial origin mostly comes from cosmic radiations. Cosmic radiations can be classified into primary and secondary cosmic radiations. Primary cosmic radiations are those which are initially incident on the earth's outer boundary of the atmosphere. They are mainly composed of protons (92%), alpha particles (7%) and about 1% of heavier nuclei of almost all atoms from Li to Ni.

Primary cosmic radiations, on interaction with earth's atmospheric gases like nitrogen and oxygen, produces secondary cosmic radiations, which in turn produces large number of radionuclide. Up to a height of 20 km above the earth's surface, all cosmic radiations are secondary. At sea level, secondary cosmic radiations mainly composed of meson (about 70%), electron-positron pairs (29%) and heavy particles (1%). Radiations from cosmic rays are found to have contributed to the radiation dose rate received by human beings, and studies conducted by Nambi *et al* (1986) have shown that the dose rate of radiation contributed by cosmic radiation is 31.96 nGy/h at sea level.

1.4. Terrestrial radionuclide:

Natural radioactivity produced by terrestrial radionuclide originates from radioactive elements present on the surface of the earth. Terrestrial radionuclide like ^{238}U, ^{232}Th and ^{40}K are prominent in nature and have a long half life which are comparable to the age of the earth, and are therefore referred to as primordial

radionuclide. Primordial radionuclide is found all around us and is detected in certain amounts in air, water, rock, soil and vegetation, from which it enters the body mainly through inhalation and ingestion. Human beings inhale or ingest many radionuclide that are present all around us, and the main exposure comes from outdoor natural terrestrial radiation that originates predominantly from upper 30 cm layer of soil present on earth (Chikasawa *et al,* 2001). Moreover, gamma radiations emitted from terrestrial radionuclide represents the main external source of irradiation of the human body (Alaamer, 2008; UNSCEAR, 1993).

Their distribution on the terrestrial surface mainly depends on the distribution of rocks from which they originate and on the processes through which they are concentrated (Mahur *et al,* 2008; Kabir *et al,* 2009). They continuously disintegrate into their radioactive daughter elements giving out α, β, and γ radiations directly or through their daughter elements. Hence, measurement of natural radionuclide is needed to identify the origin and abundance of their daughter elements like radon, thoron and their progenies.

1.4.1. Uranium:

Uranium is the heaviest trace element found at different level of concentration in all terrestrial substances. Natural uranium is present in varying amounts in rocks and soil, and due to the relatively low density of their oxides, they are found to be concentrated on the earth's crust rather than in the mantle or core. The main mineral source of uranium is pitchblende, which occurs as a primary constituent of igneous rocks, granites and pegmatite. The distribution of natural uranium in the environmental matrices is shown in Table 1.1 (UNSCEAR, 1993; National Council on Radiation Protection and Measurements (NCRP), 1999; World Health Organization (WHO), 2001).

Table 1.1: Concentration of uranium in the environmental matrices

Environmental Matrix	Concentration range
Soil	0.3 – 11.7 mg/kg
Air	2.5×10^{-8} – 10^{-7} mg/m^3
Surface Water	3×10^{-2} – 2.1 µg/l
Ground Water	3×10^{-3} – 2.0 µg/l

Natural uranium has three different isotopes which are all radioactive in nature, namely, ^{238}U, ^{235}U, and ^{234}U. Amongst the three natural isotopes of uranium, ^{238}U is the most abundant and constitute more than 99% of the total uranium present in nature. The high abundance of ^{238}U in nature makes it an isotope of interest, and its concentration and distribution in soils and rocks, as well as water could have an adverse effect on human health condition. Moreover, ^{238}U is the parent element of the most hazardous and most studied isotope of radon, ^{222}Rn (Figure 1.1).

Naturally occurring radionuclide, ^{238}U is a radioactive metal having an atomic number 92 and atomic mass of 238.03 g/mol. It is found to exist in almost every rocks, soil and water present on earth at different levels of concentration. Although ^{238}U is mostly found in rocks and soil, through the process of leaching, it can enter the water bodies as well. When water flows through soil and rocks containing ^{238}U, it gets dissolved in the flowing water and gets transported (Chandrashekara, 2017). Cothern *et al*, (1983) estimated that drinking water contributes about 85% of ingested uranium while food contributes about 15%. Though uranium is considered to be a weak radioactive element, ingestion of water containing high concentration of uranium may lead to certain health hazards.

Although the radioactive nature of uranium, especially with regards to drinking water, is considered insignificant since they are very weak in nature as compared to radioactivity from other natural sources, it has been well established that the chemical toxicity of uranium are to be considered while studying its health hazard. This is because the accumulation of uranium inside the human body can lead to

certain health effects to the internal organs, especially to the kidneys and lungs (WHO, 1998; Diwan *et al,* 2018).

Although most ingested uranium is eliminated from the body, a small amount is absorbed and carried through the bloodstream, thereby causing complications to human health. WHO recommended the safe limit value of uranium concentration in drinking water to be 30 µg/l (WHO, 2011), which was previously suggested at 15 µg/l (WHO, 2004). In India, the Atomic Energy Regulation Board has set the critical value at 60 µg/l (AERB, 2004).

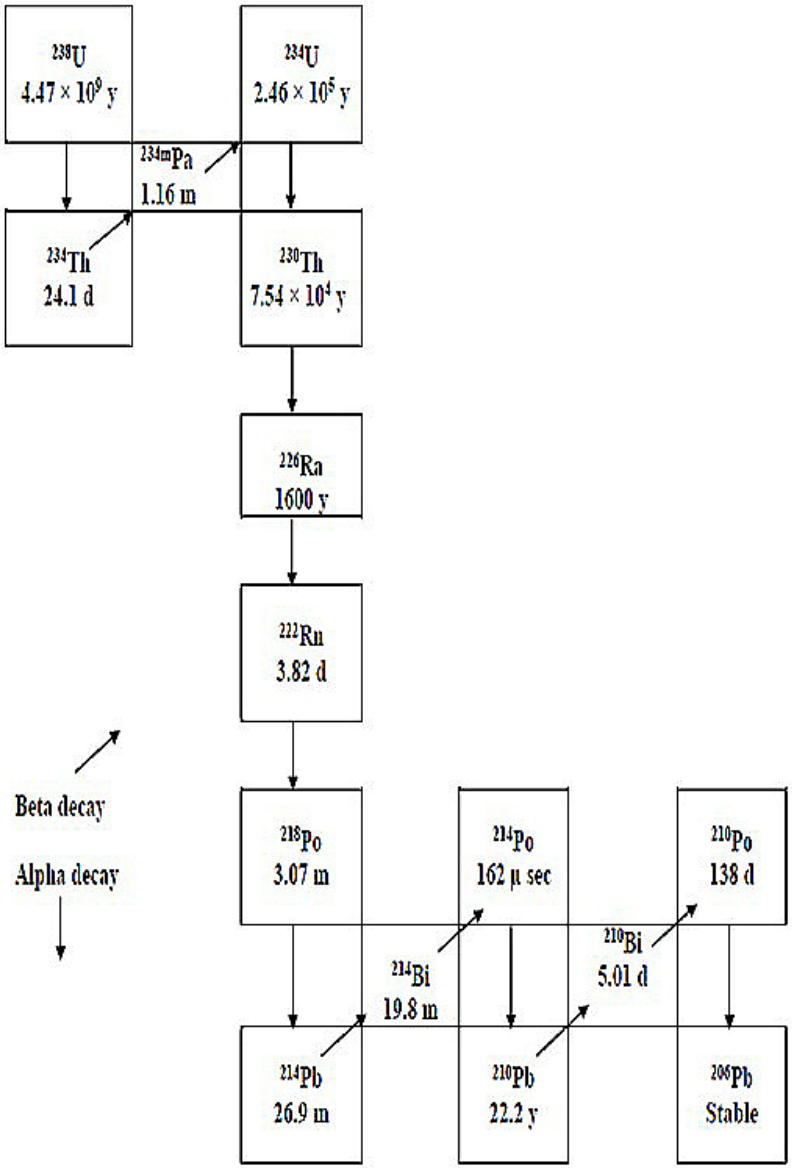

Figure 1.1: ^{238}U Decay Series

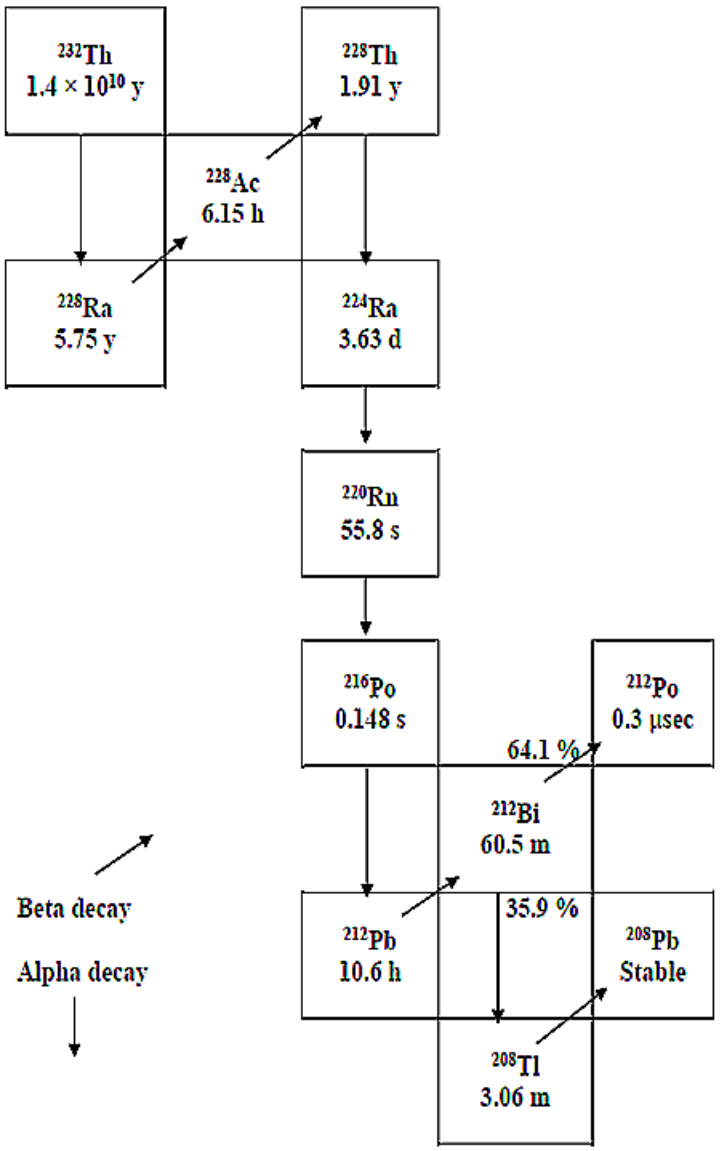

Figure 1.2: ^{232}Th Decay Series

1.4.2. Thorium:

Thorium is a naturally occurring, weak radioactive element and resembles a bright, silvery-white, soft metal. Discovered in 1828 by Jons Jacob Berzelius in Stockholm, trace levels of thorium are found in rocks, soil, water, plants and animals. 31 isotopes of thorium (whose half-lives are known) have been identified so far, with mass numbers ranging from 208 to 238. All the isotopes of thorium are radioactive and amongst the 31 known isotopes of thorium, ^{232}Th is the most stable with a half-life of 14.05 billion years and is the only primordial isotope of thorium. Also, ^{232}Th constitutes nearly 100% of thorium found on Earth. The decay series of ^{232}Th is shown in Figure 1.2.

The global average value of thorium concentration in soil is 45 Bq/kg (UNSCEAR, 2008), while for Indian soil, the average value is 18.36 Bq/kg (UNSCEAR, 2000). The abundance of thorium in nature is comparable to that of lead, and constitutes about 0.0002–0.001 wt % of the Earth's crust. Thorium is distributed in different igneous rocks such as granites, pegmatite and gneisses. However, unlike lead, thorium and its compounds do not undergo the same hydrothermal reactions that form large, concentrated mineral deposits. Although the concentration of thorium in igneous rocks is rarely higher than 1%, natural processes such as erosion can provide isolated deposits of increased thorium concentration in the form of monazite, containing about 3–10% thorium.

Although thorium is considered to be a weak radioactive element, inhalation of thorium in high dose through dust particles may increase the probability of a person developing bone and lung cancer. Studies have shown that the concentration of thorium was found to be the highest in pulmonary lymph nodes and lungs of the human body (Ibrahim *et al*, 1983; Wrenn *et al*, 1981). Since thorium is hardly soluble in water, its chemical toxicity can be considered to be quite low.

1.4.3. Potassium:

Potassium is a soft, silver-white metal and is the seventh most abundant element in the earth's crust and the sixth most abundant element in the oceans. Natural potassium comprises of three isotopes, out of which two are stable and non-radioactive, i.e., ^{39}K and ^{41}K. One isotope of natural potassium ^{40}K is radioactive and it constitutes up to one ten thousandth of the potassium found naturally. ^{40}K can be found almost everywhere, such as in human and animal tissues, soils and oceans in varying concentrations.

Along with uranium and thorium, potassium contributes to the natural radioactivity on the terrestrial surface by emitting gamma radiation of energy 1.46 MeV (McDougall *et al*, 1999). Since it is radioactive in nature, ^{40}K can produce internal as well as external health hazard and is an important radionuclide in terms of the dose associated with naturally occurring radionuclide. The global average activity concentration of ^{40}K in soil is 412 Bq/kg (Range of 4 Bq/kg to 2260 Bq/kg) (UNSCEAR, 2008) which was previously prescribed at 400 Bq/kg (UNSCEAR, 2000).

^{40}K, having a half life of 1.3 billion years, decays using either one of the two processes- about 89% of the time, it decays to ^{40}Ca by emitting a beta particle with no attendant gamma radiation and approximately 11% of the time, it decays to ^{40}Ar by electron capture with emission of an energetic gamma ray (Figure 1.3). During the electron-capture decay process, strong gamma radiation is released, making external exposure to this isotope a concern for health.

Internally, ^{40}K is known to possess a health hazard due to radiations both by beta particles and gamma rays. Once taken in, it is readily absorbed into the bloodstream and distributed throughout the body. The health hazard of ^{40}K is associated with cell damage caused by the ionizing radiation with a potential for induction of cancer (Peterson *et al*, 2001).

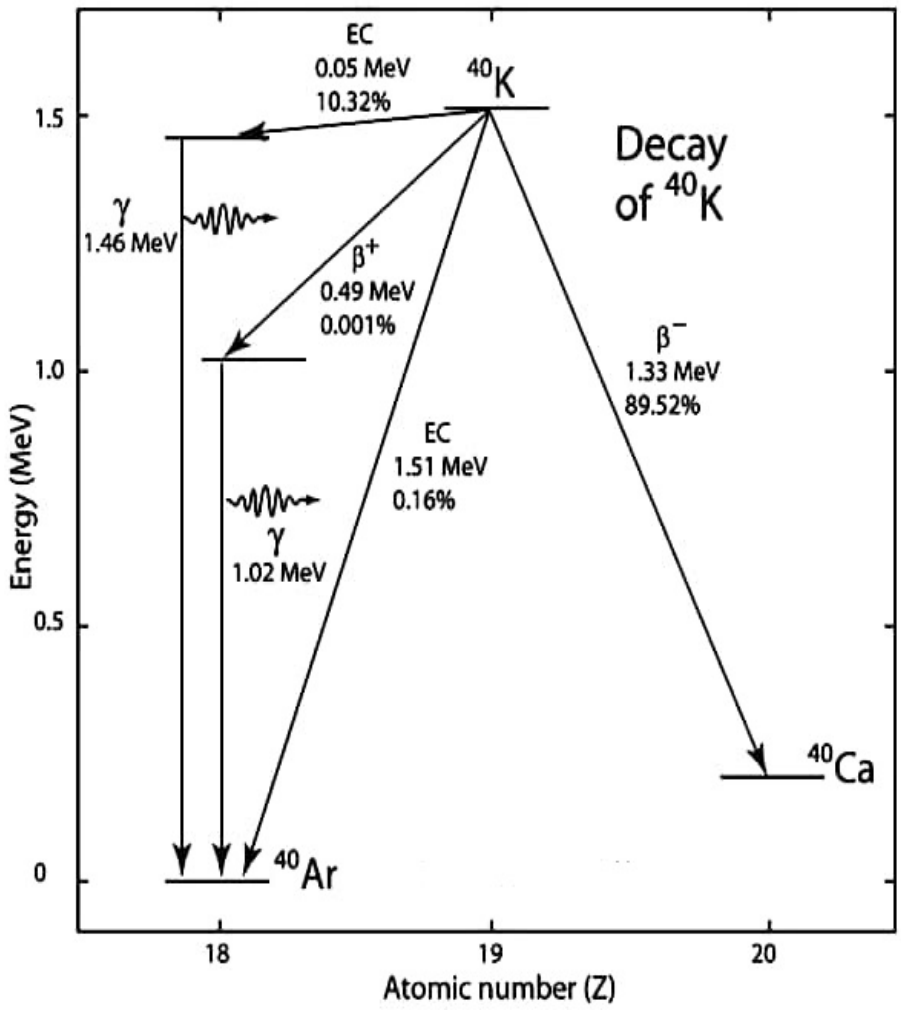

Figure 1.3: Disintegration of ^{40}K in accordance with (McDougall *et al*, 1999)

1.4.4. Radon:

Natural radioactivity arising from ^{238}U decay series is the main source of natural radiations on the earth's environment. Amongst the daughter elements of ^{238}U, ^{222}Rn is the single most contributors of natural radiations (Figure 1.4) because they are continuously being formed in the soil and released into the earth's atmosphere (UNSCEAR, 2000).

Radon, formerly identified as "Radium Emanation" was discovered in 1898 by a German Physicist known as Friedrich Ernst Dorn. Radon is known to have 35 different isotopes. Amongst the different isotopes of radon, Actinon (^{219}Rn), Thoron

(^{220}Rn) and Radon (^{222}Rn) are of natural origin and are produced as the daughter elements of the Actinium Series, the Thorium Series and the Uranium Series respectively. The most stable isotope of radon, ^{222}Rn, has a half-life of 3.82 days and along with ^{220}Rn (having a half-life of 55.6 seconds), they are the only isotopes of radon which are of significance to the environment.

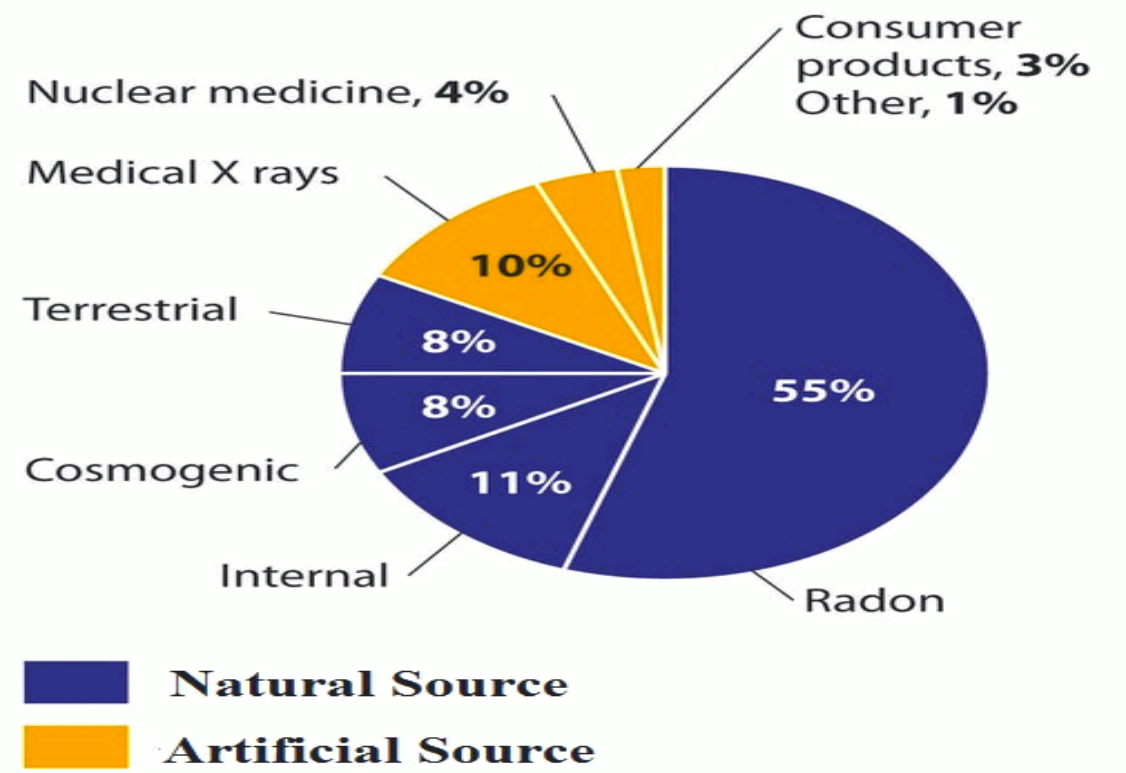

Figure 1.4: Radon, the single most contributor of radiation

Radon is a radioactive, colorless, odorless, tasteless, noble gas, having an atomic radius of 1.34 Å, occurring naturally as a decay product of Radium (^{226}Ra) along the Uranium (^{238}U) Decay Series. It is the heaviest member of the rare gas group (approximately 100 times heavier than hydrogen and about 7.5 times heavier than air) and remains a gas under normal conditions. Due to its noble nature, radon is chemically inert to reaction with other gases; hence it is able to travel freely through pores and fractures in rocks and soils, thereby releasing itself into the atmospheric air.

It has been estimated that from the total radiation dose received by human beings, radon and its decay products contributes 51% through inhalation and 0.21% through ingestion (Kumar *et al*, 2017; Gusain *et al*, 2009).

1.4.4.1. Sources of Radon:

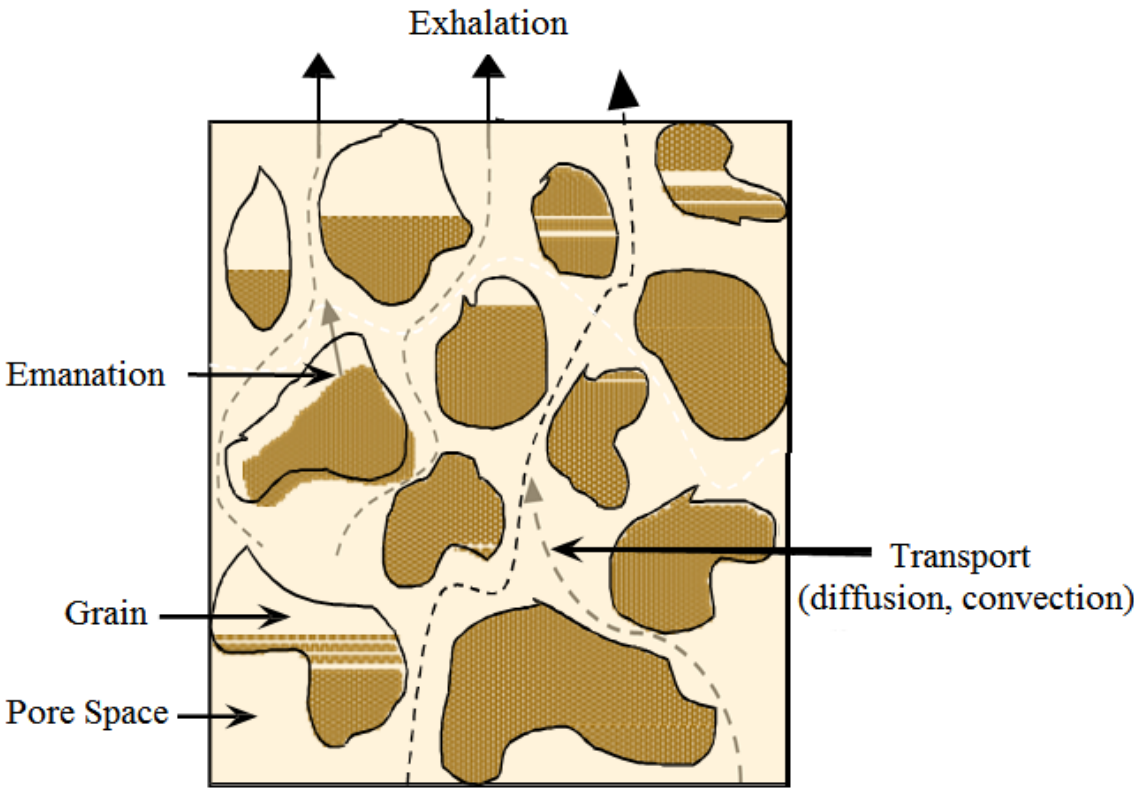

Figure 1.5.: Transport of radon form source to environment

Radon is continuously formed in the soil and its concentration in soil is greatly influenced by the amount of the parent radionuclide, i.e. ^{238}U or ^{226}Ra present in the soil, as well as the moisture content of soil, barometric pressure variations, temperature, grain size distribution and structure of soil.

Radon is transported from the source (i.e. soil or rocks) to the environment (air or water) by the following three main processes (Figure 1.5), namely; Emanation, Transport and Exhalation (Nazaroff *et al*, 1988). Emanation is defined as the release of radon from soil to small air or water pockets contained in pores between soil and

rock. By the process of diffusion and convection, emanated radon is then transported from the pore spaces between rocks and soil to the ground surface and then escapes from the ground surface into the atmosphere by a process known as exhalation.

Radon is not only found in soil and air, but also in water bodies as well. Usually, natural water contains dissolved radon due to the presence of ^{226}Ra, a member of the natural ^{238}U decay series, in soils and rocks through which the water bodies has filtered (Singh *et al,* 2009). Radon is readily soluble in water and its solubility increases with increase in pressure, but decreases with increase in temperature (Smetanova *et al*, 2010). The mole fraction solubility of radon in water is 2.3×10^{-4} at 15°C and 1.28×10^{-4} at 35°C.

Although radon concentration in water is quite low as compared to its concentration in air and soil in most cases, the presence of its parent radionuclide, i.e., uranium or radium, in high concentrations in water may result in the increase of the concentration of radon in water. The concentration of radon is known to vary depending upon the origin or sources of water. WHO (2011) has stated that radon concentration is higher in water obtained from ground water sources rather than those obtained from surface water sources. Some physical properties of radon are shown in Table 1.2.

Radon dissolved in water is also known to have contributed to the indoor radon concentration, when dissolved radon is released into household air during human activities such as bathing, washing, etc (Kumar *et al*, 2016).

Table 1.2.: Physical Properties of radon (UNSCEAR 1982)

Sl. No.	Properties	Values
1	Atomic Radius	1.34 Å
2	Atomic Volume	50.5 cm^3/mol
3	Boiling Point	-61.85 ^{0}C
4	Critical Point	377 K at 6.28 MPa
5	Critical Pressure	62 atm.
6	Critical Temperature	104 ^{0}C
7	Density	0.00973 g/cm^3 at 293 K
8	Electrical Conductivity	0.1 mOhm-cm
9	Enthalpy of Fusion	2.7 kJ/mol
10	Enthalpy of Vaporization	18.1 kJ/mol
11	Heat of Fusion	2.89 – 3.247 kJ/mol
12	Heat of Vaporization	16.4 – 18.1 kJ/mol
13	Ionization Energy	10.745 eV
14	Mean Excitation Energy	794.0 eV
15	Melting Point	-71 ^{0}C
16	Molar Volume	50.5 cm^3/mol
17	Polarizability	5.3 A^3
18	Specific Heat Capacity	94 J/kg.K
19	Thermal Conductivity	3.61 mW/m.K at 300 K
20	Thermal Entropy	176.1 kJ/mol.K (at 298.15)

1.4.4.2. Health effects of radon:

Radon is classified by International Agency for Research on Cancer as a human carcinogen (Group I) (IARC, 1988). The disintegration of radon into its progenies results in the production of alpha radiations. Although alpha particles emitted by radon and its progenies do not have the sufficient energy to penetrate even the skin of a human body, but once it is ingested or inhaled, they could easily interact with the internal organs, especially the lungs, and could alter the DNA structure, thereby causing mutations and thus resulting in cancer.

Radon is not considered to be of health hazards unless it is concentrated in enclosed spaces like caves, basement of a building or even rooms because it gets easily diluted in open spaces. But once it gets into an enclosed space, radon gets concentrated and becomes a health hazards due to the production of alpha radiations by the disintegration of radon and its progenies, namely polonium, lead and bismuth (Majumdar*,* 2000; Ahmad *et al,* 2014). The major sources of indoor radon (i.e. in an enclosed space) are:

(1) Soil gas emanation from soils and rocks.

(2) Through water and natural gas used which later off-gas into indoor air.

(**3)** Building materials.

(4) Directly from the outdoor atmospheric air through openings like doors, windows, ventilations, etc.

The decay products of ^{222}Rn are electrically charged when formed, hence, they tend to attach themselves to dusts and particulate matters which are normally present in the atmosphere. Although most of the radon inhaled is rapidly exhaled, a few of them can combine with other molecules in the air, dust particles, smoke, aerosols, etc, thus depositing itself in the airways and lung once it is inhaled. Radon progenies, having a short half life, emits ionizing alpha radiation while being lodged, and thus damage the cells which lines the airways and the sensitive cells in lung tissue, such as the basal cells of the bronchial epithelium (National Research Council (NRC), 1988). Due to this, radon and its isotopes have been identified as the second leading cause of lung cancer after tobacco smoking (Hassan *et al,* 2011; Mujahid *et al,* 2010; WHO, 2009) in the past. However, this statement is not accepted nowadays, although it is still acknowledged as a lung cancer enhancing element.

The risk of lung cancer following exposure is much higher among cigarette smokers than those among lifelong non-smokers (Darby *et al*, 2005). WHO (2009) has stated that, "Radon is much more likely to cause lung cancer in people who smoke, or who have smoked in the past, than in lifelong non-smokers. However, it is the primary cause of lung cancer among people who have never smoked". The possible effects and the nature of damage caused will depend on the exposure level.

Also, ingestion of water containing high concentrations of radon can cause certain ailments to the internal organs of the human body.

1.5. Past studies of natural radionuclide in soil and water:

Measurement of natural radioactivity is now a global trend and has covered most countries. Work has been in progress in various parts of the world in studying the concentration of natural radionuclide in air, soil and water. Initially, studies have been done mainly with the approach of correlation to epidemiological studies, identification of radioactive elements present in soil and rocks, and also in the prediction of earthquake. All this studies have led not only to the above mentioned initial approach, but also to the upgradation of instruments used for measurement and detection, as well as improvement in theoretical formulation and experimental procedures to obtain more accurate results.

Regarding epidemiological studies, the carcinogenic nature of natural radionuclide such as radon came into awareness during the study of uranium miners carried out by Jacobi (1993), Nagaratnam (1994) and others worldwide. The most extensive epidemiological study of radon exposure is the joint analysis of the 11 underground miner cohorts across countries such as China, Europe, USA and Canada (ICRP, 1984; Samiti *et al*, 1991; Lubin, 1994).

1.5.1. Soil:

Passive methods such as LR-115 nuclear track detectors and high resolution gamma-ray spectrometry have been used widely for measuring natural radioactivity in soil. In Sudan, LR-115 nuclear tract detector were being used for measuring ^{222}Rn and ^{238}U contents in soil samples giving an average value of radon exhalation rate from the soil (Hafeez *et al,*1991). Using HPGe detector, it was found that along the Chao Phraya river of Thailand, activity concentrations of ^{238}U, ^{232}Th and ^{40}K were found to be higher than the upper range of the world mean values (Santawamaitre *et al*, 2010). Solid State Nuclear Tract Detectors (SSNTDs) have been used for measuring exhalation rate of soil samples in Noonmati, Guwahati, Assam in which a good

correlation was observed between radium content and radon exhalation rate in soil samples (Sarma *et al,* 2011).

Measurements of radium, thorium and potassium using gamma spectrometry and radon exhalation rates using solid-state nuclear track detectors (LR-115, Type-II plastic) carried out in the soil samples collected from western districts of Haryana, India shows that no radiological risk was found to the residents of the studied area (Kansal *et al*, 2015). Radium and radon exhalation rates in soil samples were studied in areas of Northern Rajasthan using LR 115 type–II plastic track detectors (Duggal *et al,* 2015). A positive, but weak correlation between uranium activity contents and radon mass exhalation rates in soil samples in the Environs of Nurpur Area, Himachal Himalayas was obtained by Singh *et al* (2007). Measurements taken using NaI (Tl) detector in Devadurga and Lingasugur of Raichur Districts of Karnataka, India shows that the concentration of ^{238}U, ^{232}Th and ^{40}K in the soil samples were found to have a little higher values in comparison to other places of India and world literature values (Rajesh *et al*, 2017).

1.5.2. Water:

Ingestion of water containing natural radionuclide is known to contribute to the radiation dose received by human beings, and due to the radiation-induced public health hazards they caused, measurement of uranium and dissolved radon levels in water remains a topic of interest.

In Lebanon, a preliminary national average radon level was determined to be about 11.4 Bq/l. Since these determined concentrations were well below the 100 and 146 Bq/l revised reference levels proposed in the European Union and the United States respectively, it was concluded that there is no reason to believe these water sources pose any radon-related hazard (Abdallaha *et al,* 2007).

Preliminary studies on groundwater samples from selected wells in three communities in the Greater Accra region of Ghana was carried out to determine the concentration of ^{222}Rn using gamma spectrometry and the average activity concentration obtained was 8.1 Bq/l with an average annual effective dose of 59.2 μSv. This result was found to be within the range published by other countries and the

recommended limit for radon in drinking water set by the World Health Organization (Darko *et al,* 2009). In Amritsar city of Punjab in India, radon concentration was estimated in drinking water samples using RAD7 and the values of radon concentration in these samples were found below the recommended limit proposed by the United States Environmental Protection Agency (USEPA, 1991) and European Commission (2001) (Kumar *et al,* 2016). Radon exhalation rate from the soil shows a positive correlation with radon concentration in water in summer season in Budhakedar, Garhwal Himalaya (Prasad *et al*, 2009).

In a study conducted by Sahoo *et al* (2010) on packaged drinking water samples using laser fluorimetry, the total uranium content varies from 0.04 - 3.88 μg/l, which was well within the USEPA drinking water limit of 30 μg/l (USEPA, 2000a) and WHO limit of 15 μg/l (WHO, 2004). Measurement of uranium and radon concentration in drinking water was also conducted by Singh *et al* (2008), Kaur *et al* (2017), Singh *et al* (2014), Bajwa *et al* (2003) in different parts of India and their results were found to be within the safe limit. Poor correlation between radon dissolved in water and uranium concentration was observed by Kumar *et al* (2017) in Jalandhar district of Punjab. Similar result was reported by Ryan *et al* (2003) in Wicklow, Ireland. The possible reason for this poor correlation may be due to the fact that radon in ground water is transported to very limited distance due to its lower half-life (3.82 days) as compared to uranium, which can travel a very long distance.

1.5.3. Natural radioactivity monitoring in Mizoram:

The status of monitoring of natural radionuclide in Mizoram is still at a budding stage. Most of the works done in the study of radon and other natural radionuclide were mainly in relation to indoor and outdoor air. One of the early works regarding natural radionuclide measurement in Mizoram was done in 1996 by Srivastava *et al* (1996), when they conduct measurements of potential alpha energy of radon and its progenies in some regions of Aizawl, Kolasib, Saiha and Khawlian. Almost a decade later, measurement of radon, thoron and their progeny concentrations was carried out in 17 dwellings in Mizoram (Ramachandran *et al*, 2003). In 2009, measurement of radon and thoron concentrations in Aizawl,

Champhai and Kolasib districts of Mizoram were done by Rohmingliana *et al* (2009) and Vanchhawng *et al* (2009).

Regarding earthquake studies, Jaishi *et al* (2015) had carried out soil gas radon and thoron concentration measurements using LR-115 type-II detectors and found a positive correlation between radon/thoron data and seismic activities that occurred around the measuring site. Recently, Chhangte (2018) had carried out an extensive analysis of radon and thoron in dwellings, with special reference to Saiha and Lawngtlai districts of Mizoram.

Since limited work has been done in Mizoram, and most of the work done have been mainly with respect to soil and air, this study will offer a new approach by surveying the concentrations of natural radionuclide available in water sources and surrounding soils in Aizawl and Kolasib districts of Mizoram.

In this research work, study on natural radioactivity was conducted by measuring natural radionuclide concentrations in water samples as well as soil samples collected within Aizawl and Kolasib district of Mizoram. Lattitudinal and longitudinal coordinates of each sampling sites were marked by Global Positioning System (GPS) device and at the time of sampling, background gamma radiation level were taken at a height of 1 meter above the ground at each spots using a Gamma Survey Meter PM 1405. For measurement of radon concentration in water and radon mass exhalation rates, a scintillation based radon detector, Smart RnDuo (developed by BARC, Mumbai) was employed.

Because radon belongs to the decay chain of uranium series, measurement of uranium concentration in water was also conducted using a device called LED Fluorimeter, LF-2a, which works on the principle of detection of fluorescence produced by uranyl complexes in water samples. Soil radioactivity measurement was carried out by measuring the activity concentration of three specific prominent primordial radionuclide; namely; ^{238}U, ^{232}Th and ^{40}K. A gamma ray spectrometer, i.e., Sodium Iodide (NaI) detector, doped with thallium (Tl) and coupled with a personal computer based 1K multi-channel analyzer; GSPEC-SA was employed for this purpose.

The objective of the present study includes:

- To monitor the seasonal variation of radon and uranium concentrations in water in Aizawl and Kolasib Districts of Mizoram.
- To determine the seasonal variation of radon mass exhalation from soil near the water sources in Aizawl and Kolasib Districts of Mizoram.
- To determine the activity and type of radioactive sources present in the collected soil samples.

The results obtained in this study will help in understanding the status of natural radionuclide concentration in Aizawl and Kolasib districts of Mizoram. This study is also expected to help in identification of high radioactive regions within the study area and also obtain a baseline data for further studies, as well as providing necessary data to implement radiation safety measures, if required. Radioactivity measurement in soil will also help in identifying the type and concentration of radionuclide that are present within the study area. The influence of monsoon rain and dry season on radon concentration in water as well as radon mass exhalation rate for soil will also be obtained by measuring the seasonal variation of the radon concentration in water and radon mass exhalation rate of soil.

2

Theory and Methodology

In this chapter, we shall discuss the theoretical formulation as well as the different methodology employed in the present research work. This chapter will also explain the detailed description of the detectors or instruments used. In the present work, study was conducted by measuring uranium and radon concentration in water samples collected from different water sources, mostly employed for domestic consumption and irrigation purposes, within Aizawl and Kolasib Districts of Mizoram.

For measurement of uranium concentration, LED Fluorimeter (LF 2-a) was employed, which works on the principle of measurement of the fluorescence given out by uranyl ions. Scintillation-based radon detector, Smart RnDuo was used for measurement of radon concentration in water, and this instrument works on the principle of measurement of the alpha scintillations produced by radon.

Spot background gamma radiation was measured at each sampling sites (at a height of 1 metre above the ground) at the time of sampling using a gamma survey meter PM 1045. Also, soil samples were collected at each sampling sites and from these collected samples, the activity concentration of uranium, potassium and thorium were measured using a gamma spectrometer, Sodium Iodide, NaI (Tl) Detector, coupled with a personal computer based 1K multi channel analyzer, GSPEC-SA. The radon mass exhalation rate from each soil samples were also measured using the instrument Smart RnDuo.

The instruments employed for carrying the proposed research works, including the theoretical working of the instruments, the specifications and methods for carrying out the proposed works are given below:-

2.1. Smart RnDuo:

Figure 2.1: Scintillation-based radon detector Smart RnDuo

Scintillation-based radon detector, Smart RnDuo is a portable, advanced continuous radon/thoron detector developed by Bhabha Atomic Research Centre, Mumbai, India and has multiple applications in radon and thoron studies (Figure 2.1). For measurement of radon concentration, the sample gas was collected into a scintillation cell (150 cc) by the process of diffusion. The gas was allowed to pass through a "progeny filter" and "thoron discriminator", where the concentrations of radon/thoron progenies and thoron are eliminated (Figure 2.2). The thoron discriminator is based on "diffusion-time delay", which means that the short-lived thoron ^{220}Rn, having a half-life of 55.6 seconds only, is not allowed to pass through.

The measurement of radon concentration using Smart RnDuo is based on the detection of alpha particles emitted from radon and its decay products, formed inside a scintillation cell volume (Handbook of Radon, 2017). The alpha scintillations produced by radon and its decay products formed inside the cell are continuously counted by the Photo Multiplier Tube and the associated counting electronics.

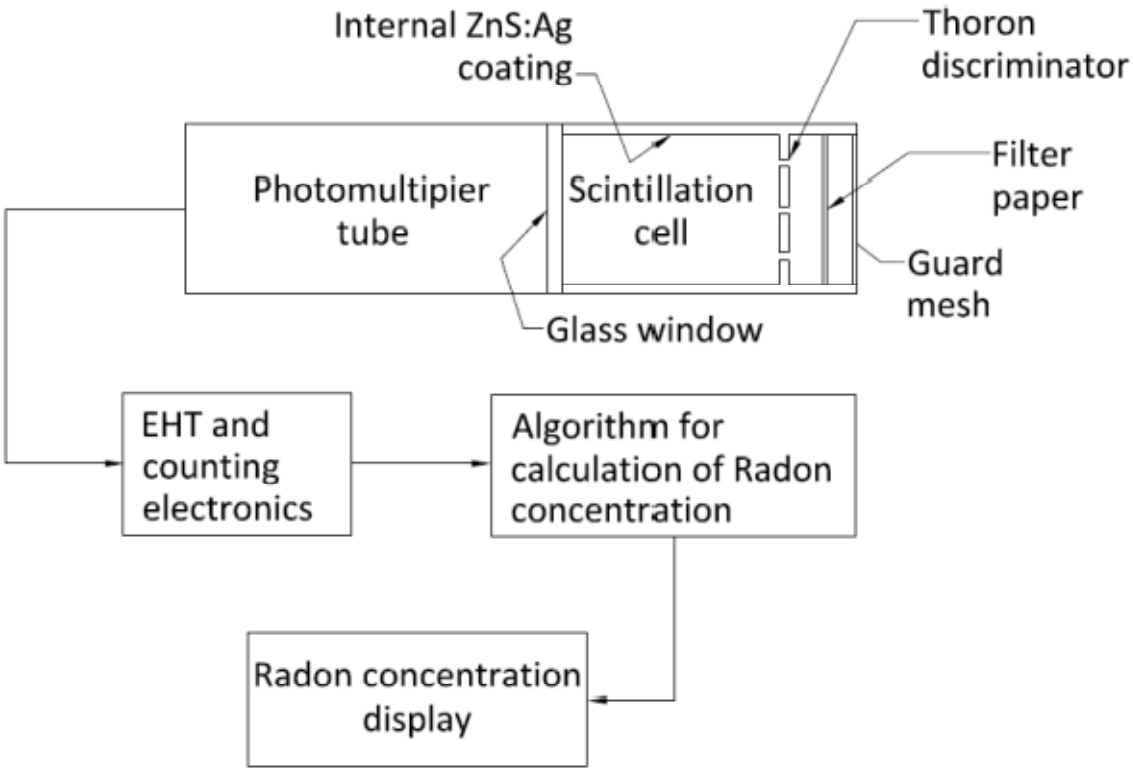

Figure 2.2: Schematic diagram of the working of RnDuo

The build-up and the decay of radon progenies inside the scintillation cell due to varying radon concentrations are complicated, and they never attain equilibrium with radon. Due to this, the automated continuous monitoring of radon was not possible without reckoning the decay product activities. To eliminate this shortcoming, an in-built algorithm was developed for successful deployment of scintillation technology to measure continuously the radon concentration.

The in-built algorithm mentioned above, is based on the theoretical decay and growth of decay products of radon during the ongoing measurement cycle and from the radon concentration in history. The alpha counts so obtained while measuring the concentration of radon, is processed by a microprocessor unit as per the developed algorithm, and then the actual concentration of radon is displayed on the monitor. The instrument has a very good sensitivity and low detector volume which makes it a favorable instrument for radon detection. Due to its favorable properties as well as its

ease of portability, Smart RnDuo was used in this research work to measure the radon concentration in water as well as the radon mass exhalation rate in soil.

The different technical specifications of Smart RnDuo monitor are given below (Table 2.1):

Table 2.1: Technical specifications of Smart RnDuo

Detector type	Scintillation cell	
Scintillation coating	Internally coated ZnS:Ag	
Scintillation cell active volume	153 cm^3	
Radon sensitivity	1.2 CPH/(Bq/m^3)	44.5 CPH/ (pCi/L)
Thoron sensitivity	0.8 CPH/(Bq/m^3)	30 CPH/ (pCi/L)
Sampling type	Diffusion / Flow	
Sampling flow rate	0.5 to 0.7 L/min with inbuilt pump	
Measurement cycle time	15 / 30 / 60 min	
Response time	15 minutes for attaining 95% of radon / thoron	
Minimum detection limit	Radon: 8 Bq/m^3 at 1 σ and 1 h cycle Thoron: 15 Bq/m^3 at 1 σ and 1 h cycle	
Upper detection limit	50 MBq/m^3	
Effect of sample humidity and trace gases on sensitivity	Practically nil until humidity is not condensed on scintillator surface.	
Thoron interference	< 5% with sniffing mode of sampling	
Power	External: 110 - 240V AC 50/60 Hz Internal: 6 V DC Battery	
Dimension	37 cm x 20 cm x 12 cm	

2.1.1. Smart RnDuo for measurement of radon in water:

Radon concentration measurements in liquid samples are important for ingestion as well as inhalation dosimetry. Ingestion of radon dissolved in water is known to contribute to the annual effective dose received by human beings. In addition, radon dissolved in water readily escapes into the surrounding environment, thereby increasing the concentration of radon in the surrounding air. Although there are different processes for measurement of radon concentration in liquid, in this research work, we employ the bubbling technique for measurement, because this process takes shorter time while providing accurate results. Moreover, for the detection of radon concentration, Smart RnDuo monitor was employed. This instrument is a suitable and preferable detector for this purpose because the instrument is free from humidity interference.

The liquid samples were collected in a leak tight sampling bottle provided with the RnDuo system. While sampling the liquid into the bottle, caution was taken to avoid formation of air pocket or bubble in the liquid. The bottle was filled completely and the bottle cap closed tightly, so that no air volume remains in the bottle. Radon concentration in the collected liquid samples was measured within 4-5 hours after the sampling so that dissolved radon does not escape into the surrounding environment before the start of the detection procedure.

After connecting RnDuo monitor along with bubbler attachment to the sampling bottle using flexible tubing (Figure 2.3), measurements were taken in a cycle of 15 minutes for a period of 1 hour. This means that four readings for the radon concentration will be obtained for each liquid sample within the mentioned measurement period. The first reading of the measurements was ignored and the average of the later readings was taken as C_{air}.

The radon concentration in liquid (C_{liq}) (Bq/m^3) is estimated from the concentration measured in air (C_{air}) with RnDuo as under (Handbook of Radon, 2017).

$$C_{liq} = C_{air}\left(K + \frac{V_{air}}{V_{liq}}\right) \qquad \text{---------- (2.1)}$$

Where,

K is the partition coefficient of radon in liquid with respect to air (0.25 for water),

V_{air} is volume of air enclosed in the closed loop setup (m^3) (Bubbler volume + tubing volume + detector volume),

V_{liq} is volume of liquid in sampling bottle (m^3).

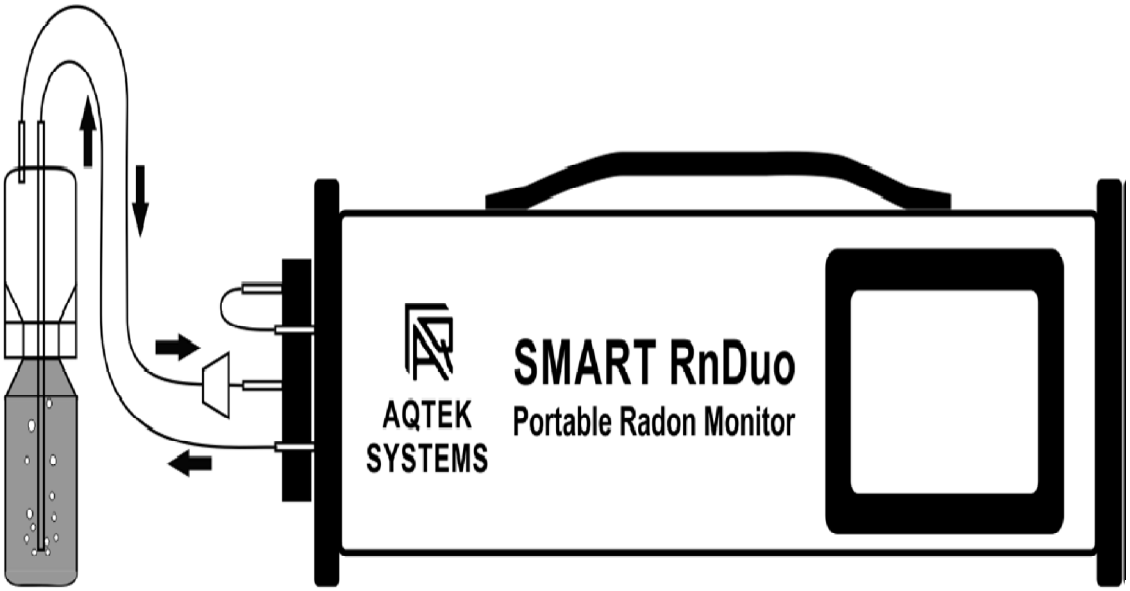

Figure 2.3: Measurement of radon content in water using Smart RnDuo.

2.1.1.1. Ingestion dose due to radon in water:

Taking the average of water consumed by a human being in a year as 60 litres, the annual effective ingestion dose due to radon concentration in water was calculated by using the following equation: (UNSCEAR, 2000 (Annex A))

$$D_{ing}\ (\mu Sv/yr) = {}^{222}Rn\ conc.\ (Bq/l) \times 720\ (l/yr) \times 10^{-3} \times 3.5\ (nSv/Bq) \quad \text{------ (2.2)}$$

Where,

D_{ing} (μSv/yr) is the annual effective ingestion dose due to radon concentration in water and,

3.5 (nSv/Bq) is the conversion coefficient for ingestion dose.

2.1.1.2. Inhalation dose due to radon in water:

Since radon dissolved in water escapes easily into the surrounding environment, the contribution of radon in water to the inhalation dose received by human beings is being considered in this research work. The annual effective inhalation dose due to radon concentration in water was calculated by using the parameters established in UNSCEAR (2000 (Annex A)):

$$D_{inh}\ (\mu Sv/yr) = {}^{222}Rn\ conc.\ (Bq/l) \times 7000\ (hr/\ yr) \times 10^{-4}\ Bq/m^3 \times 0.4 \times 9\ (nSv/\ Bq/hr/m^3) \quad \text{---------- (2.3)}$$

Where,

Average indoor occupancy time per person is about 7000 hr/year,

Ratio of radon in air to radon in water supply is in the range of 10^{-4} Bq/m^3;

Equilibrium factor between radon and its progeny is equal to 0.4,

Dose conversion factor for radon exposure is 9 nSv/Bq/hr/m^{-3} (Duggal *et al*, 2013).

2.1.2. Smart RnDuo for measurement of radon mass exhalation rate from soil

The emission potential of radon from soil is governed by the radon mass exhalation rate (J_m). Active and passive methods of measurement have been widely used for measurement of the radon mass exhalation rate. Although both methods of measurement provides accurate and comparable results, active methods are found to be favorable for exhalation studies because they take much shorter time for measurement, mainly about 1-2 days, while passive method of measurement, mostly using a solid state nuclear track detector, usually takes about 3 months at a time. In this research work, the radon mass exhalation rate of collected soil samples were measured using active method, by employing Smart RnDuo monitor coupled with a radon mass exhalation chamber provided by BARC, Mumbai (Figure 2.4).

Figure 2.4.: Radon Mass Exhalation Rate using Smart RnDuo

Figure: 2.5: Mass exhalation chamber

The accumulation chamber (Figure 2.5) is a stainless steel cylinder having an inner height of about 8 cm and radius 4.5 cm. The scintillation detector was attached directly on the upper or top side of the accumulation chamber, hence acting as a lid to provide a closed loop measurement system. The closed loop measurement system helps in the build-up of radon concentration inside the chamber, and provides accurate radon mass exhalation measurement. The principle of measurement is based on the detection of α-particles given out by radon gas emitted from soil samples and its decay progeny formed inside the detector volume by scintillation with ZnS (Ag). The response time of RnDuo is about 20 min for 63% of chamber radon concentration and 40 min for 95% of chamber radon concentration.

At each sampling sites, soil samples were taken carefully by first removing the top or upper part of the soil (up to a few centimetres), and then collecting the resulting soil using a plastic/ polythene bag. For measuring radon mass exhalation rate, the collected sample was first weigh and its volume taken, and then put inside the radon mass exhalation chamber. The scintillation detector is then mounted on top of the exhalation chamber, and build up data of radon was retrieved every 60 minutes for a period ranging from 10 to 24 hours. Least square fitting of the data obtained was carried out using the following equation given below (Sahoo *et al,* 2007; Lekshmi *et al,* 2018):

$$C(t) = \left(\frac{J_m M}{V} \right) t + C_o \qquad \text{---------- (2.4)}$$

Where,

$C\ (t)$ is ^{222}Rn concentration (Bq/m^3) at time t,

C_o is the ^{222}Rn concentration (Bq/m^3) present in the chamber volume at t = 0,

M is the total mass of the dry sample (kg),

V is the effective volume (volume of detector + porous volume of sample + residual air volume of mass exhalation chamber) (m^3).

The porous volume (V_p) can be estimated using the following equation,

$$V_P = V_s - \left(\frac{M}{\rho_g} \right) \qquad \text{---------- (2.5)}$$

Where,

V_s is the sample volume in the mass exhalation chamber,

ρ_g is the specific gravity of the sample.

On least square fitting of the data to the above equation, one may obtain J_m from the fitted parameters with the information of the mass M of the sample.

2.1.2.1. Emanation Factor:

Radon gas is formed continuously in the soil matrix due to the presence of its parent radionuclide, i.e., radium. After formation, it escapes from the soil matrix into

the surrounding air or water pockets contained within the pores between rocks or soils by a process known as emanation. The fraction of radon atoms generated, that escape the solid phase in which they are formed and become free to migrate through the bulk medium is defined as the emanation factor of radon. The emanation factor (f) is calculated using the formula: (Lekshmi *et al*, 2018)

$$f = \frac{J_m}{C R_a \lambda} \qquad \text{---------- (2.6)}$$

Where,

C_{Ra} is the radium activity concentration (Bq/kg),

λ is the decay constant of radon (in hour),

J_m is the mass exhalation rate of radon (mBq/kg/hr).

2.2. Gamma Spectrometry using NaI (Tl) Detector

Fig 2.6: Sodium Iodide, NaI (Tl) detector housing

Gamma spectrometry is a technique used for determining the identity as well as the activity concentration of various radioisotopes contained in a given sample. This technique is based on the analysis of the different gamma energies and the peak areas of the full-energy peaks of the gamma lines emitted by the radioactive isotopes. Using this technique, it is possible to measure simultaneously the activity concentration, and identifies the different radionuclide in a given sample without the requirement of any chemical separation.

The measurement of activity concentration of ^{238}U, ^{232}Th and ^{40}K in the collected soil samples was carried out by using a Thallium (Tl) activated 5" X 4" Sodium Iodide (NaI) detector (Figure 2.6.). The detector was coupled to a personal computer based 1 K multi-channel analyzer, GSPEC-SA (Version 2.5 X), which was manufactured by Electronic Enterprises (India) Pvt. Ltd, Mumbai, Maharashtra, India (Figure 2.7). The GSPEC-SA allows control and analysis of the detector output by employing in-built computer-based application software (SAAS – Spectrum Acquisition and Analysis).

Fig 2.7: GSPEC-SA multichannel analyzer

To overcome the effects of background radiation from the surrounding environment, the detector is enclosed in a cylindrical lead and iron shield. The Multi-Channel Analyzer was pre-calibrated so that detection of gamma energies between 0 keV and 3000 keV is possible. Two Standard sources, ^{137}Cs, having an energy peak at 661.99 keV, and ^{60}Co, having two energy peaks at 1173 keV and 1332 keV was employed for this purpose (Figure 2.8). The initial settings of the GSPEC-SA multi-channel analyzer is shown in Table 2.2.

2.2.1 Efficiency and Energy Calibration of NaI (Tl) Detector

For efficiency calibration, IAEA standard source of ^{238}U, ^{232}Th and ^{40}K (Figure 2.8) with known activity was analyzed using the GSPEC-SA multichannel analyzer for a period of 10800 seconds (3 hours). This calibration established the detection efficiency of the detector as a function of the energy of radiation. To minimize error due to attenuation of gamma radiation, all the three standard sources were prepared in similar geometry as well as matrix. Also, to avoid coincidence summing of the gamma rays, a gamma ray standard of the same radionuclide as the one to be monitored was used (Agarwal, 2011).

Table 2.2: Initial Settings of GSPEC-SA

Gain	HV	LLD	^{137}Cs Ch & Energy		^{60}Co Ch & Energy		^{60}Co Ch & Energy	
			Channel	keV	Channel	keV	Channel	keV
6	650	1	231	661.99	403	1173	455	1332.01

The gamma ray photon emitted from the radioactive decay chain of the standard sources undergo various types of interactions with the detector, thus leading to a complex detector response of continuous energy distribution, having certain full energy peaks. This continuous energy distribution is due to part absorption of the photon energy inside the detector volume, while the remaining photon energy escapes from the detector. The full energy peaks arise due to the complete absorption of gamma photons within the detector, either by the photoelectric effect or by various multiple interactions. For the gamma energy peak obtained, the efficiency was calculated using the formula:

$$\eta(\%) = \frac{Area/_{sec}}{dps} X \frac{100}{Ab\%} X100 \qquad \text{---------- (2.7)}$$

Where,

$\eta(\%)$ = Percent Efficiency

Area/sec = Net peak area per second (background subtracted)

dps = Source strength

$Ab\%$ = Gamma ray abundance factor

Before measuring the natural radioactivity present in a sample, a three-point energy calibration was carried out using sources containing a mixture of radionuclide (ISO 18589-3:2007(E)). In this study, the energy calibration is achieved by counting given standard sources of ^{60}Co and ^{137}Cs for a period of 500 seconds. This calibration allows the establishment of the relationship between the channel numbers of the analyzer and the known energy of the photons (BIPM, 2004). Three photo peak areas were obtained and after analysis of the region of interests (ROI's), the necessary calibration was performed by inputting the obtained data into the computer software.

Figure 2.8: IAEA Standard Sources for Energy and Efficiency Calibration

2.2.2 Activity Concentration Measurement

The collected samples were first dried, and then heated using a heater at a temperature of about 110 ^{o}C. The samples were then grinded into a fine powder-size and sieved using a 500 μm mesh. It was then sealed inside an airtight container of 250 ml, and was kept undisturbed for a minimum period of 30 days to attain radioactive equilibrium. Since some radionuclide of the natural decay chains such as ^{238}U and ^{232}Th can be determined only by measuring their respective daughter radionuclide, it is necessary to ensure a radioactive equilibrium between the parent radionuclide and the daughter radionuclide before the start of measurement.

The activity concentration of the sample was obtained by analyzing with the GSPEC-SA Multichannel Analyzer for a period of 50,000 seconds. The activity concentrations were determined for three primordial radionuclide, viz., ^{238}U, ^{232}Th and ^{40}K after removing the background radiation content using the multichannel analyzer software. In this research work, the activity concentration was determined only for ^{238}U, ^{232}Th and ^{40}K radionuclide because they are the most prominent and the most abundant natural radionuclide found in nature.

The activity concentration of ^{238}U and ^{232}Th in the soil samples, as mentioned before, cannot be determined directly by using gamma spectroscopy. However, as secular equilibrium is established between ^{238}U, ^{232}Th, and their decay products, the ^{238}U concentration was determined from the activity concentrations of its daughter radionuclide, ^{214}Pb and that of ^{232}Th was determined from the activity concentrations of its decay radionuclide, ^{228}Ac. The activity concentrations of ^{238}U-series (^{214}Pb), ^{232}Th- series (^{228}Ac), as well as ^{40}K, are all expressed in Bq/kg. After measurement, the weights of the samples were taken and the activity concentration (A) was obtained for each samples using the formula given below:

$$A = \frac{N}{T} X \frac{100}{\gamma\%} X \frac{100}{\eta\%} X \frac{1}{Wt} \qquad \text{---------- (2.8)}$$

Where,

$\frac{N}{T}$ = Background subtracted net photo peak counts in time 'T'.

$\gamma\%$ = Gamma-ray abundance factor/branching intensity.

η % = obtained percentage Efficiency of the standard source.

Wt = weight of the sample

2.2.3. Determination of Radium Equivalent Activity:

Uniformity of natural radioactivity in soil with respect to exposure to radiation is defined in terms of the Radium equivalent activity (Ra_{eq}). It is a comparison of the specific activity of materials containing different amounts of ^{226}Ra, ^{232}Th and ^{40}K. Since, radioactive equilibrium between the parent radionuclide and the daughter

radionuclide was achieved for all the soil samples, the activity level of ^{238}U obtained in this study corresponds to the activity level of its daughter radionuclide, ^{226}Ra.

Radium equivalent activity (Ra_{eq}) is simply the representation the activity levels of ^{226}Ra, ^{232}Th and ^{40}K by a single quantity, taking into account the radiation hazards associated with them. It is defined by assuming that 370 Bq/kg for ^{226}Ra, 259 Bq/kg for ^{232}Th and 4810 Bq/kg for ^{40}K produce the same gamma dose rate and is represented as given below (Beretka *et al*, 1985):

$$Ra_{eq} = C_{Ra} + 1.43\ C_{Th} + 0.07\ C_K \quad \text{---------- (2.9)}$$

Where,

C_{Ra} represents the activity concentrations of ^{226}Ra (in Bq/kg)

C_{Th} is the activity concentrations of ^{232}Th (in Bq/kg)

C_K is the activity concentrations of ^{40}K (in Bq/kg).

2.3. Measurement of Uranium in water using LED Fluorimeter:

Figure 2.9: LED Fluorimeter, LF-2a

Fluorimetry using Light Emitting Diode (LED) is a simple, effective and low-time consuming spectroscopic technique used for the detection and measurement of trace quantities of uranium in aqueous solution such as water. This technique is based on the principle of measurement of fluorescence of uranium complexes in aqueous sample formed by the addition of an inorganic reagent (Rathore, 2008; Kutahyali *et al*, 2011).

When Ultra-violet light of suitable wavelength falls on uranium complexes contained in a given aqueous sample, it excites the uranium complex, thus emitting green fluorescence, which can be measured by a Photomultiplier Tube (PMT). The fluorescence yield obtained is proportional to the intensity of the excitation source and the concentration of uranium in the sample, therefore, the fluorescence obtained in this method corresponds to the uranium concentration in the given sample. The fluorescence yield for different uranium complexes contained in a sample is different, so, to convert all the complexes into a single valence state of U (IV), and also to increases the fluorescence lifetime and yield, an organic reagent known as Fluorescence enhancing reagent (Fluren) is added to the aqueous sample.

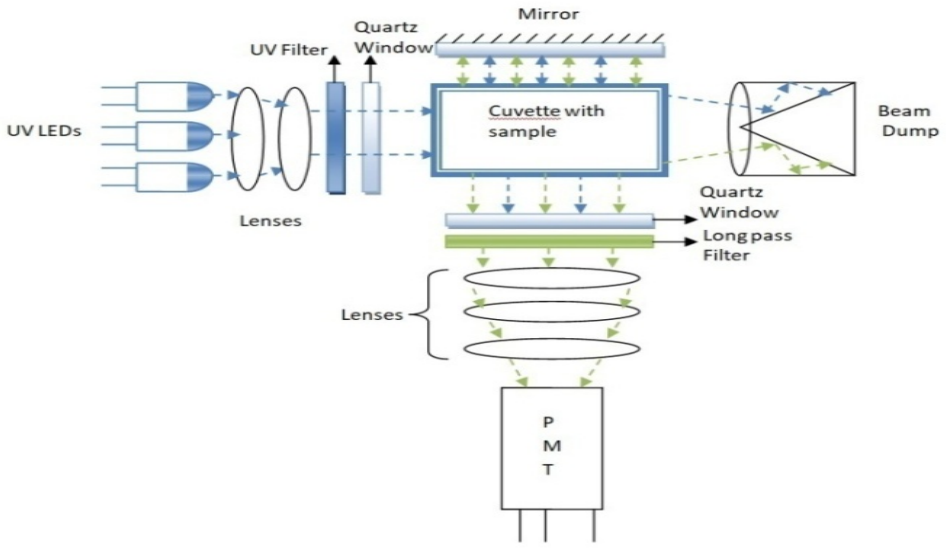

Figure 2.10: Working of LED Fluorimeter, LF-2a

The uranium concentration in collected water samples were measured using LED Fluorimeter LF-2a, manufactured by Quantalase Enterprises Private Limited, Indore, India (Figure 2.9). The instrument consist of an arrangements of Light

Emitting Diode (LED) which emits pulses at wavelength of 405 nm, having a repetition rates of 1000 pps and about 20 µsec pulse duration (Figure 2.10). The emitted light passes through a UV filter, which allows only the required UV light to pass through and then eventually falls on the cuvette containing the sample. This excites the uranium complexes in the sample, thereby emitting green fluorescence. The uranium fluorescence so obtained then pass through the long pass filter (350 nm), and is then focused by the lens into the photomultiplier tube. The long pass filter acts as a filter for blocking unwanted Ultra-violet light as well as other fluorescence emitted by the sample to enter into the Photo-multiplier Tube. In the above given arrangement, the quartz window acts as a shield to block environmental effects, while the beam dump absorbs the UV light and other light emitted from the sample. The detector is time gated so that the fluorescence will be measured only after the reduction of the background substantially.

The buffer solution required in this technique was prepared by adding Sodium pyrophosphate solution (5%) in double distilled water. The pH value of the resultant solution was adjusted to 7.0 by the addition of dilute Ortho-phosphoric acid (OPA) solution drop-wise to it. This solution acts as fluorescence enhancing reagent (Fluren) (Virk, 2016). Standard solution was prepared by the dilution of Uranium Standard (ICP-MS-66N-0.01X-1) using double distilled water.

Collected water samples were filtered using a filter paper to remove unwanted impurities before the start of analysis. Background count was measured by putting 5ml double distilled water along with 10% Fluren (Buffer solution) inside the quartz cuvette. Standard addition method was employed in this research to overcome the effect of interfering materials during analysis. The mean value and standard deviations were then analyzed using Microsoft Excel. The limit of detection obtained using this method was as low as 0.2 ppb. The concentration of uranium (µg/l) in samples was calculated using the following formula (Patra *et al*, 2013):

$$U = \frac{D_1}{D_2 - D_1} \text{ x } \frac{V_1 C}{V_2} \qquad \text{---------- (2.10)}$$

Where,

D_1 is the fluorescence due to sample alone,

D_2 is the fluorescence due to sample and U-standard,

V_1 is the volume of U-standard added (ml),

V_2 is the volume of sample used for analysis (ml),

C is the concentration of U in U-standard solution (µg/l).

2.3.1. Annual effective dose due to ingestion of uranium:

The annual effective radiation dose received by a human being due to ingestion of water containing uranium is calculated by using the following equation, which was established by WHO (2004):

$$AED\ (\mu Sv/year) = U_{act}\ (Bq/l) \times F\ (mSv/Bq) \times 10^3 \times 1480\ (l/year) \quad \text{-------- (2.11)}$$

Where,

AED (µSv/year) is the annual effective dose due to ingestion of uranium,

U_{act} (Bq/l) is the uranium activity concentration (taking 1 µg/l = 0.02528 Bq/l),

F (mSv/Bq) is the effective dose per unit ingestion (4.5×10^{-5}),

1480 (l/year) is the amount of water consumed in a single year (HDR, 2009).

2.4. Spot background gamma detection

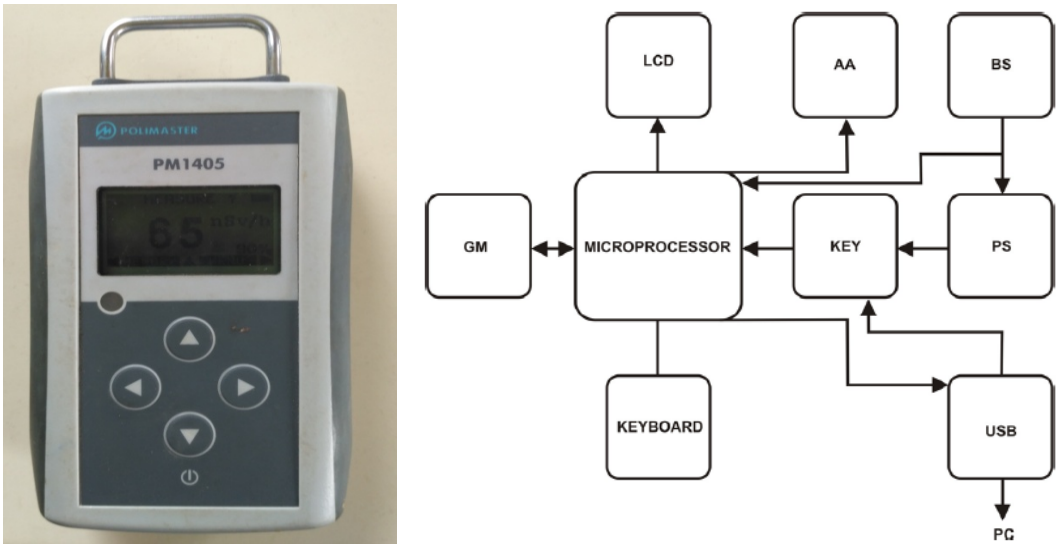

Figure 2.11: Gamma Survey Meter PM 1405

Spot background gamma radiation detection was carried out using an electronic dosimeter known as Gamma Survey Meter PM 1405, developed by Polimaster, Minsk, Belarus. The instrument is able to operate in an environmental condition where the ambient air temperature ranges from minus 10^{o}C upto plus 50^{o}C; relative humidity up to 95 % at the temperature of 35^{o}C and lower. The instrument comprises the following main blocks and modules (Figure 2.11):

- Geiger-Muller detection bloc (GM);
- Main microprocessor controller (Microprocessor);
- LCD;
- Keyboard;
- Audible alarm (AA);
- Key;
- Batteries set (BS);
- Power supply (PS);
- USB interface unit (USB).

The instrument is lightweight, portable and works on a detection bloc based on Geiger-Muller counter by transformation of photon to electro-pulses. The instrument's operating algorithm ensures continuity of the measurement process, static handling of measurement results, fast adaptation to radiation rate changes and effective output of the information obtained on the LCD. The microprocessor controls the instrument's operating modes, USB interface, keyboard, backlight, non-volatile memory, matrix LCD, necessary calculations, self-diagnostics, as well as information gathering from the detection bloc. The measurement range for gamma radiations using this instrument is between the ranges of 0.1μSv/h to 100 mSv/h.

Detection was carried out at each site at the time of sampling and the detector was put 1 metre above the ground level so that background gamma radiations coming from cosmic and terrestrial sources are detected. The level of background gamma radiation obtained in this method could help in tracing the origin of the radiations, i.e., whether cosmetic or terrestrial.

2.5. Soil Type and Grain Size Determination

Radon mass exhalation rate is found to be greatly affected by the soil moisture content. Different types of soil have different grain size, and the grain size determines the ability for soil to retain moisture. Therefore, identification of soil type and grain size determination is an important factor in this regard.

Figure 2.12.: Mechanical Sieve Shaker

For identification of soil type using the process of sieving, a Mechanical Sieve Shaker was employed to enable quality assurance of the result (Figure 2.12). This is because mechanical parameters such as sieving time, speed and amplitude are carried out with exact reproducibility in a Mechanical Sieve Shaker.

Collected soil samples were dried and placed in the uppermost sieve in a set of stacked sieves. The stack of sieves was arranged in order so that the coarsest sieve is

at the top with finer ones below. A pan was placed at the bottom of the stacked sieves to catch any sediment that passes through the lowest and finest sieve. The stack of sieves was then placed on the shaking machine for about 15 to 20 minutes.

Five different sieves of sieve mesh number, namely, 60 (grain size 0.25 mm which corresponds to medium sand), 120 (grain size 0.125 mm which corresponds to fine sand), 230 (grain size 0.0625 mm which corresponds to very fine sand), 325 (grain size 0.044 mm which corresponds to silt/mud) and >325 (grain size smaller than 0.044 mm which corresponds to clay) was used to identify the grain size distribution.

The soil that had collected on each sieve was then removed and the weight taken. Percentage of the grain size distribution obtained was then plotted using a triangular plot. The triangle plot consists of three main primary classifications, namely, sand, silt and clay. These three classifications are further divided into 12 classes. A triangular plot, called the USDA triangle was employed for this purpose (García-Gaines *et al*, 2015). The different grain size obtained in this study were named in accordance with the Udden-Wentworth size term (Wentworth, 1922).

3

Experimental Determination of Radon and Uranium Concentration in Water

The experimental determination of radon concentration and uranium concentration in water in Aizawl and Kolasib District of Mizoram will be presented in this chapter. The detailed critical discussion of the result will also be presented. The seasonal variation of radon concentration in water, as well as how the concentration of radon and uranium differs with respect to the sample source will be shown. The obtained results will be compared with the global average values whenever possible. The radon concentration and uranium concentration obtained in this present study will also be correlated.

The geographical area of sampling sites (Figure 3.1) extends from 23˚34'23.6'' to 23˚54'8.8'' latitude and from 92˚39'51.9'' to 92˚57'57.9'' longitude, with an altitude ranging from 1170 ft to 4140 ft above sea level in Aizawl district. In Kolasib district, the sampling area extends from 23˚58'56.5'' to 24˚30'43.5'' latitude and from 92˚35'54.4'' to 92˚46'23.7'' longitude, with an altitude ranging from 150 ft to 2967 ft above sea level. Samples were collected from different available water sources such as streams, springs, bore-wells, government supplied water etc. A total of 66 locations: 39 from Aizawl district and 27 from Kolasib district was chosen for this research work.

In Kolasib District, samples were collected from 10 Town/Villages, namely; Kolasib, Vairengte, Bilkhawthlir, Rengtekawn, Pangbalkawn, Saihapui, Thingdawl, Bualpui, Kawnpui and Taitow. While in Aizawl District, 14 City/Town/Villages, namely; Aizawl, Sihphir, Hlimen, Lungleng, Falkawn, Sateek, Tachhip, Seling, Thingsulthliah, Darlawng, Tlungvel, Tuikhurhlu, Keifang and Saitual were selected for measurement.

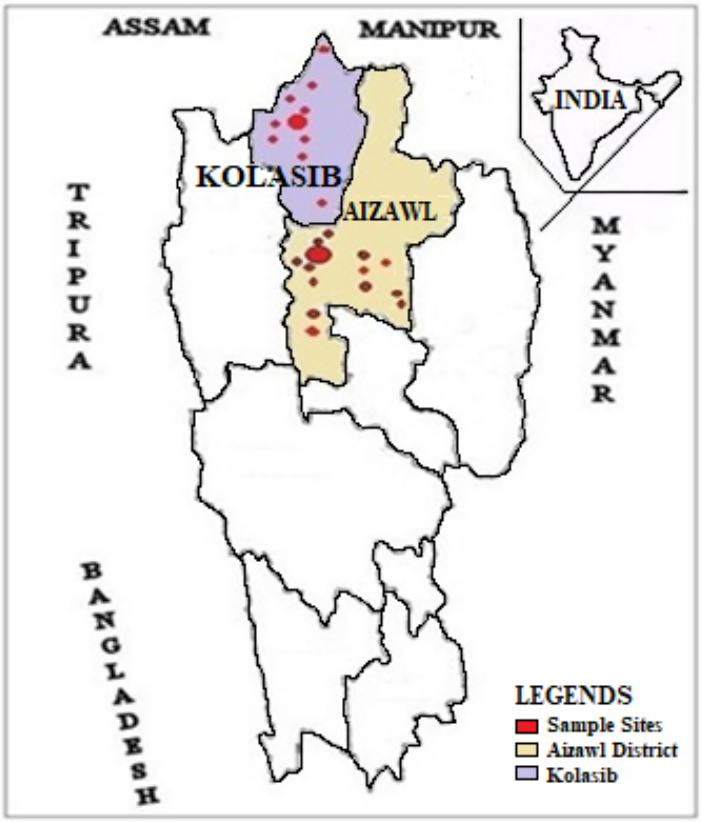

Figure 3.1: Geographical Map showing the studied regions of Aizawl and Kolasib District

3.1. Determination of ^{222}Rn Concentration in Water

Smart RnDuo Monitor is used for the determination of radon concentration in water. The principle of measurement of this instrument is based on the detection of alpha particles formed inside the scintillation cell volume, the alpha particles being emitted by radon/thoron contained in the water samples. The liquid samples were collected from different water sources, such as springs, streams, bore-wells, enclosed springs, open wells and government supplied water. Samples were collected in a leaked tight glass bottle, and were completely filled to avoid any air trappings inside the bottle. The detailed protocols for measurement of radon concentration in water are given below:

1. Before start of the each experiment, whatever radon gas that is trapped in the setup, including detector volume was flushed for a period of about 5 minutes by putting "Pump setting = On" in Rn222 mode in open loop.
2. Connection of RnDuo monitor with the bubbler attachment to the sampling bottle was made as shown in Figure 2.3 using flexible tubing. The liquid samples were handled carefully to avoid disturbing it, so that dissolved radon does not escape before being counted.
3. Special attention was given to ensure that the direction of flow is exactly as shown in Figure 2.3. This is because any wrong connection may lead to the liquid entering the monitor and thus, damage the pump as well as the scintillation cell.
4. "Pump setting = ON" in Rn222 mode in closed setup was selected manually, which turned on the pump for about 2 minutes.
5. A delay of 5 minutes was given after turning the pump off and the measurement with started by inputting the following configuration in RnDuo:

   Mode = Rn222

   Modify cycle = 15 minutes

   Pump Settings = OFF
6. Measurement was done for a period of about 1 hour. The first reading was ignored and the average values of the later reading were taken as C_{air}.
7. When more than one samples were analyzed continuously, instead of stopping the measurement at the end of 1 hour, the sampling bottle was removed and the set up was flushed for about 5 minutes in open loop (by putting "ON" the pump in RnDuo).
8. After flushing the cell for 5 minutes, the pump was then again turned "OFF" and the measurement procedure described above was repeated for subsequent sample analysis.

At the end of the measurement, four readings for C_{air} was obtained and after discarding the first reading to ensure that there is no error due to background radon counts from former samples, the average of the latter readings were taken. The volume of the liquid samples used and also the volume of air enclosed in the closed

loop system were then manually measured. The radon concentration in the water sample was then calculated using Equation 2.1.

3.1.1. Results and Discussions

Seasonal data of radon concentration in water were taken at each sampling sites. The period of sampling for winter season ranges from November 2016 to February 2017, for summer season, it ranges from March 2017 to June 2017 and for monsoon season; the period ranges from July 2017 to October 2017.

Table 3.1: Radon Concentration in water in Kolasib District

Code	Source	Location	Radon in water (Bq/l)					
			Winter		Summer		Monsoon	
			Conc.	Error	Conc.	Error	Conc.	Error
K-1	Borewell	Vairengte-I	14.55	0.74	9.29	0.41	11.84	0.67
K-2	Spring	Vairengte-II	1.27	0.07	1.75	0.13	1.83	0.13
K-3	Spring	Vairengte-III	3.75	0.41	9.24	0.52	14.86	0.38
K-4	Spring	Vairengte-IV	5.58	0.45	1.96	0.08	2.52	0.11
K-5	Spring	Bilkhawtlir-I	2.72	0.20	12.08	0.57	15.33	0.87
K-6	Spring	Bilkhawthlir-II	2.3	0.24	1.21	0.06	0.44	0.10
K-7	Spring	Bilkhawthlir-III	1.77	0.26	1.66	0.12	0.26	0.09
K-8	Borewell	Rengtekawn-I	7.62	0.60	11.49	0.57	6.81	0.49
K-9	Spring	Rengtekawn-II	10.12	0.67	4.69	0.21	26.85	0.92
K-10	Spring	Kolasib-I	2.16	0.12	8.13	0.19	38.63	1.01
K-11	Spring	Kolasib-II	1.63	0.14	19.82	0.88	12.42	0.71
K-12	Spring	Kolasib-III	2.38	0.13	7.4	0.50	31.18	0.94
K-13	Openwell	Kolasib-IV	8.49	0.68	8.92	0.57	41.68	0.97
K-14	Spring	Kolasib-V	9.19	0.83	17.34	0.59	18.89	0.34
K-15	Spring	Pangbalkawn	1.79	0.17	1.36	0.24	2.62	0.16
K-16	Spring	Tuichhuahen	1.18	0.16	6.6	0.48	1.61	0.11
K-17	Spring	Saihapui	1.11	0.20	1.25	0.36	1.61	0.12
K-18	Spring	Kolasib outskirt	1.3	0.15	1.01	0.20	10.4	0.64

K-19	Spring	Thingdawl-I	9.58	0.17	4.92	0.29	15.95	0.41
K-20	Spring	Thingdawl-I	6.51	0.70	8.29	0.38	17.67	0.59
K-21	Spring	Khuangpuilam	15.72	0.88	17.47	0.89	20.9	0.53
K-22	Spring	Kolasib-VI	2.58	0.23	18.99	0.85	37.62	0.92
K-23	Spring	Kolasib-VII	5.01	0.51	17.53	0.88	19.04	0.86
K-24	Borewell	Bualpui	10.4	1.03	7.37	0.74	21.18	0.33
K-25	Spring	Kawnpui-I	6.05	0.54	0.99	0.09	6.55	0.48
K-26	Spring	Kawnpui-II	22.18	0.91	0.66	0.04	10.76	0.66
K-27	Borewell	Taitow	17.11	0.82	4.57	0.34	12.97	0.37

Table 3.2: Radon Concentration in water in Aizawl District

Code	Source	Location	Radon in water (Bq/l)					
			Winter		Summer		Monsoon	
			Conc.	Error	Conc.	Error	Conc.	Error
A-1	Borewell	Bawngkawn-I	3.9	0.24	N.D.	N.D.	7.49	0.61
A-2	Spring	Bawngkawn-II	20.74	0.82	19.72	0.85	21.06	0.92
A-3	Borewell	Chhinga Veng	9.03	0.49	9.02	0.31	10.98	0.73
A-4	Spring	Ramhlun-I	4.5	0.42	4.34	0.37	0.4	0.17
A-5	Borewell	Ramhlun-II	2.72	0.49	4.55	0.47	4.75	0.37
A-6	Borewell	Sihphir-I	32.53	1.03	24.9	0.57	24.86	0.98
A-7	Spring	Sihphir-II	9.41	0.85	6.88	0.84	11.89	0.64
A-8	Spring	Selesih-I	3.23	0.44	6.64	0.67	14.08	0.62
A-9	Borewell	Selesih-II	21.86	0.81	22.64	0.91	31.28	0.72
A-10	Borewell	Durtlang	26.42	0.88	8.16	0.32	15.46	0.66
A-11	Spring	Bungkawn-I	6.97	0.44	12.66	0.40	8.67	0.58
A-12	Borewell	Bungkawn-II	3.21	0.33	6.6	0.34	0.41	0.13
A-13	Stream	Tuikual Lui	1.65	0.20	2.59	0.30	0.46	0.18
A-14	Borewell	Luangmual	15.53	0.68	12.55	0.23	12.58	0.70
A-15	Borewell	Mission VT	5.35	0.45	1.01	0.06	5.13	0.54
A-16	Borewell	Republic VT	5.35	0.48	3.83	0.17	9.35	0.60

A-17	Spring	Mission Veng	2.37	0.53	1.82	0.06	3.72	0.57
A-18	Borewell	Mualpui	1.48	0.32	2.2	0.06	5.9	0.34
A-19	Borewell	Hlimen-I	6.3	0.54	5.72	0.20	7.57	0.42
A-20	Spring	Hlimen-II	2.26	0.20	1.19	0.05	5.96	0.47
A-21	Spring	Lungleng	6.3	0.57	1.03	0.05	5.96	0.52
A-22	Borewell	Hlimen-III	27.5	0.97	29.7	0.59	17.46	0.88
A-23	Borewell	Falkawn	2.05	0.15	0.92	0.04	0.36	0.23
A-24	Borewell	Sateek-I	3.91	0.30	5	0.12	12.66	0.50
A-25	Spring	Sateek-II	2.86	0.33	1.5	0.04	0.85	0.16
A-26	Spring	Tachhip	3.27	0.31	0.53	0.06	7	0.47
A-27	Stream	Ramthar	4.88	0.59	12.66	0.67	10.13	0.52
A-28	Stream	Chite Lui-I	0.02	0.44	1.62	0.11	0.55	0.09
A-29	Stream	Chite Lui-II	2.2	0.34	1.34	0.20	2	0.30
A-30	Spring	Zemabawk	3.16	0.52	11.98	0.70	3.75	0.31
A-31	Spring	Seling	1.04	0.06	0.74	0.11	2.4	0.13
A-32	Spring	Thingsulthliah-I	2.85	0.05	15.01	0.54	3.69	0.21
A-33	Stream	Thingsulthliah-II	1.23	0.06	12.56	0.61	2.37	0.11
A-34	Stream	Darlawng	6.57	0.54	8.12	0.75	5.54	0.32
A-35	Spring	Tlungvel	4.9	0.42	6.29	0.87	7.65	0.31
A-36	Stream	Tuikhurhlu	6.13	0.27	1.44	0.08	8.62	0.50
A-37	Supplied	Govt. Tanky	0.31	0.04	0.66	0.06	0.47	0.05
A-38	Stream	Keifang	0.44	0.05	0.49	0.04	3.71	0.12
A-39	Borewell	Saitual	1.96	0.53	2.07	0.05	6.54	0.41

The annual average radon concentration obtained ranges from 1.23 ± 0.16 Bq/l to 19.73 ± 0.66 Bq/l, having an average value of 9.66 ± 0.46 Bq/l in Kolasib district. In Aizawl district, the annual average radon concentration was found ranged from 0.48 ± 0.05 Bq/l to 27.43 ± 0.86 Bq/l, having an average value of 7.25 ± 0.41 Bq/l.

Table 3.1 shows the measured values of radon concentration in water in Kolasib district during winter, summer and monsoon. Radon concentrations were

found to be in the range of 1.11 ± 0.2 Bq/l to 22.18 ± 0.91 Bq/l, with an average of 6.45 ± 0.44 Bq/l and standard deviation (SD) of 5.66 during the winter season. In summer, radon concentration ranged from 0.66 ± 0.04 Bq/l to 19.82 ± 0.88 Bq/l, having an average value of 7.63 ± 0.41 Bq/l and SD of 6.19. And, in monsoon season, the radon concentration was found to be in the range of 0.26 ± 0.09 Bq/l to 41.68 ± 0.97 Bq/l, having an average value of 14.91 ± 0.52 Bq/l and SD of 12.03.

Table 3.2 shows the measured results of radon concentration in water in Aizawl district during winter, summer and monsoon. Radon concentration was found to be in the range of 0.02 ± 0.44 Bq/l to 32.53 ± 1.03 Bq/l, having an average value of 6.83 ± 0.44 Bq/l and SD of 8.07 during the winter. While in summer, it ranged from 0.49 ± 0.04 Bq/l to 29.70 ± 0.59 Bq/l, with an average value of 7.12 ± 0.34 Bq/l and SD of 7.38. Also, in monsoon season, it ranged from 0.40 ± 0.17 Bq/l to 31.28 ± 0.72 Bq/l, having an average of 7.79 ± 0.44 Bq/l and SD of 6.99. Sample code A-1 of Aizawl district for the summer season was marked as "Not Defined (N.D.)" because at the time of sampling, no water was found as the water source has dried up. So, measurement of radon in this case, was not possible during this time.

The measured values of radon concentration in water for Kolasib and Aizawl district, for all the three seasons (i.e. winter, summer and monsoon), with the exception of sample code K-13 of Kolasib district (of monsoon season), were found to be well within the safe limit range of 4-40 Bq/l for radon concentration in drinking water as recommended by UNSCEAR (1993). These values were also found to be much lower than the European Commission recommended reference level for radon in drinking water, which is 100 Bq/l (European Commission, 2001). Although sample code K-13 of Kolasib district, during the monsoon season, exceeds the safe limit range of radon concentration in water prescribed by UNSCEAR (1993) by 1.68 Bq/l, the annual average radon concentration in water for this particular sample is found to be 19.70 Bq/l, which was well within the mentioned safe limit range.

Figure 3.2 shows the graphical representation of the seasonal variation of the measured average radon concentration in water in both Aizawl and Kolasib District. In both districts, it was found that the radon concentration was found to be highest

during the monsoon season, followed by summer season, and the lowest concentration of radon was observed during the winter season.

The possible reason for this result may be due to the fact that there is possibility of higher collection of radon emanated from different soil surface into the rain water as it flows through several soil during the monsoon season. Hence, absorption of radon from soil into the water will be higher. At the same time, winter is dry compared to summer and monsoon. And in summer, we observed some rain, but not as heavy as monsoon season.

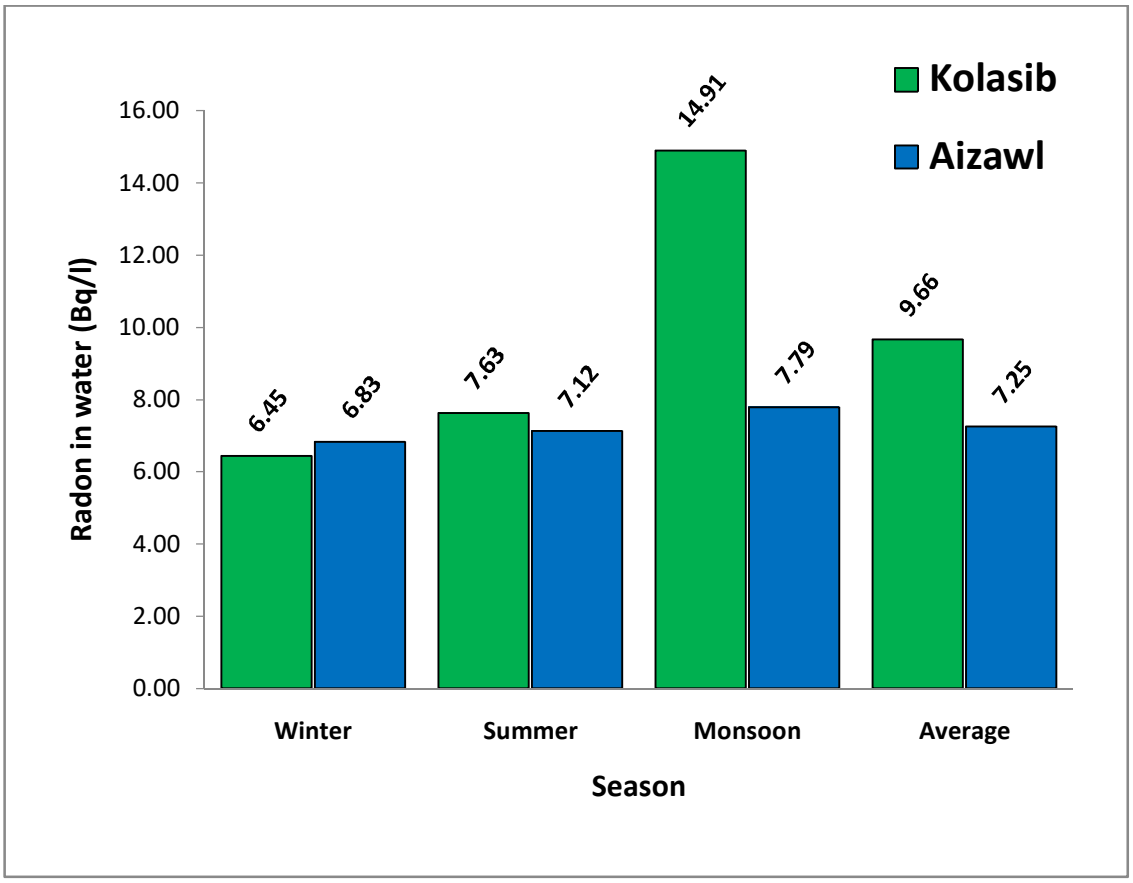

Figure 3.2: Seasonal variation of radon concentration in water

Depending upon their source or origin, collected water samples were classified into two types. Samples collected from water sources such as streams, springs and government supplied water are collectively labeled as "surface water", while those

samples taken from water sources like bore wells, open wells and enclosed springs are labeled as "ground water".

For Kolasib district, the radon concentration for surface water sources was found to be in the range of 1.11 ± 0.2 Bq/l to 22.18 ± 0.91 Bq/l, having an average value of 5.41 ± 0.38 Bq/l during the winter. In summer, it ranges from 0.66 ± 0.04 Bq/l to 19.82 ± 0.88 Bq/l, with an average value of 7.44 ± 0.4 Bq/l. Also, for monsoon season, the radon concentration ranged from 0.26 ± 0.09 Bq/l to 37.62 ± 0.92 Bq/l, having an average of 12.82 ± 0.48 Bq/l. For samples taken from ground water sources, the concentration ranged from 2.16 ± 0.12 Bq/l to 17.11 ± 0.82 Bq/l, having an average of 10.05 ± 0.67 Bq/l during the winter season. In summer, the value ranges from 4.57 ± 0.34 Bq/l to 11.49 ± 0.57 Bq/l, having an average of 8.29 ± 0.47 Bq/l. And, for monsoon, it ranged from 6.81 ± 0.49 Bq/l to 41.68 ± 0.97 Bq/l, having an average of 22.19 ± 0.64 Bq/l.

In Aizawl district, the radon concentration from surface water sources ranges from 0.02 ± 0.44 Bq/l to 20.74 ± 0.82 Bq/l, having an average value of 4.23 ± 0.37 Bq/l during the winter. In summer, the value ranges from 0.49 ± 0.04 Bq/l to 19.72 ± 0.85 Bq/l, having an average of 5.73 ± 0.37 Bq/l. And, for monsoon, the radon concentration was found to be in the range of 0.40 ± 0.17 Bq/l to 21.06 ± 0.92 Bq/l, having an average value of 5.69 ± 0.36 Bq/l. For samples taken from ground water sources, the radon concentration in winter ranges from 1.48 ± 0.32 Bq/l to 32.53 ± 1.03 Bq/l, having an average of 10.57 ± 0.54 Bq/l. In summer, the value ranges from 0.92 ± 0.04 Bq/l to 29.70 ± 0.59 Bq/l, having an average of 9.26 ± 0.3 Bq/l. And, for monsoon, the value was found to range from 0.36 ± 0.23 Bq/l to 31.28 ± 0.72 Bq/l, having an average of 10.80 ± 0.55 Bq/l.

Figure 3.3 shows the graphical representation of the comparison of radon concentration between water samples having its sources from groundwater and surface water. Similar trends of radon concentration being higher in samples taken from groundwater sources rather than those taken from surface water sources was observed in both districts, in all of the three seasons. The result obtained is in accordance with WHO (2011), which states that radon concentration is higher in water obtained from ground water sources than those from surface water sources. The

possible reason for this result is due to the fact that radon escapes more readily from surface water rather than from groundwater.

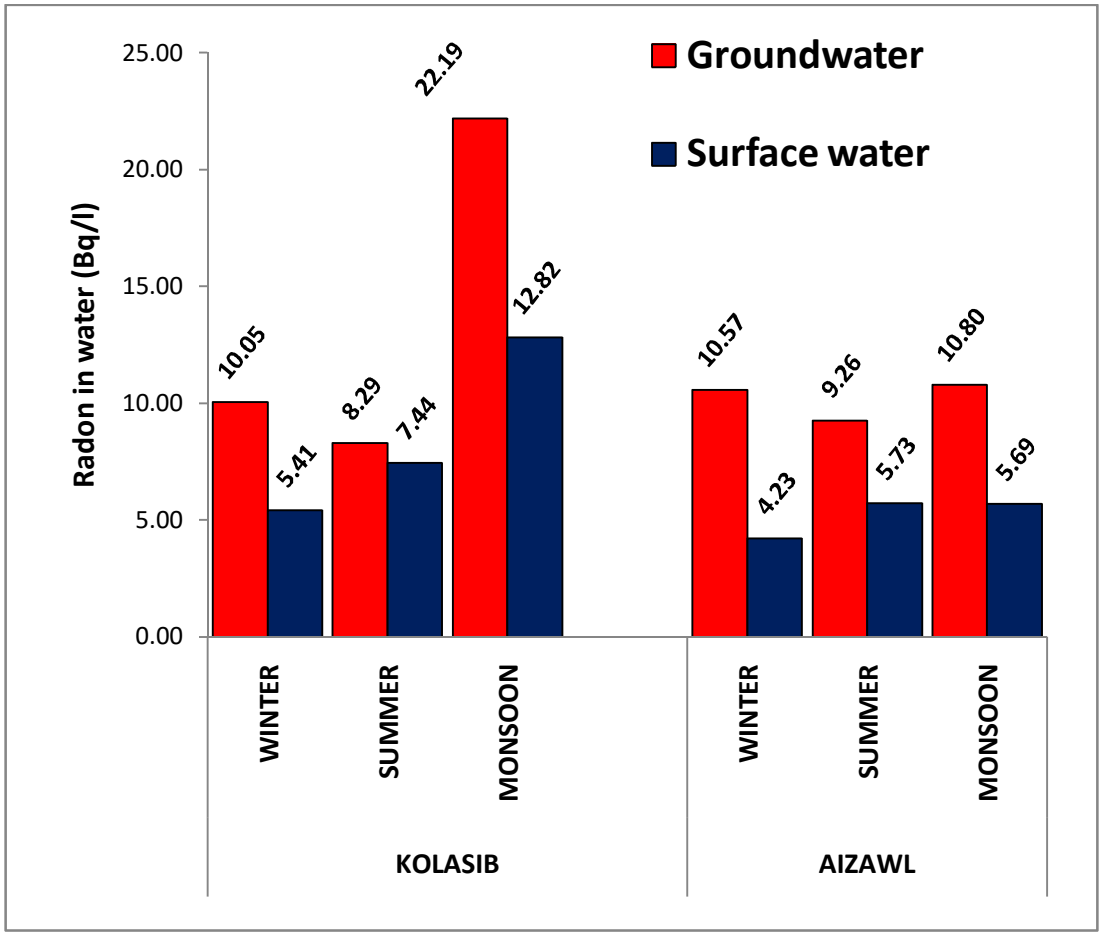

Figure 3.3: Comparison of radon concentration with respect to sample source

3.2. Annual Ingestion, Inhalation and Total Effective Dose Due to Radon Concentration in Water

The presence of radon in water not only possess a direct health hazard to human beings through the process of ingestion, it is also known to increase the concentration of radon in surrounding environment, when dissolved radon in water escapes to the surrounding air when it is being disturbed. Since ingestion and inhalation of radon contributes to the annual effective radiation dose received by human beings, it is therefore important to measure the inhalation and ingestion dose due to radon.

Using the obtained values of radon concentration in water (Table 3.1 and Table 3.2) and taking the average water consumed by a human being in a year as 720 litres (UNSCEAR, 2000), the effective ingestion dose due to radon (D_{ing}) was calculated by using equation 2.2. Also, for estimation of effective inhalation dose (D_{inh}), the average indoor occupancy time per person is taken as 7000 hour/year and with the data obtained for radon concentration; equation 2.3 is used for calculation. The total effective dose due to radon (D_{tot}) is then calculated by adding the measured values of inhalation dose and ingestion dose.

3.2.1. Results and Discussions

Table 3.3: Ingestion, inhalation & Total Dose Due to ^{222}Rn in Kolasib District

Sample Code	Dose due to ^{222}Rn (μSv/yr)								
	Winter			Summer			Monsoon		
	D_{ing}	D_{inh}	D_{tot}	D_{ing}	D_{inh}	D_{tot}	D_{ing}	D_{inh}	D_{tot}
K-1	3.05	36.65	39.71	1.95	23.42	25.37	2.49	29.83	32.31
K-2	0.27	3.19	3.46	0.37	4.42	4.79	0.38	4.61	4.99
K-3	0.79	9.45	10.24	1.94	23.29	25.23	3.12	37.44	40.56
K-4	1.17	14.06	15.23	0.41	4.94	5.35	0.53	6.36	6.89
K-5	0.57	6.86	7.44	2.54	30.45	32.99	3.22	38.63	41.85
K-6	0.48	5.79	6.27	0.25	3.05	3.30	0.09	1.11	1.20
K-7	0.37	4.45	4.82	0.35	4.18	4.53	0.05	0.65	0.70
K-8	1.60	19.21	20.81	2.41	28.95	31.37	1.43	17.17	18.60
K-9	2.12	25.49	27.62	0.99	11.83	12.81	5.64	67.66	73.30
K-10	0.45	5.43	5.89	1.71	20.48	22.18	8.11	97.36	105.47
K-11	0.34	4.12	4.46	4.16	49.95	54.11	2.61	31.29	33.90
K-12	0.50	5.99	6.49	1.55	18.64	20.19	6.55	78.58	85.13
K-13	1.78	21.40	23.18	1.87	22.47	24.34	8.75	105.04	113.80
K-14	1.93	23.15	25.08	3.64	43.70	47.34	3.97	47.60	51.57
K-15	0.38	4.50	4.88	0.29	3.42	3.71	0.55	6.60	7.16

K-16	0.25	2.97	3.22	1.39	16.64	18.02	0.34	4.07	4.41
K-17	0.23	2.81	3.04	0.26	3.16	3.42	0.34	4.07	4.41
K-18	0.27	3.27	3.55	0.21	2.55	2.76	2.18	26.21	28.39
K-19	2.01	24.13	26.15	1.03	12.41	13.44	3.35	40.18	43.53
K-20	1.37	16.42	17.79	1.74	20.88	22.62	3.71	44.52	48.23
K-21	3.30	39.61	42.91	3.67	44.02	47.68	4.39	52.68	57.07
K-22	0.54	6.50	7.04	3.99	47.87	51.85	7.90	94.79	102.69
K-23	1.05	12.61	13.66	3.68	44.17	47.85	4.00	47.98	51.98
K-24	2.18	26.21	28.39	1.55	18.56	20.11	4.45	53.37	57.82
K-25	1.27	15.26	16.53	0.21	2.51	2.71	1.38	16.51	17.89
K-26	4.66	55.89	60.55	0.14	1.68	1.82	2.26	27.13	29.39
K-27	3.59	43.13	46.72	0.96	11.52	12.48	2.72	32.69	35.41

Table 3.3 shows the result for the measurement for ingestion, inhalation and total effective dose due to radon during the winter, summer and monsoon seasons for Kolasib District. For winter season, the ingestion dose ranges between 0.23 μSv/yr to 4.66 μSv/yr, with an average of 1.35 μSv/yr and SD of 1.19, while the inhalation dose ranges between 2.81 μSv/yr to 55.89 μSv/yr, with an average value of 16.24 μSv/yr and SD of 14.26, and the total effective dose ranges between 3.04 μSv/yr to 60.55 μSv/yr, with an average of 17.60 μSv/yr and SD of 15.45.

For summer season, the measured values of ingestion dose ranges between 0.14 μSv/yr to 4.16 μSv/yr, with an average of 1.60 μSv/yr and SD of 1.3, while the inhalation dose ranges between 1.68 μSv/yr to 49.95 μSv/yr, with an average value of 19.23 μSv/yr and SD of 15.59, and the total effective dose ranges between 1.82 μSv/yr to 54.11 μSv/yr, with an average of 20.83 μSv/yr and SD of 16.89.

Also, for monsoon season, the ingestion dose ranges between 0.05 μSv/yr to 8.75 μSv/yr, with an average of 3.13 μSv/yr and SD of 2.53, while the inhalation dose ranges between 0.65 μSv/yr to 105.04 μSv/yr, with an average value of 37.56 μSv/yr and SD of 30.32, and the total effective dose ranges between 0.7 μSv/yr to 113.8 μSv/yr, with an average of 40.69 μSv/yr and SD of 32.85.

Table 3.4: Ingestion, inhalation & Total Dose Due to ^{222}Rn in Aizawl District

Sample Code	Dose due to ^{222}Rn (µSv/yr)								
	Winter			Summer			Monsoon		
	D_{ing}	D_{inh}	D_{tot}	D_{ing}	D_{inh}	D_{tot}	D_{ing}	D_{inh}	D_{tot}
A-1	0.82	9.83	10.65	N.D	N.D	N.D	1.57	18.87	20.45
A-2	4.36	52.26	56.62	4.14	49.69	53.84	4.42	53.07	57.49
A-3	1.90	22.76	24.65	1.89	22.73	24.62	2.31	27.67	29.98
A-4	0.95	11.34	12.29	0.91	10.94	11.85	0.08	1.01	1.09
A-5	0.57	6.85	7.43	0.96	11.47	12.42	1.00	11.97	12.97
A-6	6.83	81.98	88.81	5.23	62.75	67.98	5.22	62.65	67.87
A-7	1.98	23.71	25.69	1.44	17.34	18.78	2.50	29.96	32.46
A-8	0.68	8.14	8.82	1.39	16.73	18.13	2.96	35.48	38.44
A-9	4.59	55.09	59.68	4.75	57.05	61.81	6.57	78.83	85.39
A-10	5.55	66.58	72.13	1.71	20.56	22.28	3.25	38.96	42.21
A-11	1.46	17.56	19.03	2.66	31.90	34.56	1.82	21.85	23.67
A-12	0.67	8.09	8.76	1.39	16.63	18.02	0.09	1.03	1.12
A-13	0.35	4.16	4.50	0.54	6.53	7.07	0.10	1.16	1.26
A-14	3.26	39.14	42.40	2.64	31.63	34.26	2.64	31.70	34.34
A-15	1.12	13.48	14.61	0.21	2.55	2.76	1.08	12.93	14.00
A-16	1.12	13.48	14.61	0.80	9.65	10.46	1.96	23.56	25.53
A-17	0.50	5.97	6.47	0.38	4.59	4.97	0.78	9.37	10.16
A-18	0.31	3.73	4.04	0.46	5.54	6.01	1.24	14.87	16.11
A-19	1.32	15.88	17.20	1.20	14.41	15.62	1.59	19.08	20.67
A-20	0.47	5.70	6.17	0.25	3.00	3.25	1.25	15.02	16.27
A-21	1.32	15.88	17.20	0.22	2.60	2.81	1.25	15.02	16.27
A-22	5.78	69.30	75.08	6.24	74.84	81.08	3.67	44.00	47.67
A-23	0.43	5.17	5.60	0.19	2.32	2.51	0.08	0.91	0.98
A-24	0.82	9.85	10.67	1.05	12.60	13.65	2.66	31.90	34.56
A-25	0.60	7.21	7.81	0.32	3.78	4.10	0.18	2.14	2.32
A-26	0.69	8.24	8.93	0.11	1.34	1.45	1.47	17.64	19.11

A-27	1.02	12.30	13.32	2.66	31.90	34.56	2.13	25.53	27.65
A-28	0.0042	0.05	0.05	0.34	4.08	4.42	0.12	1.39	1.50
A-29	0.46	5.54	6.01	0.28	3.38	3.66	0.42	5.04	5.46
A-30	0.66	7.96	8.63	2.52	30.19	32.71	0.79	9.45	10.24
A-31	0.22	2.62	2.84	0.16	1.86	2.02	0.50	6.05	6.55
A-32	0.60	7.18	7.78	3.15	37.83	40.98	0.77	9.30	10.07
A-33	0.26	3.10	3.36	2.64	31.65	34.29	0.50	5.97	6.47
A-34	1.38	16.56	17.94	1.71	20.46	22.17	1.16	13.96	15.12
A-35	1.03	12.35	13.38	1.32	15.85	17.17	1.61	19.28	20.88
A-36	1.29	15.45	16.73	0.30	3.63	3.93	1.81	21.72	23.53
A-37	0.07	0.78	0.85	0.14	1.66	1.80	0.10	1.18	1.28
A-38	0.09	1.11	1.20	0.10	1.23	1.34	0.78	9.35	10.13
A-39	0.41	4.94	5.35	0.43	5.22	5.65	1.37	16.48	17.85

Table 3.4 shows the result for the measurement for ingestion, inhalation and total effective dose due to radon during the three seasons in Aizawl District. For winter season, the ingestion dose ranges between 0.0042 μSv/yr to 6.83 μSv/yr, with an average of 1.43 μSv/yr and SD of 1.69, while the inhalation dose ranges between 0.05 μSv/yr to 81.98 μSv/yr, with an average value of 17.21 μSv/yr and SD of 20.33, and the total effective dose ranges between 0.054 μSv/yr to 88.81 μSv/yr, with an average of 18.65 μSv/yr and SD of 22.02.

For summer season, the measured ingestion dose ranges between 0.1 μSv/yr to 6.24 μSv/yr, with an average of 1.50 μSv/yr ad SD of 1.55, while the inhalation dose ranges between 1.23 μSv/yr to 74.84 μSv/yr, with an average value of 17.95 μSv/yr and SD of 18.59, and the total effective dose ranges between 1.33 μSv/yr to 81.08 μSv/yr, with an average of 19.45 μSv/yr and SD of 20.14. Also, for monsoon season, the ingestion dose ranges between 0.08 μSv/yr to 6.57 μSv/yr, with an average of 1.64 μSv/yr and SD of 1.47, while the inhalation dose ranges between 0.91 μSv/yr to 78.83 μSv/yr, with an average value of 19.62 μSv/yr and SD of 17.62, and the total effective dose ranges between 0.98 μSv/yr to 85.39 μSv/yr, with an average of 21.26 μSv/yr and SD of 19.09.

The total effective dose due to ingestion and inhalation of radon in water for all the seasons obtained for both the studied districts in this study were mostly found to be within the safe limit value of 100 µSv/yr set by WHO (2004). But three samples from Kolasib, namely Sample Code K-10, K-13 and K-22 were found to exceed the safe limit value during the monsoon season. But, taking the seasonal average of the total effective dose, they were found to be well within the safe limit value set by WHO (2004).

Figure 3.4 shows the graphical representation of seasonal variation of average values of ingestion, inhalation and total effective dose in Kolasib District. It can be seen that the measured results of average values of ingestion, inhalation and total effective dose are highest during the monsoon season, followed by summer season, while it is lowest during the winter season. Since the effective doses measured in this research work is directly proportional to the radon concentration values contained in that particular sample, so the result obtained in this work is as expected.

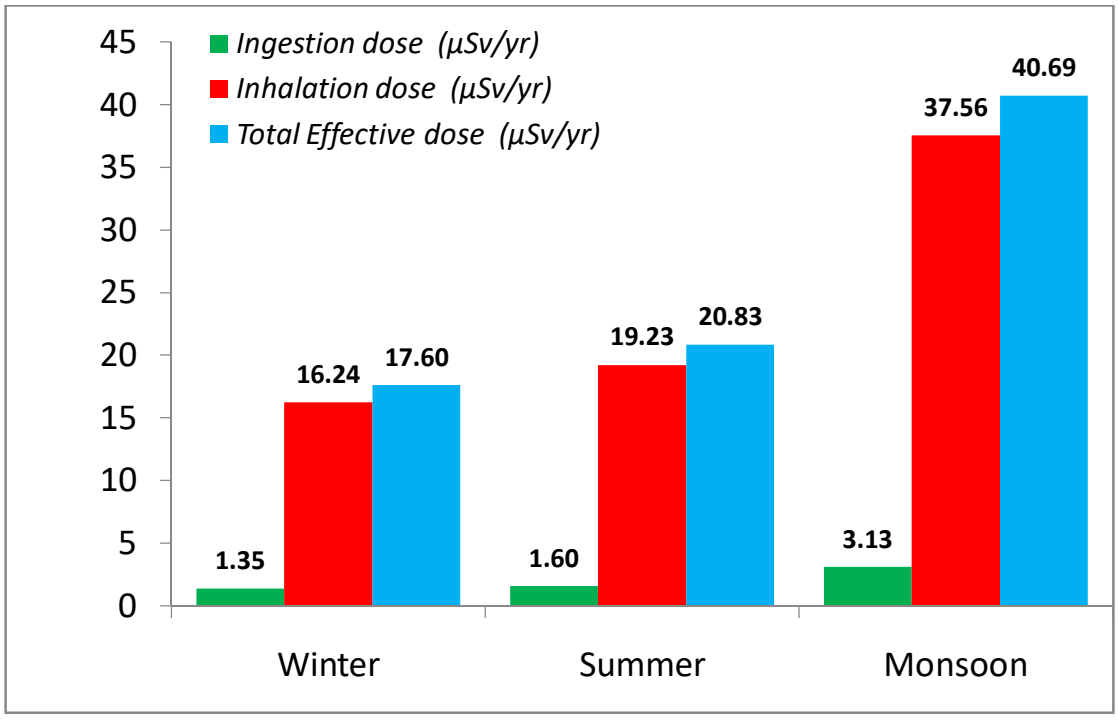

Figure 3.4: Seasonal variation of ingestion, inhalation and total effective dose in Kolasib district.

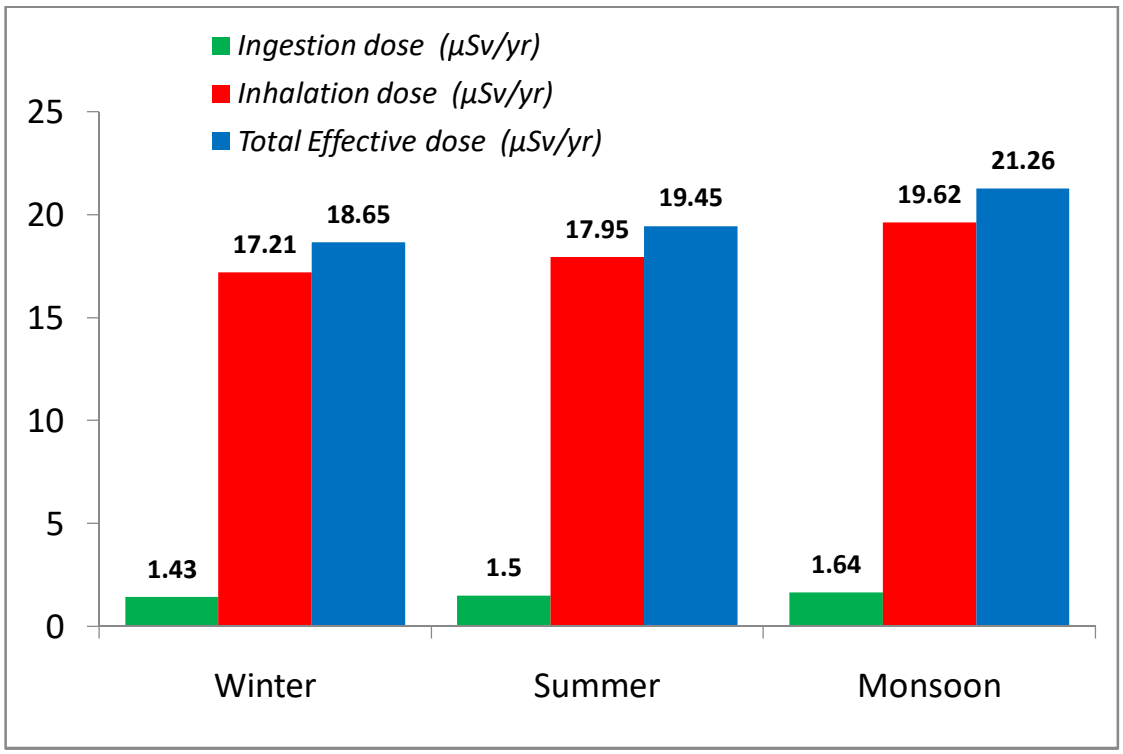

Figure 3.5: Seasonal variation of ingestion, inhalation and total effective dose in Aizawl district.

Similar trends was observed in Fig 3.5, which shows the graphical representation of seasonal variation of average values of ingestion, inhalation and total effective dose in Aizawl District. As in Kolasib District, the measured results of average values of ingestion, inhalation and total effective dose in Aizawl District are highest during the monsoon season, followed by summer season, while it is lowest during the winter season.

3.3. Determination of Uranium Concentration in Water

The uranium concentration in collected water samples are measured using LED Fluorimeter LF-2a. The Fluorimeter works on the principle of measurement of green uranium fluorescence on the addition of a suitable buffer solution. Standard addition method of measurement was employed for this research work and the uranium fluorescence emitted by the samples were counted in Calibrated Fluorescence mode, i.e. a proper calibration of the instrument was done before each measurement. This is achieved by measuring a blank solution, which is simply a

mixture of buffer solution and doubled distilled water (containing zero uranium concentration), using the Fluorimeter before the start of each experiment. Water samples were collected from different sampling sites within the study area using a 60ml Tarsons plastic bottles, and filtering of the samples were done before each measurement using a filter paper to avoid any suspended particles from interfering with the fluorescence.

3.3.1. Preparation of Standard Solution, Buffer Solution and Blank Solution

ICP Uranium Standard (ICP-MS-66N-0.01X-1), manufactured by AccuStandard, Connecticut, United States of America, is used for preparing the required standard solution used in this research work. The uranium standard is basically a 100 µg/ml uranium concentration in 2-5% Nitric acid. The required uranium standard is obtained by dilution of 100 µg/ml uranium concentration standard to about 500 ppb standard using doubled distilled water in a glass beaker or flask. A precision pipette was used so that accurate required standard concentration is obtained. The freshly prepared standard solution is then put in a plastic bottle for longer storage.

The addition of buffer solution to a sample, while measuring the uranium concentration in liquid samples, not only increases the uranium fluorescence yield of the samples by orders of magnitude, it also convert all the uranium complexes (having different fluorescence yield) into a single valence state U (IV), thus emitting only one type of fluorescence. For measurements, it is recommended that 1 part of buffer solution is added to 10 parts of uranium solution / sample. The buffer solution is prepared by taking 5 grams of Sodium Pyrophosphate into a flask / plastic bottle and adding 100 ml of double distilled water to it. The flask / plastic bottle was shook until all the Sodium Pyrophosphate salts dissolves. Ortho-phosphoric Acid was then added drop by drop while monitoring the pH value of the solution, and the required buffer is obtained when a pH of 7 is reached. While measuring the uranium concentration using a Fluorimeter, a blank solution is always required to eliminate the possible effects of any fluorescing compounds present in a buffer solution. The blank solution is prepared by take 1 ml of Buffer solution and adding 10 ml of double distilled water

to it. The blank solution is essentially a sample with zero uranium concentration. Fluorescence of blank solution is always measured when calibrating the detector/instrument and also when measuring unknown uranium concentration samples. The uranium concentration in the water sample was then calculated using Equation 2.10.

3.3.2. Results and Discussions

Table 3.5: Uranium Concentration in water in Kolasib District

Sample Code	Uranium in water (μg/l)	Error (μg/l)	Sample Code	Uranium in water (μg/l)	Uranium in water (μg/l)
K-1	0.20	0.06	K-15	0.25	0.11
K-2	0.35	0.15	K-16	0.21	0.12
K-3	0.22	0.11	K-17	0.28	0.13
K-4	0.41	0.15	K-18	0.25	0.12
K-5	0.89	0.23	K-19	0.58	0.19
K-6	0.22	0.11	K-20	0.79	0.19
K-7	0.38	0.15	K-21	0.45	0.17
K-8	0.29	0.14	K-22	0.25	0.11
K-9	0.52	0.17	K-23	0.36	0.13
K-10	0.31	0.14	K-24	0.24	0.12
K-11	0.20	0.09	K-25	0.25	0.11
K-12	0.56	0.19	K-26	0.28	0.12
K-13	0.22	0..8	K-27	0.30	0.15
K-14	0.62	0.19			

Table 3.5 shows the measured values of uranium concentration in water for Kolasib district. A total of 27 samples were collected within the mentioned district and the samples were taken from water having different sources, 21 samples from surface water sources and 6 samples originating from ground water sources. All the water from these sampling sites were essentially used as a source of irrigation and

domestic consumption, so the measured uranium concentration values have a great implication on the health hazards associated with it. The measured values of uranium concentration in water in Kolasib district was found to be in the range of 0.20 ± 0.06 µg/l to 0.89 ± 0.23 µg/l, with a mean of 0.37 ± 0.14 µg/l and Standard Deviation (SD) of 0.18. The results obtained were found to be well within the safe limit values for drinking water, i.e. 30µg/l as prescribed by WHO (2011).

Table 3.6: Uranium Concentration in water in Aizawl District

Sample Code	Uranium in water (µg/l)	Error (µg/l)	Sample Code	Uranium in water (µg/l)	Error (µg/l)
A-1	0.64	0.28	A-21	0.86	0.19
A-2	0.32	0.14	A-22	0.20	0.13
A-3	0.46	0.20	A-23	0.33	0.09
A-4	0.33	0.13	A-24	0.7	0.39
A-5	0.47	0.18	A-25	0.34	0.15
A-6	0.46	0.35	A-26	0.29	0.12
A-7	0.29	0.17	A-27	0.24	0.13
A-8	0.86	0.36	A-28	3.77	0.60
A-9	1.78	0.44	A-29	2.28	0.46
A-10	0.27	0.06	A-30	0.91	0.26
A-11	0.78	0.22	A-31	0.54	0.25
A-12	0.51	0.17	A-32	0.62	0.25
A-13	0.25	0.17	A-33	1.2	0.56
A-14	0.45	0.18	A-34	0.56	0.24
A-15	0.95	0.32	A-35	0.24	0.17
A-16	0.67	0.26	A-36	0.33	0.13
A-17	0.35	0.18	A-37	0.23	0.19
A-18	0.38	0.20	A-38	0.38	0.24
A-19	0.8	0.09	A-39	0.94	0.32
A-20	1.74	0.56			

Table 3.6 shows the measured values of uranium concentration in water for Aizawl district. In Aizawl, a total of 39 samples, 16 samples from ground water sources and 23 samples from surface water sources were collected and like Kolasib, all the samples were used as a source of drinking and domestic consumption.

The measured values of uranium concentration in water in Aizawl district was found to be in the range of 0.20 ± 0.13 μg/l to 3.77 ± 0.60 μg/l, with a mean of 0.71 ± 0.24 μg/l and SD of 0.68. Again, the results obtained in this district were found to be well within the safe limit value of 30μg/l for drinking water as prescribed by WHO (2011).

The measured uranium concentration in water samples were divided into two categories depending upon their source or origin. Those samples taken from bore wells, enclosed springs and open wells are collectively categorized as "ground water", while samples collected from springs, streams and government water supply are categorized as "surface water". In both Kolasib and Aizawl district, water samples which were taken from "surface water sources" are found to have higher average uranium concentration than those taken from "ground water sources".

The possible reason for this result probably due to the "leaching" of uranium into the water bodies as it flows through soil and rocks. There is always a possibility of higher collection of uranium in "surface water" rather than from "ground water" because water from surface sources flows through several soils and rocks before collecting itself, thereby having a higher probability of leaching of uranium into the water body.

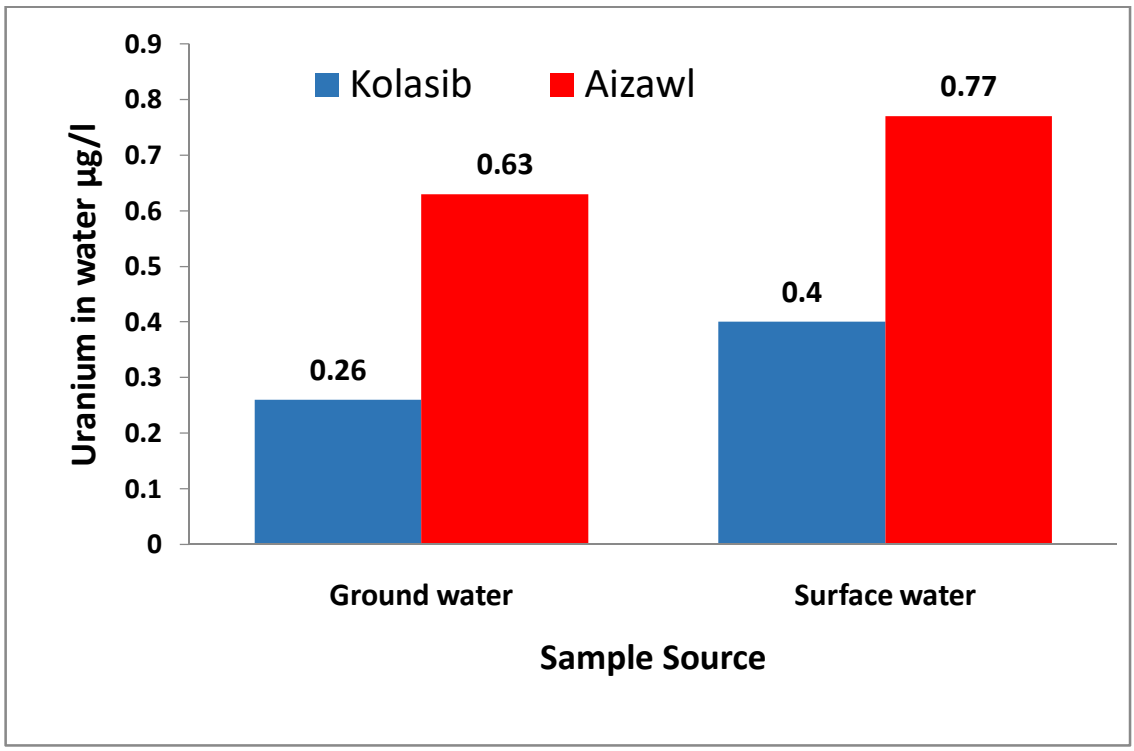

Figure 3.6: Comparison of Uranium in water with respect to water sources

3.4. Annual Effective Dose Due to Ingestion of Uranium

The annual effective ingestion dose is an important terminology while studying the health effects of uranium ingestion and is basically the radiation dose received by human beings due to ingestion of uranium. Taking 1 µg/l = 0.02528 Bq/l, the uranium activity concentration from each sample is calculated from the measured uranium concentration and equation (2.11) is then employed to calculate the annual effective dose due to ingestion of uranium in water.

3.4.1. Results and Discussions

The measured values of annual effective dose due to ingestion of uranium in Kolasib district is shown in table 3.7. The annual effective dose ranges from 0.337 µSv/yr to 1.498 µSv/yr, having an average value of 0.616 µSv/yr and SD of 0.309.

Also, Table 3.8 shows the measurement of annual effective dose due to ingestion of uranium in Aizawl district. The annual effective dose ranges from 0.337 µSv/yr to 6.347 µSv/yr, having an average value of 1.197 µSv/yr and SD of 1.146.

In all the samples measured in both district, we found that the annual effective dose due to ingestion of uranium in water were all well within the safe limit reference level for effective radiation dose, which was prescribed at 100 μSv/year by WHO (2004).

Table 3.7: Annual Effective Ingestion Dose due to ^{238}U in Kolasib District

Code	^{238}U Activity Conc. (Bq/l)	Annual effective ingestion dose (μSv /yr)	Code	^{238}U Activity Conc. (Bq/l)	Annual effective ingestion dose (μSv /yr)
K-1	0.005	0.337	K-15	0.006	0.421
K-2	0.009	0.589	K-16	0.005	0.354
K-3	0.006	0.370	K-17	0.007	0.471
K-4	0.010	0.690	K-18	0.006	0.421
K-5	0.022	1.498	K-19	0.015	0.977
K-6	0.006	0.370	K-20	0.020	1.330
K-7	0.010	0.640	K-21	0.011	0.758
K-8	0.007	0.488	K-22	0.006	0.421
K-9	0.013	0.875	K-23	0.009	0.606
K-10	0.008	0.522	K-24	0.006	0.404
K-11	0.005	0.337	K-25	0.006	0.421
K-12	0.014	0.943	K-26	0.007	0.471
K-13	0.006	0.370	K-27	0.008	0.505
K-14	0.016	1.044			

Table 3.8: Annual Effective Ingestion Dose due to ^{238}U in Aizawl District

Code	^{238}U Activity Conc. (Bq/l)	Annual effective ingestion dose (µSv /yr)	Code	^{238}U Activity Conc. (Bq/l)	Annual effective ingestion dose (µSv /yr)
A-1	0.016	1.078	A-21	0.022	1.448
A-2	0.008	0.539	A-22	0.005	0.337
A-3	0.012	0.774	A-23	0.008	0.556
A-4	0.008	0.556	A-24	0.018	1.179
A-5	0.012	0.791	A-25	0.009	0.572
A-6	0.012	0.774	A-26	0.007	0.488
A-7	0.007	0.488	A-27	0.006	0.404
A-8	0.022	1.448	A-28	0.095	6.347
A-9	0.045	2.997	A-29	0.058	3.839
A-10	0.007	0.455	A-30	0.023	1.532
A-11	0.020	1.313	A-31	0.014	0.909
A-12	0.013	0.859	A-32	0.016	1.044
A-13	0.006	0.421	A-33	0.030	2.020
A-14	0.011	0.758	A-34	0.014	0.943
A-15	0.024	1.599	A-35	0.006	0.404
A-16	0.017	1.128	A-36	0.008	0.556
A-17	0.009	0.589	A-37	0.006	0.387
A-18	0.010	0.640	A-38	0.010	0.640
A-19	0.020	1.347	A-39	0.024	1.583
A-20	0.044	2.930			

3.5. Correlation between Radon and Uranium Concentration in Water

Since radon is a noble gas and uranium is a metal, their behavior in liquid samples will vary greatly. However, radon being in the decay chain of the uranium series, the two parameters are correlated in this study.

3.5.1. Results and Discussions

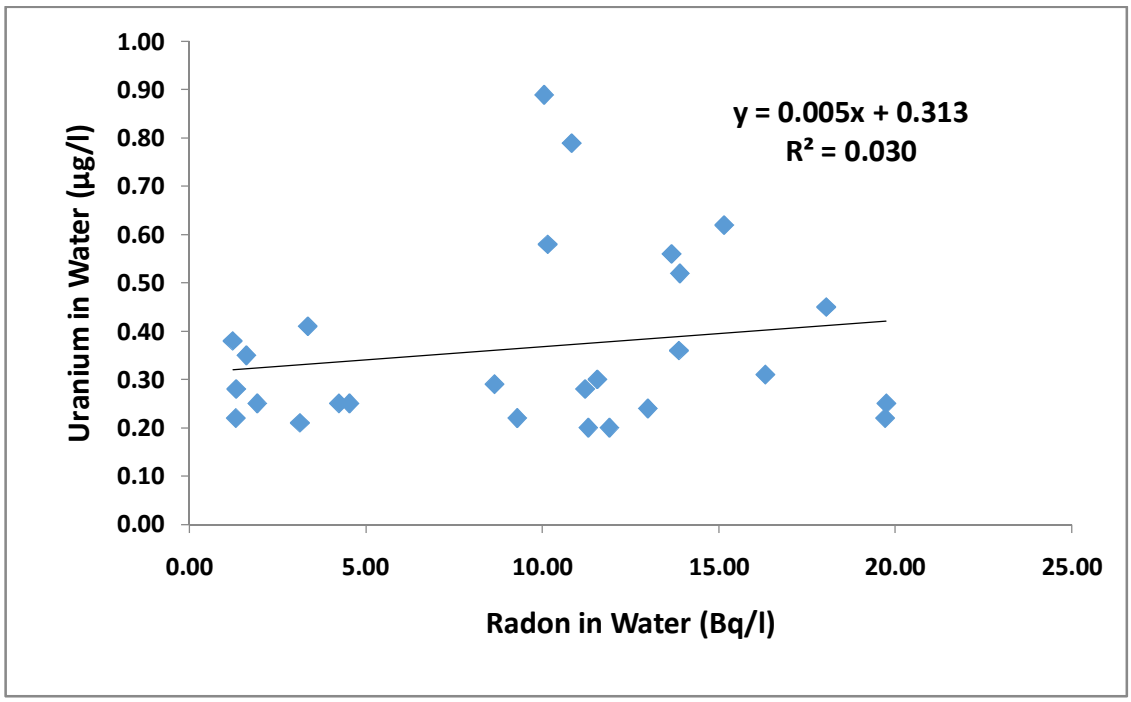

Figure 3.7: Correlation between radon and uranium in water in Kolasib district

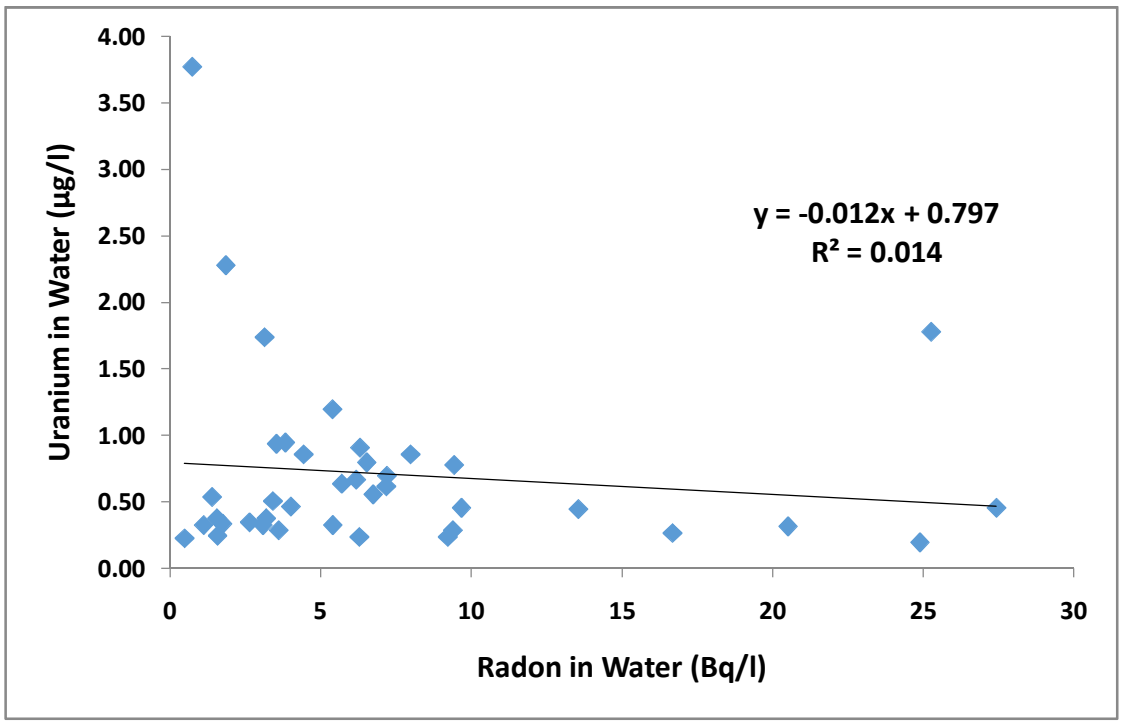

Figure 3.8: Correlation between radon and uranium in water in Aizawl district

Figure 3.7 and Figure 3.8 shows the correlation between the measured values of radon and uranium concentration in Kolasib district and Aizawl district respectively. In Kolasib district, it was found that correlation coefficient, i.e, R^2 = 0.030, while in Aizawl district, R^2 = 0.014. In both cases, the values obtained are found to be very close to zero, which shows that there is a very poor correlation between the measured values of radon and uranium concentration obtained in this study. The possible reason for this weak correlation may be due to the fact that radon being a gas, readily escapes into the surrounding air when water containing dissolved radon is being disturbed. Whereas uranium does not necessarily deposit itself to the surrounding soil, its concentration in water body rather increases as the water flows through rocks and soils.

4

Experimental Determination of Natural Radioactivity and Radon Mass Exhalation Rate in Soil and Measurement of Spot Background Gamma Radiation

The experimental determination of natural radioactivity and radon mass exhalation rate in surrounding soils of the sampling sites in Aizawl and Kolasib District of Mizoram will be presented in this chapter. Also, spot background gamma radiation taken at each time of sampling will be presented along with the soil type identification and grain size determination of the soil samples taken for study. The detailed result as well as the critical discussion of the result will also be presented. The seasonal variation of radon mass exhalation rate and spot background gamma radiation will be shown and the obtained results in this study will be compared with the global average values whenever possible.

4.1. Determination of Natural Radioactivity in Soil

Radiation arising from naturally occurring radionuclide material is the main source of irradiation to the human body (UNSCEAR, 1993). Since terrestrial radiations originate mainly from the upper 30 cm of soil layer of the earth's crust (Chikasawa *et al,* 2001), soil is considered to be the main contributor of natural radioactivity. Hence, measurement of activity concentration of different radionuclide in soil is important in this regard.

In the present work, estimation of natural radioactivity is carried out using the process of gamma spectrometry, by employing a 5"x4" Sodium Iodide (NaI) detector, doped with thallium (Tl). Using this gamma spectrometer, the radioactivity concentration of ^{238}U, ^{232}Th and ^{40}K was determined from the soil samples collected at the chosen sampling sites within the study area of Aizawl and Kolasib district of Mizoram. A personal computer based 1K Multichannel analyzer GSPEC-SA, coupled with the detector is used for acquisition and analysis of the spectrum obtained in this research. The Spectrum Acquisition & Analysis Software of the GSPEC-SA has an

in-built algorithm which subtracts the unwanted background radiation, thus providing accurate counts for each measurement.

To establish the detection efficiency of the detector as a function of the energy of radiation, the instrument was first calibrated using IAEA standard source of ^{238}U, ^{232}Th and ^{40}K and the efficiency of the instrument was obtained by using equation 2.7. Also, to establish a relationship between the channel numbers of the analyzer and the known energy of the photons, energy calibration was performed before the start of each experiment using standard sources of ^{60}Co and ^{137}Cs. After performing the necessary efficiency and energy calibration, the activity concentration for the collected soil sample was measured and then calculated using equation 2.8. The detailed method of efficiency and energy calibration as well as activity concentration measurement performed is shown in Appendix-I, Appendix-II and Appendix-III respectively.

4.1.1. Results and Discussions

Table 4.1 shows the measured values of the activity concentration for ^{238}U, ^{232}Th and ^{40}K radionuclide in Kolasib district. The activity concentration of ^{238}U ranges from 12.90 ± 2.85 Bq/kg to 43.39 ± 2.06 Bq/kg, with an average value of 26.84 ± 2.30 Bq/kg and standard deviation (SD) of 8. For ^{232}Th nuclide, the activity concentration ranges from 34.39 ± 7.61 Bq/kg to 115.67 ± 5.49 Bq/kg, with an average value of 71.55 ± 6.14 Bq/kg and SD of 21.34. And for ^{40}K radionuclide, the activity concentration ranges from 372.99 ± 5.01 Bq/kg to 978.48 ± 3.83 Bq/kg, with an average value of 627.27 ± 4.54 Bq/kg and SD of 180.64.

Table 4.2 shows the measured activity concentration for ^{238}U, ^{232}Th and ^{40}K radionuclide in Aizawl district. Activity concentration of ^{238}U ranges from 18.10 ± 3.32 Bq/kg to 60.40 ± 2.03 Bq/kg, with an average value of 34.26 ± 2.78 Bq/kg and SD of 10.31. For ^{232}Th nuclide, it ranges from 53.45 ± 10.90 Bq/kg to 161.03 ± .41 Bq/kg, with an average value of 87.49 ± 7.31 Bq/kg and SD of 26.66. And for ^{40}K radionuclide, the activity concentration ranges from 279.58 ± 7.09 Bq/kg to 964.62 ± 3.56 Bq/kg, with an average value of 764.20 ± 5.00 Bq/kg and SD of 159.55.

Table 4.1: Activity concentration of ^{238}U, ^{232}Th and ^{40}K in Kolasib District

Sample Code	Activity of Soil (Bq/kg)					
	U-238	**Error**	**Th-232**	**Error**	**K-40**	**Error**
K-1	43.39	2.06	115.67	5.49	870.56	4.22
K-2	24.58	1.99	65.53	5.31	502.79	4.22
K-3	20.28	2.49	54.05	6.63	441.21	4.86
K-4	20.73	2.60	55.26	6.93	441.02	5.34
K-5	30.97	2.60	82.55	6.94	505.61	5.34
K-6	28.00	2.62	74.66	6.98	917.91	4.25
K-7	24.83	2.66	66.18	7.09	623.86	4.85
K-8	25.83	2.30	68.86	6.12	758.63	4.12
K-9	25.83	2.30	68.86	6.12	758.63	4.12
K-10	23.28	2.36	62.08	6.29	539.34	4.58
K-11	31.13	2.20	83.00	5.87	423.20	5.39
K-12	25.27	2.15	67.38	5.74	591.29	3.94
K-13	36.60	1.86	97.58	4.97	764.80	3.72
K-14	32.92	2.24	87.77	5.96	478.11	5.04
K-15	12.90	2.85	34.39	7.61	375.75	4.46
K-16	15.28	3.12	40.72	8.33	519.92	5.55
K-17	20.10	1.56	53.59	4.16	732.49	3.97
K-18	15.28	3.36	40.74	8.97	660.57	4.54
K-19	32.54	1.81	86.76	4.82	829.70	3.50
K-20	33.83	1.82	90.20	4.86	566.87	4.02
K-21	38.23	2.35	101.91	6.27	870.94	4.52
K-22	26.65	1.72	71.04	4.60	978.48	3.83
K-23	17.87	3.18	47.64	8.49	594.60	5.75
K-24	33.69	1.89	89.81	5.04	581.17	4.16
K-25	21.82	2.26	58.18	6.03	372.99	5.01
K-26	41.49	2.08	110.62	5.55	398.36	5.62
K-27	21.28	1.70	56.73	4.54	837.61	3.57

Table 4.2: Activity concentration of ^{238}U, ^{232}Th and ^{40}K in Aizawl District

Sample Code	Activity of Soil (Bq/kg)					
	U-238	**Error**	**Th-232**	**Error**	**K-40**	**Error**
A-1	37.07	3.95	114.54	10.54	872.32	6.83
A-2	21.74	2.71	57.95	7.23	909.18	3.93
A-3	43.31	2.52	55.31	6.71	573.74	3.02
A-4	32.38	2.03	86.32	5.41	894.45	3.53

A-5	32.38	3.37	86.32	5.41	894.45	3.53
A-6	29.29	2.28	78.08	6.09	914.35	4.07
A-7	33.59	4.49	88.11	11.96	611.96	3.92
A-8	39.05	2.19	90.19	5.83	942.00	6.34
A-9	39.05	3.16	81.84	8.44	942.00	6.18
A-10	50.81	1.82	135.46	4.86	919.07	3.61
A-11	18.10	3.32	102.46	8.86	872.25	5.05
A-12	18.10	3.51	92.10	9.36	872.25	4.98
A-13	20.26	2.18	54.01	5.80	588.68	4.00
A-14	37.87	2.69	61.35	7.16	782.62	3.87
A-15	38.23	3.49	74.16	9.29	827.86	7.21
A-16	58.69	3.11	122.18	8.29	536.94	6.35
A-17	37.84	1.96	100.88	5.24	964.62	3.56
A-18	38.30	2.09	102.11	5.56	835.29	3.88
A-19	27.30	2.17	54.26	5.79	639.82	6.45
A-20	27.30	3.04	107.43	8.11	639.82	4.65
A-21	35.02	2.07	93.35	5.52	690.84	4.64
A-22	40.09	1.59	106.89	4.25	809.82	3.32
A-23	23.23	4.09	53.45	10.90	770.16	3.71
A-24	38.23	3.90	60.08	10.39	803.22	4.80
A-25	38.23	2.38	100.96	6.34	803.22	6.62
A-26	28.43	1.73	75.79	4.61	642.74	3.29
A-27	31.06	1.78	82.80	4.74	911.81	3.28
A-28	21.20	1.67	56.53	4.46	479.76	3.71
A-29	60.40	2.03	161.03	5.41	847.52	4.04
A-30	47.95	3.65	84.43	9.73	820.14	5.72
A-31	43.43	2.03	115.79	5.40	279.58	7.09
A-32	35.90	2.31	81.45	6.16	746.93	6.20
A-33	36.69	4.21	66.05	11.21	764.61	6.70
A-34	20.13	2.86	53.68	7.63	792.48	5.04
A-35	41.03	3.28	63.81	8.73	794.68	5.16
A-36	40.99	2.83	91.01	7.54	895.12	4.98
A-37	20.52	2.77	118.25	7.38	508.57	7.65
A-38	28.05	3.43	60.63	9.14	503.73	7.08
A-39	24.96	3.68	141.22	9.82	905.26	7.01

It had been found that in all of the samples measured in this study, ^{40}K was the most abundant amongst the natural radionuclide which was taken into account; this

was followed by ^{232}Th and ^{238}U respectively. The result obtained in this report shows that the overall average activity concentrations of ^{238}U nuclides were found to be well within the worldwide average value of 35 Bq/kg (UNSCEAR, 2000). But, it was found that the average activity concentrations of ^{232}Th and ^{40}K nuclides were found to be higher than the corresponding worldwide average values of 30 Bq/kg and 400 Bq/kg respectively (UNSCEAR, 2000). Although the average activity concentrations of ^{232}Th and ^{40}K were high as compared to worldwide average, they were found to be well within the critical value set by the International Atomic Energy Agency (IAEA, 2004), the critical values being 10,000 Bq/kg for ^{40}K and 1000 Bq/kg for both ^{238}U and ^{232}Th radionuclide. Also, activity concentrations for ^{238}U, ^{232}Th and ^{40}K obtained in this study were quite comparable to those reported by Chhangte (2018) and Hmingchungnunga (2020).

4.2. Estimation of Radium Equivalent Activity

The activity concentration obtained from the natural radioactivity estimation of soil contains a mixture of activity concentration of different types of radionuclide and therefore, are not uniform. To represent the activity levels of ^{226}Ra (which is similar to the activity level of ^{238}U since equilibrium is established), ^{232}Th and ^{40}K into a single quantity with respect to exposure to radiation or dose, radium equivalent activity (Ra_{eq}) was calculated using equation 2.9.

4.2.1. Results and Discussions

Figure 4.1 and 4.2 shows the measured radium equivalent activity concentration in soil samples collected from Kolasib and Aizawl district respectively. In Kolasib district, the radium equivalent activity concentration ranges from 88.38 Bq/kg to 269.73 Bq/kg, with an average value of 173.06 Bq/kg and standard deviation (SD) of 43.62. While in Aizawl district, the radium equivalent activity concentration ranges from 135.62 Bq/kg to 350 Bq/kg, with an average value of 212.87 Bq/kg and SD of 46.45. The measured values of radium equivalent activity in all the samples were found to be lower than the critical value of 370 Bq/kg prescribed by the Organization for Economic Co-operation and Development (OECD, 1979).

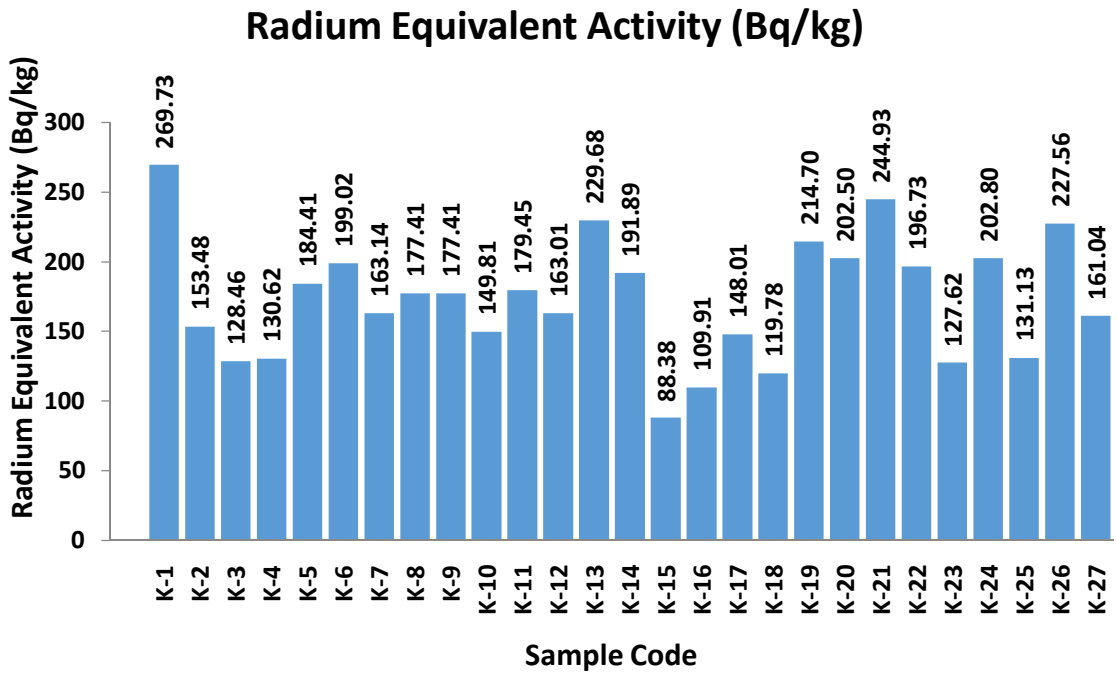

Figure 4.1: Radium Equivalent Activity of soil in Kolasib District

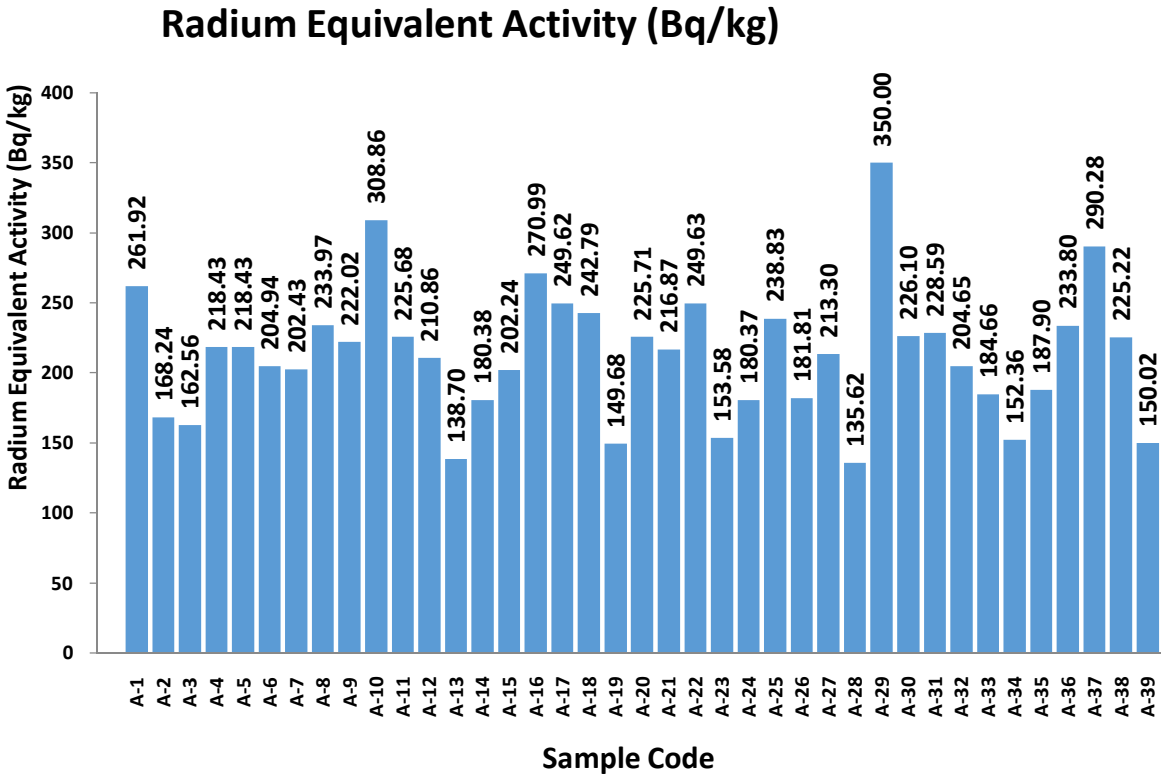

Figure 4.2: Radium Equivalent Activity of soil in Aizawl District

4.3. Measurement of radon mass exhalation rate

The radon mass exhalation rate is defined as the rate at which radon exhalate or escapes from a sample of unit mass. It is expressed in mBq/kg/hr.

In this research, the radon mass exhalation rate is calculated using Smart RnDuo monitor. The detection of radon using this instrument is basically free from humidity interference; hence, the instrument allows accurate measurement of radon exhalation. Soil samples of about 350 – 500g were first collected inside the "radon mass exhalation chamber" provided with the RnDuo system, the scintillation detector was then attached on the upper side of the chamber, thus acting as a lid and hence providing a closed loop measurement system. The build-up of radon concentration inside the chamber was measured by following the measurement protocol given below:

1. For the measurement of radon mass exhalation rate, we use the "Radon Mass Accumulation Chamber" provided with the RnDuo measurement system.
2. The scintillation cell, if previously used for another measurement, was replaced with a background free scintillation cell (which was stored for at least 3 hours after radon flushing).
3. The RnDuo was put in the "ON" state. The mode of measurement was then put in Rn222 mode. The instrument is then configured by adjusting the parameters as shown below:
   Modify cycle = 1 hour
   Pump Settings = OFF
4. The RnDuo and the mass accumulation chamber were connected as shown in Figure 2.4 for diffusion mode.
5. The amount of sample used for measurement was taken up to the full level (below neck) of the accumulation chamber.
6. The monitoring was then started after enclosing the sample and connecting the setup as shown in Figure 2.4, and measurement was done for a period of 12-18 hours to obtain the radon concentration build up data. The measurement time was adjusted so that a proper growth and decay of the radon concentration curve is achieved.

At the end of the measurements, the build-up data of radon with elapsed time was least square fitted to Equation 2.4 using Origin software and from the slope of the curve obtained, the radon exhalation rate was calculated.

4.3.1. Results and Discussions

Table 4.3: Radon Mass Exhalation Rate (J_m) in Kolasib District

Sample Code	Radon Mass Exhalation Rate, Jm (mBq/kg/hr)					
	Winter		Summer		Monsoon	
	Jm	Error	Jm	Error	Jm	Error
K-1	41.24	6.99	18.69	2.36	24.51	3.68
K-2	26.09	1.82	19.24	8.41	41.53	1.63
K-3	37.86	1.65	33.85	3.37	21.22	3.46
K-4	3.81	3.10	21	3.06	17.96	2.09
K-5	34.94	1.21	28.17	1.68	20.51	1.93
K-6	49.56	1.75	27.27	2.17	22.45	5.90
K-7	15.87	7.34	26.5	3.79	43.2	5.01
K-8	23.67	3.02	32.71	3.00	24.81	1.70
K-9	23.67	3.02	26.37	2.42	24.81	1.70
K-10	9.16	0.86	18.51	4.11	16.25	5.66
K-11	35.76	1.92	50.47	7.29	19.31	7.39
K-12	35.18	2.20	34.06	6.14	21.88	2.24
K-13	48.24	3.01	26.6	4.80	26.2	2.88
K-14	45.91	1.58	37.49	3.36	22.43	6.74
K-15	24.27	1.10	25.52	4.37	27.6	1.61
K-16	15.37	1.04	32.62	3.66	27.36	2.17
K-17	0.99	5.33	40.77	4.14	31.77	1.78
K-18	1.93	1.53	15.04	3.40	43.77	2.18
K-19	51.97	2.51	24.39	2.96	63.06	3.90
K-20	36.78	1.37	22.77	3.00	20.49	2.44
K-21	36.93	2.88	46.9	8.11	50.74	4.89
K-22	37.89	2.51	21.21	3.94	12.35	2.24
K-23	31.32	1.87	43.77	8.92	22.45	2.17
K-24	24.61	1.56	21.8	6.83	16.92	2.51
K-25	5.87	4.66	35	2.45	21.48	3.78
K-26	17.63	5.09	15.84	2.96	4.51	2.48
K-27	0.92	0.97	29.55	2.68	15.43	1.69

The annual value of radon mass exhalation rate obtained in this study ranges from 12.66 ± 3.51 mBq/kg/hr to 46.47 ± 3.12 mBq/kg/hr, with an average value of 27.14 ± 3.42 mBq/kg/hr and SD of 8.28 in Kolasib district. While in Aizawl district, the annual value of radon mass exhalation rate was found to range from 12.09 ± 1.71 mBq/kg/hr to 48.30 ± 2.94 mBq/kg/hr, with an average value of 30.70 ± 3.36 mBq/kg/hr and SD of 11.27.

Table 4.3 shows the measured values of radon mass exhalation rate in Kolasib district of Mizoram. The measured values of radon mass exhalation rate ranges from 0.92 ± 0.97 mBq/kg/hr to 51.97 ± 2.51 mBq/kg/hr, with an average value of 26.97 ± 2.89 mBq/kg/hr and SD of 15.77 during the winter season. In summer, the radon mass exhalation rate ranges from 15.04 ± 3.40 mBq/kg/hr to 50.47 ± 7.29 mBq/kg/hr, with an average of 28.75 ± 4.20 mBq/kg/hr and SD of 9.35. While in monsoon, the measured value ranges from 4.51 ± 2.84 mBq/kg/hr to 63.06 ± 3.90 mBq/kg/hr, with an average of 26.11 ± 3.18 mBq/kg/hr and SD of 12.54.

Table 4.4: Radon Mass Exhalation Rate (J_m) in Aizawl District

Sample Code	Radon Mass Exhalation Rate (mBq/kg/hr)					
	Winter		Summer		Monsoon	
	Jm	Error	Jm	Error	Jm	Error
A-1	37.72	3.66	47.94	3.19	29.77	1.93
A-2	46.87	5.24	24.7	27.09	45.68	2.42
A-3	26.43	2.30	16	1.79	29.26	2.94
A-4	18.06	5.27	48.69	2.99	74.94	2.52
A-5	18.06	5.27	48.69	2.99	74.94	2.52
A-6	14.28	10.03	13.57	2.04	32.19	1.80
A-7	42	2.86	19.02	2.17	37.66	2.14
A-8	53.48	5.17	44	1.21	41.06	2.44
A-9	53.48	5.17	44	1.21	41.06	2.44
A-10	36.71	6.82	20.71	1.69	25.9	1.52
A-11	40.05	3.35	54.89	2.05	49.97	3.42
A-12	40.05	3.35	54.89	2.05	49.97	3.42
A-13	19.11	2.22	17.56	1.92	21.99	2.40
A-14	43.18	4.63	14.68	2.21	13.29	2.54
A-15	44.78	4.75	18.28	1.95	16.92	2.12
A-16	28.49	6.26	43.57	2.16	33.01	1.55

A-17	58.11	9.01	58.65	2.11	23.4	1.60
A-18	40.14	4.85	19.03	3.00	28.89	1.93
A-19	15.68	2.67	26.79	1.81	18.71	1.50
A-20	15.68	2.67	26.79	1.81	18.71	1.50
A-21	22.36	11.82	21.02	1.39	43.93	1.94
A-22	31.49	5.06	38.02	2.70	36.92	4.31
A-23	22.05	3.18	7.42	2.19	11.26	1.39
A-24	33.25	4.01	57.14	2.99	36.7	2.39
A-25	33.25	4.01	57.14	2.99	36.7	2.39
A-26	22.35	3.66	41.78	1.36	21.09	2.88
A-27	14.92	4.25	23.33	1.84	34.3	2.46
A-28	8.28	10.02	17.37	4.86	21.98	1.52
A-29	18.94	1.50	32.12	2.33	21.04	1.46
A-30	55.4	5.17	18.26	1.93	16.79	2.87
A-31	16.9	6.11	11.46	1.44	13.04	2.82
A-32	26.35	1.81	11.28	2.53	8.86	2.01
A-33	40.97	5.75	24.35	3.10	34.81	4.11
A-34	29.16	7.08	11.59	2.25	32.3	1.52
A-35	44.31	3.53	58.66	3.76	41.19	1.88
A-36	28.64	4.58	29.8	1.49	11.01	2.68
A-37	4.72	3.66	45.65	4.03	29.47	2.77
A-38	34.99	1.77	37.42	2.42	10.21	1.56
A-39	15.5	1.41	11.6	2.49	9.18	1.23

Table 4.4 shows the measured values of radon mass exhalation rate in Aizawl district of Mizoram. The measured values of radon mass exhalation rate ranges from 4.72 ± 3.66 mBq/kg/hr to 58.11 ± 9.01 mBq/kg/hr, with an average value of 30.67 ± 4.84 mBq/kg/hr and SD of 13.80 during the winter season. In summer, the radon mass exhalation rate ranges from 7.42 ± 2.19 mBq/kg/hr to 58.66 ± 3.76 mBq/kg/hr, with an average of 31.23 ± 2.96 mBq/kg/hr and SD of 16.31. While in monsoon, the measured value ranges from 8.86 ± 2.01 mBq/kg/hr to 74.94 ± 2.52 mBq/kg/hr, with an average of 30.21 ± 2.28 mBq/kg/hr and SD of 15.73.

Figure 4.3 shows the graphical representation of the seasonal variation of the measured values of radon mass exhalation rate in soil samples collected from both Aizawl and Kolasib District. In both the districts, it was found that the radon mass

exhalation rate highest during the summer season, followed by winter season, and the lowest rate of radon mass exhalation was observed during the monsoon season.

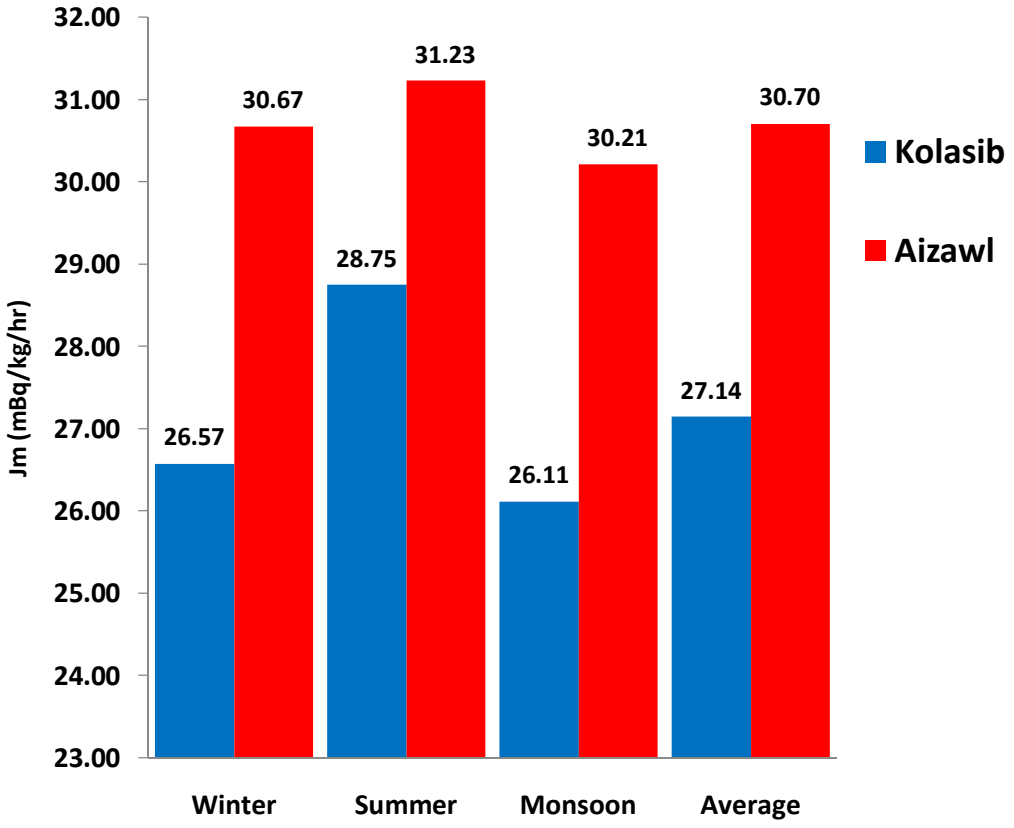

Fig. 4.3: Seasonal Variation of ^{222}Rn Mass Exhalation Rate

The possible reason for this result of seasonal variation of radon mass exhalation rate from soil in this study is mainly due to the soil moisture content. Radon mass exhalation rate is known to be increased by the presence of moisture in soil, but eventually decreases if the moisture content is increased to a much larger value (Owczarski *et al*, 1990; Stranden *et al*, 1984). In this study, the average value of radon mass exhalation rate was found to be highest during the summer season, when there is small amount of moisture in soil due to light rainfall observed during this time. In monsoon, heavy rainfall was observed, which results in increase of soil moisture and hence the decrease of radon mass exhalation rate compared to other seasons. While in winter, since no rainfall is observed, the soil was much drier and the

mass exhalation rate therefore, was found to be lower than those observed during the summer season.

4.4. Estimation of emanation factor/coefficient

Before exhalation of radon from soil surfaces or volume, a fraction of radon atoms escape the solid phase in which they are formed into the surrounding pore spaces through the process of emanation. Thus, emanation factor (f) is a dimensionless parameter which characterizes the behaviour of radon in soils or rocks and is calculated by employing the measured activity concentration of radium/uranium and the radon mass exhalation rate obtained previously, through Equation 2.6. The detailed calculated data for Emanation factor in Kolasib and Aizawl district is shown in Appendix IV and Appendix V respectively.

4.4.1. Results and Discussions

Figure 4.4 shows the graphical representation of the measured emanation factor in Kolasib District. The emanation factor ranges from 0.04 to 0.27, with an average value of 0.15 and SD of 0.05. Also, Figure 4.5 shows the graphical representation of the measured emanation factor or coefficient in Aizawl District, where the emanation factor ranges from 0.04 to 0.36, with an average value of 0.13 and SD of 0.07. The radon emanation coefficient is usually found to be in the range of about 0.05 to 0.70 in typical rocks and soils (Nazaroff *et al.* 1988). In this research, the results obtained were quite comparable to the given mentioned ranges.

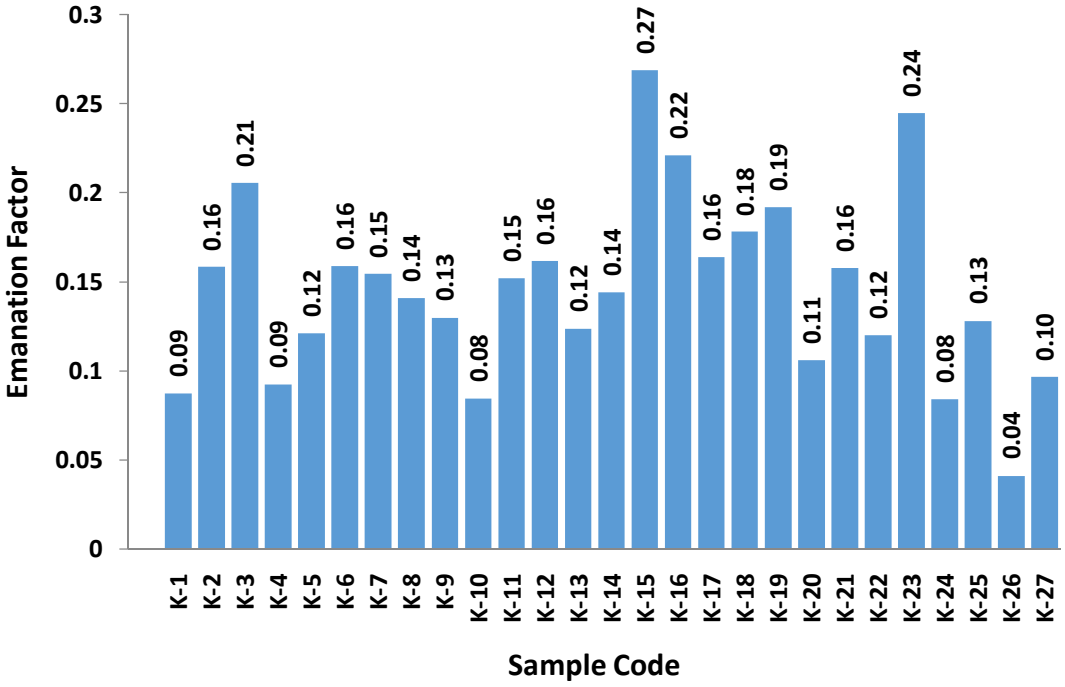

Fig. 4.4: Emanation Factor in Kolasib District

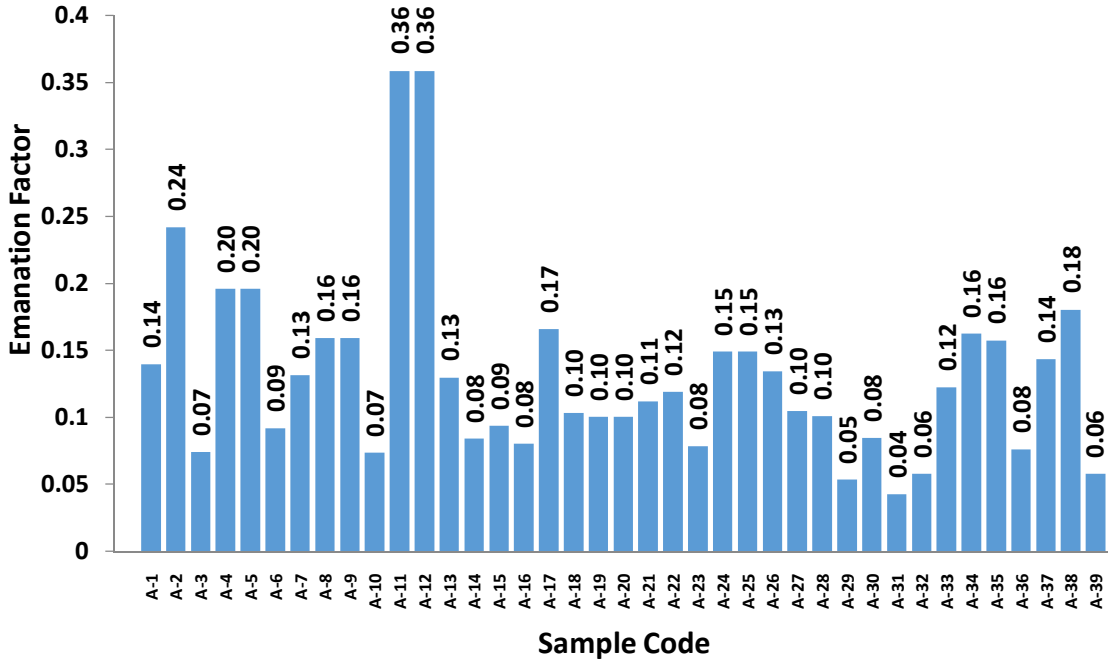

Fig. 4.5: Emanation Factor in Aizawl District

4.5. Soil type identification and Grain size determination

Soil type identification and grain size determination of collected soil samples was performed using a mechanical sieve shaker, since the ability of soil to retain moisture (which in turn affects the radon mass exhalation rate), as well as the radioactivity content is greatly determined by the soil type and grain size distribution of the soil sample. Five different set of sieve, having different mesh number, was arranged in an order such that the coarsest sieve is at the top while the finer ones are below. Three main classifications of soils, namely, sand, silt and clay was used in accordance with the Udden-Wentworth size term (Wentworth, 1922). These three classifications were further divided into 12 sub-classes while performing a triangular plot using the United States Department of Agriculture (USDA) triangle.

4.5.1. Results and Discussions

Table 4.5: Grain size distribution in soil samples collected from Kolasib District.

Sample Code	Soil Composition (%)			Sample Code	Soil Composition (%)		
	Sand	Silt	Clay		Sand	Silt	Clay
K-1	99.21	0.23	0.01	K-15	94.63	4.26	0.31
K-2	99.65	0.27	0.02	K-16	92.18	6.52	0.73
K-3	93.02	5.04	1.08	K-17	94.02	5.00	0.19
K-4	91.66	6.48	1.02	K-18	91.27	7.76	0.33
K-5	93.67	5.19	0.42	K-19	95.48	3.17	0.44
K-6	96.65	2.65	0.14	K-20	97.91	1.44	0.05
K-7	88.84	7.71	3.06	K-21	95.36	3.34	0.95
K-8	98.78	0.77	0.13	K-22	98.88	0.62	0.01
K-9	98.78	0.77	0.13	K-23	94.94	4.41	0.23
K-10	90.73	8.39	0.22	K-24	93.19	6.40	0.27
K-11	95.50	3.98	0.14	K-25	91.61	6.79	0.88
K-12	98.56	0.54	0.02	K-26	95.46	3.87	0.07
K-13	96.01	3.32	0.12	K-27	99.51	0.07	0.01
K-14	95.91	3.83	0.03				

Table 4.6: Grain size distribution in soil samples collected from Aizawl District.

Sample Code	Soil Composition (%)			Sample Code	Soil Composition (%)		
	Sand	Silt	Clay		Sand	Silt	Clay
A-1	94.87	4.26	0.11	A-21	98.29	0.41	0.07
A-2	99.38	0.08	0.02	A-22	95.18	4.26	0.05
A-3	96.10	3.39	0.01	A-23	91.48	8.01	0.05
A-4	97.80	2.09	0.03	A-24	95.45	3.89	0.15
A-5	97.80	2.09	0.03	A-25	95.45	3.89	0.15
A-6	93.64	4.93	0.27	A-26	94.46	4.83	0.07
A-7	95.84	3.74	0.14	A-27	92.64	7.08	0.12
A-8	96.53	2.91	0.02	A-28	94.64	4.79	0.46
A-9	96.53	2.91	0.02	A-29	97.12	2.05	0.13
A-10	94.79	4.34	0.03	A-30	94.61	4.48	0.24
A-11	95.14	4.45	0.23	A-31	99.28	0.48	0.01
A-12	95.14	4.45	0.23	A-32	94.33	4.80	0.17
A-13	95.94	3.57	0.04	A-33	96.92	2.27	0.08
A-14	94.47	4.23	0.71	A-34	89.19	8.91	1.00
A-15	93.63	5.60	0.46	A-35	88.39	7.72	3.72
A-16	91.38	8.01	0.23	A-36	93.13	5.12	0.98
A-17	89.08	10.07	0.70	A-37	95.12	3.15	0.91
A-18	97.63	1.78	0.01	A-38	93.57	5.81	0.29
A-19	89.89	9.70	0.39	A-39	90.66	7.72	0.70
A-20	89.89	9.70	0.39				

Table 4.5 shows the measured values of grain size distribution for soil samples collected from Kolasib district and Table 4.6 shows the measured values of grain size distribution for soil samples collected from Aizawl district. In both the tables, it can be seen that in all the measured collected samples, a very high percentage of grain size were found to fall dominantly under “Sand”, which was followed by “Silt” and then a very small percentage of grain size falls under “Clay”. From the grain size

distribution obtained, a triangular plotting proposed by USDA (United States Department of Agriculture) was performed using "Origin" computer software to identify the soil type of the collected samples (García-Gaines et al. 2015).

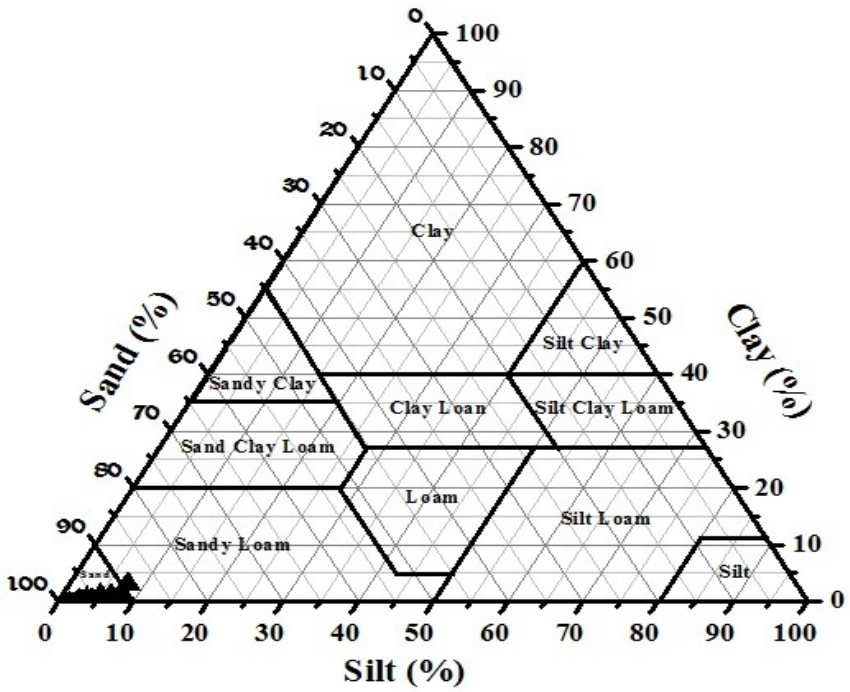

Fig 4.6: USDA Triangular Plot for Kolasib District.

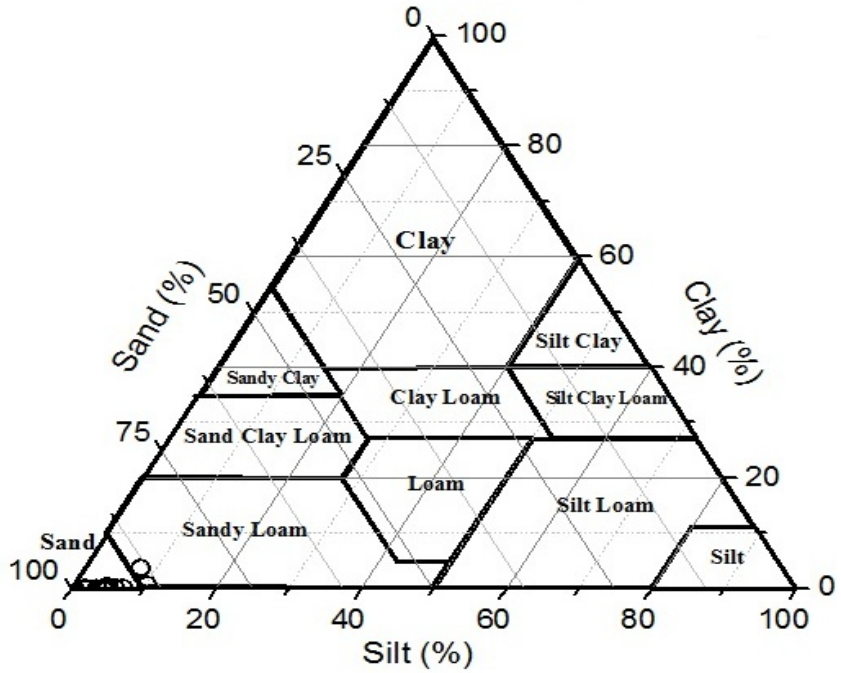

Fig 4.7: USDA Triangular Plot for Aizawl District.

Figure 4.8 and figure 4.9 shows respectively the United States Department of Agriculture (USDA) Triangular Plot for determination of soil type for Aizawl District and Kolasib District. The plot shows that the soil type of most of the samples fall under "sand", while a very few of them are "sandy loam". Since the grain size distribution and soil type of all the soil samples collected falls more or less under the same category, it cannot be used to justify the variations observed in the radioactivity content and radon mass exhalation rate in soil.

4.6. Spot Background Gamma Radiation

Background gamma radiation was taken at each sampling sites using a gamma survey meter PM 1405. The survey meter was put 1 metre above the ground to assess the gamma radiation coming from terrestrial as well as cosmic origin.

4.6.1. Results and Discussions

Table 4.7.: Background Gamma Radiation for Kolasib District.

Sample Codes	Background Gamma Level (nSv/hr)					
	Winter	Error	Summer	Error	Monsoon	Error
K-1	157	19	147	18	139	17
K-2	192	23	182	22	195	23
K-3	192	23	164	20	152	18
K-4	207	25	161	19	144	17
K-5	202	24	179	21	148	18
K-6	180	22	191	23	161	19
K-7	208	25	166	20	174	21
K-8	154	18	124	15	144	17
K-9	154	18	124	15	144	17
K-10	158	19	134	16	147	18
K-11	180	22	161	19	121	15
K-12	183	22	130	16	194	23
K-13	160	19	149	18	140	17
K-14	170	20	134	16	165	20
K-15	130	16	145	17	134	16

K-16	155	19	162	19	127	15
K-17	126	15	155	19	141	17
K-18	215	26	147	18	188	23
K-19	185	22	152	18	217	26
K-20	185	22	125	15	193	23
K-21	190	23	118	14	143	17
K-22	190	23	143	17	195	23
K-23	200	24	155	19	162	19
K-24	157	19	137	16	135	16
K-25	180	22	141	17	155	19
K-26	160	19	125	15	130	16
K-27	170	20	138	17	135	16

Table 4.8.: Background Gamma Radiation for Aizawl District.

Sample Codes	Background Gamma Level (nSv/hr)					
	Winter	**Error**	**Summer**	**Error**	**Monsoon**	**Error**
A-1	166	20	155	19	160	19
A-2	153	18	198	24	177	21
A-3	190	23	166	20	171	21
A-4	182	22	168	20	197	24
A-5	182	22	168	20	197	24
A-6	148	18	135	16	158	19
A-7	211	25	177	21	162	19
A-8	164	20	163	20	151	18
A-9	164	20	163	20	151	18
A-10	187	22	129	15	166	20
A-11	171	21	162	19	183	22
A-12	171	21	162	19	183	22
A-13	156	19	162	19	168	20
A-14	189	23	138	17	175	21
A-15	135	16	143	17	140	17
A-16	156	19	165	20	167	20
A-17	163	20	199	24	192	23
A-18	136	16	155	19	152	18

A-19	168	20	154	18	126	15
A-20	168	20	154	18	126	15
A-21	171	21	189	23	212	25
A-22	180	22	147	18	145	17
A-23	174	21	159	19	135	16
A-24	180	22	140	17	156	19
A-25	180	22	140	17	156	19
A-26	160	19	146	18	145	17
A-27	186	22	153	18	150	18
A-28	182	22	157	19	150	18
A-29	163	20	174	21	170	20
A-30	188	23	148	18	172	21
A-31	163	20	132	16	170	20
A-32	150	18	145	17	143	17
A-33	171	21	118	14	180	22
A-34	172	21	204	24	167	20
A-35	158	19	147	18	147	18
A-36	190	23	185	22	172	21
A-37	190	23	183	22	190	23
A-38	128	15	135	16	128	15
A-39	128	15	147	18	143	17

Table 4.7 shows the measured values of spot background gamma radiation for Kolasib district and Table 4.8 shows the measured values of spot background gamma radiation for Aizawl district. In Kolasib District, the measured values of background gamma radiation ranged from 126 ± 15 *nSv/hr* to 215 ± 26 *nSv/hr*, with an average value of 176 ± 21 *nSv/hr* and a standard deviation (SD) of 22.85 in winter. In summer, it ranged from 118 ± 14 *nSv/hr* to 191 ± 23 *nSv/hr*, with an average value of 148 ± 18 *nSv/hr* and SD of 18.94, while in monsoon, it ranged from 121 ± 15 *nSv/hr* to 217 ± 26 *nSv/hr*, with an average value of 156 ± 19 *nSv/hr* and SD of 25.51.

The measured values of background gamma radiation within Aizawl District ranged from 128 ± 15 *nSv/hr* to 211 ± 25 *nSv/hr*, with an average value of 169 ± 20 *nSv/hr* and SD of 18.32 in winter. In summer, it ranged from 118 ± 14 *nSv/hr* to 204 ± 24 *nSv/hr*, with an average value of 158 ± 19 *nSv/hr* and SD of 19.89, while in

monsoon, it ranged from 126 ± 15 *nSv/hr* to 212 ± 25 *nSv/hr*, with an average value of 162 ± 19 *nSv/hr* and SD of 20.49.

In both district, the background gamma radiation level obtained were all found to be higher in comparison with the values reported by UNSCEAR (2000) for different countries (mean of 59 nGy/h in the range of 18- 93 nGy/h), but was within the given range of background gamma level for India (89 nGy/h in the range of 27–3051 nGy/h) as reported by Nambi *et al.* (1986).

4.6.1(a). *Correlation between Background Gamma and Radium Equivalent Activity*

Figure 4.10 and Figure 4.11 shows respectively graphical representation of the correlation between the measured values of background gamma level and radium equivalent activity in Kolasib and Aizawl district of Mizoram. The correlation coefficients obtained are found to be very close to zero in both cases, which denotes that there is a a very poor correlation between the two measured parameters.

It is a known fact that the background gamma radiation measured using the gamma survey meter measures the gamma radiations coming from both terrestrial and cosmic sources. Here, the possible reason for the poor correlation may be due to the fact that there is some contribution from cosmic radiations to the background gamma level measured at each sampling sites. Moreover, the radium equivalent activity accounts only for the activity concentration measured from three terrestrial radionuclide, namely ^{238}U, ^{232}Th and ^{40}K. Also, there may be other gamma-emitting terrestrial radionuclide which contributes to the background gamma level, but was not taken into account while measuring the radium equivalent activity.

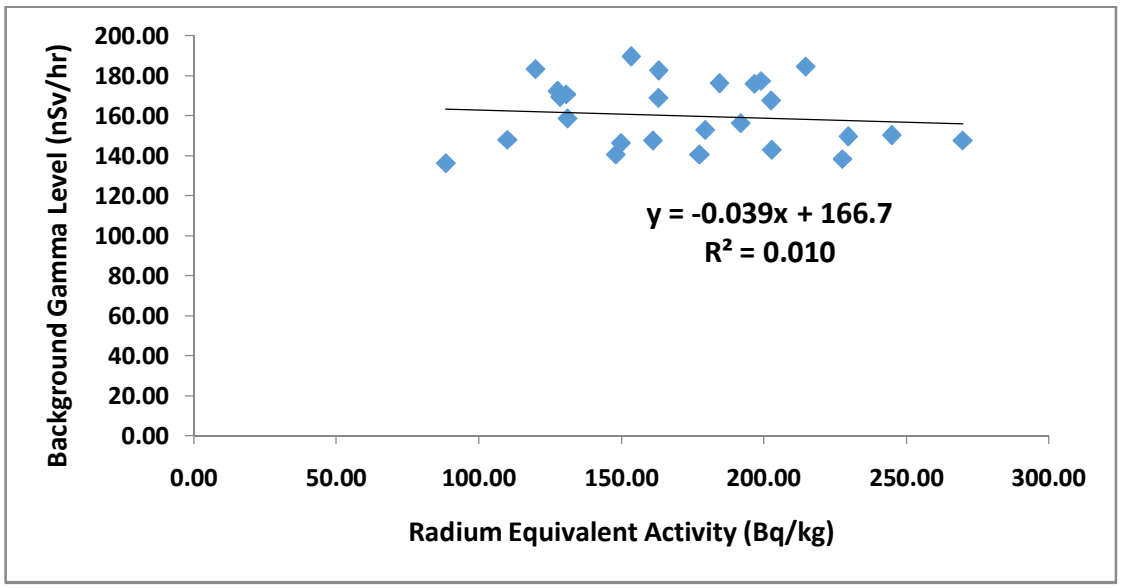

Fig 4.8: Correlation between background gamma level and radium equivalent activity in Kolasib District.

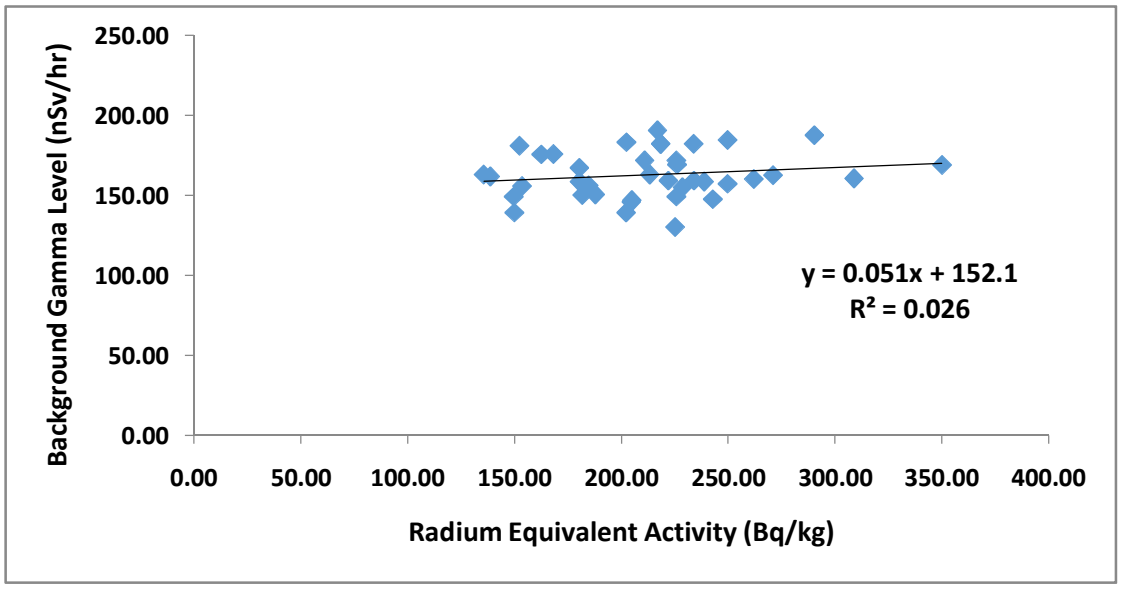

Fig 4.9: Correlation between background gamma level and radium equivalent activity in Aizawl District.

5

Conclusion

This chapter will give the conclusions drawn out from the thesis titled, "Concentrations of Natural Radionuclides in Water Sources and its Surrounding Soil in Aizawl and Kolasib Districts of Mizoram". Active methods of measurements which yield sufficient results in a short time period, using suitable detectors or instruments, were used for the determination of the concentration of different natural radionuclide in water sources and its surrounding soil within the mentioned studied area. This study was performed with a hope to create a deeper understanding of the properties, behaviour and abundance of the natural radionuclide present in the studied area. Moreover, radiation dosimetry performed in this study is an important aspect in studying the implications of natural radionuclide towards human health. The following conclusions are drawn based on measurements carried out during the present study:

- The geographical location of the study area extends from 23˚34'23.6'' to 23˚54'8.8'' latitude and from 92˚39'51.9'' to 92˚57'57.9'' longitude, with an altitude ranging from 1170 ft to 4140 ft above sea level in Aizawl district. In Kolasib district, the sampling area extends from 23˚58'56.5'' to 24˚30'43.5'' latitude and from 92˚35'54.4'' to 92˚46'23.7'' longitude, with an altitude ranging from 150 ft to 2967 ft above sea level. Samples were collected from a total of 66 locations: 39 from Aizawl district and 27 from Kolasib district. The sampling period for winter season ranges from November 2016 to February 2017, for summer season, it ranges from March 2017 to June 2017 and for monsoon season; the period ranges from July 2017 to October 2017. Radon concentration in water was measured using a scintillation based radon detector, Smart RnDuo. Except for sample code K-13 of Kolasib district (of monsoon season), the measured values of radon concentration in water were found to be within the safe limit value of 4-40 Bq/l for drinking water as recommended by UNSCEAR (1993). But, these values were found to be much lower than the reference level of 100 Bq/l recommended by the European Commission (2001). To assess the health hazards due to radiation

dose associated with it, the annual effective dose for inhalation and ingestion due to radon in water was calculated and the total effective radiation dose due to radon in water was obtained from these two results. Only three samples from Kolasib district, namely Sample Code K-10, K-13 and K-22, measured during the monsoon season, were found to exceed the safe limit value of 100 μSv/yr prescribed by WHO (2004). Since these three samples exceeds the safe limit value only during the monsoon season, the seasonal average value for each of the mentioned three samples was taken and it was found that the average total effective dose obtained were all well within the safe limit value of 100 μSv/yr. Hence, these three samples were considered to be safe for irrigation purposes and domestic consumption.

- Seasonal variation of the measured radon concentration in water shows that the concentration was highest during the monsoon season, followed by summer season, and the lowest concentration of radon was observed during the winter season. This result can be related to the amount of rainfall experienced during the different seasons. During monsoon season, heavy rainfall was observed, which led to the possibility of higher collection of radon emanated from soil surface into the rain water as it flows through several soils. This possibility decreases when the amount of rainfall was decreased during the summer season. Also, since no rainfall was observed during the winter season, there is lower absorption of radon from soil into the water, hence the lowest concentration. A similar trend of seasonal variation was observed for the measured values of ingestion, inhalation and total effective dose. The ingestion, inhalation and total effective dose are found to be the highest during the monsoon season, followed by summer season, while it is lowest during the winter season. Since, the effective doses measured is directly proportional to the radon concentration values contained in a sample, the season variation trends obtained is as expected.
- The measured values of radon concentrations in water were classified into two categories, depending upon the sampling source or origin. Those samples collected from water sources such as streams, springs and government supplied water are collectively labeled as “surface water” and samples taken from water sources like bore wells, open wells and enclosed springs are labeled as “ground

water". The results obtained in both districts shows that radon concentration was higher in samples taken from groundwater sources rather than those taken from surface water sources. This result was in accordance with WHO (2011), which states that radon concentration in ground water is higher those from surface water. Radon dissolved in water, being a gas, readily escapes from water surfaces when disturbed. Likewise, water present on the surface always has a higher possibility of being disturbed than water presents inside the ground, hence the result.

- The uranium concentration in water samples were measured by using LED Fluorimeter LF-2a, which works on the principle of measurement of green fluorescence produced by uranium on the addition of a buffer solution. The measured values of uranium concentration in Kolasib district and Aizawl district were found to be well within the safe limit value of 30 μg/l for drinking water as prescribed by WHO (2011). The values obtained were also much lower that the critical value of 60 μg/l, suggested in India by the Atomic Energy Regulation Board (AERB, 2004). To assess the radiological effects of uranium on human health due to ingestion, the annual effective ingestion dose of uranium was calculated using equation (2.11). The calculated annual effective ingestion dose in Kolasib district (mean of 0.616 μSv/yr in the range of 0.337 μSv/yr to 1.498 μSv/yr) and Aizawl district (mean of 1.197 μSv/yr in the range of 0.337 μSv/yr to 6.347 μSv/yr) were found to be much lower than the safe limit reference level of 100 μSv/yr for effective radiation dose, as prescribed by WHO (2004). Hence, there is no radiological risk due to ingestion of water containing uranium in this study.
- "Leaching" is an important property of uranium and can be explained as the process in which uranium in soil or rocks gets dissolved into water bodies as the water flows through uranium containing rocks or soils. The measured values of uranium concentrations in water were classified into two categories depending upon their source of origin, namely "surface water" and "ground water". The results obtained in both districts shows that uranium concentration was higher in samples taken from surface water sources than those taken from ground water sources. The possible reason for this result may be due to the fact that there is of

higher possibility of collection of uranium in "surface water" rather than from "ground water", because water from surface sources flows through several soils and rocks, thereby having a higher probability of leaching of uranium into the water body. Whereas ground water remains stagnant for a long time, therefore, there is minimum possibility of leaching of uranium into ground water bodies.

- The radon concentration and the uranium concentration in water obtained in this study were correlated since these two elements belong to the same decay series of ^{238}U, ^{222}Rn being the daughter element of ^{238}U. The correlation coefficient obtained for Kolasib district ($R^2 = 0.030$) and Aizawl district ($R^2 = 0.014$) were found to be very close to zero. This means that there is very poor correlation at all between the two measured values. The possible reason for this weak correlation may be due to the fact that radon being a gas, readily escapes into the surrounding air when water containing dissolved radon is being disturbed, while uranium does not necessarily deposit itself to the surrounding soil, its concentration in water body rather increases as the water flows through rocks and soils. Hence, the concentration of uranium and radon in water are not in good correlation in this regard.
- Since soil is considered to be the main source of natural radioactivity, the natural radioactivity present in soil was calculated using a sodium iodide (NaI) detector, having thallium (Tl) as a doping agent. The detector was coupled with a PC based 1K Multichannel analyzer called GSPEC-SA. The radioactivity concentration was determined for three specific radionuclide, namely ^{238}U, ^{232}Th and ^{40}K from the soil samples collected from the sampling sites. The average values of activity concentration of ^{238}U in Kolasib district and Aizawl district were found to be within the worldwide average value of 35 Bq/kg, given in UNSCEAR (2000). However, the average activity concentration of ^{232}Th and ^{40}K nuclide were found to exceed the corresponding worldwide average values of 30 Bq/kg and 400 Bq/kg respectively (UNSCEAR, 2000). Although the results obtained for ^{232}Th and ^{40}K were higher than the corresponding worldwide average values, the average radioactivity concentration obtained for the three radionuclide were all found to be well within the critical value set by IAEA (2004), the critical values being 10,000

Bq/kg for ^{40}K and 1000 Bq/kg for both ^{238}U and ^{232}Th radionuclide. To represent the activity concentration of ^{238}U, ^{232}Th and ^{40}K into a single quantity with respect to exposure to radiation, the radium equivalent activity was calculated using equation 2.9. The measured values of radium equivalent activity concentration for Kolasib district (Average of 173.06 Bq/kg in the range of 88.38 Bq/kg to 269.73 Bq/kg) and Aizawl district (Average of 212.87 Bq/kg in the range of 135.62 Bq/kg to 350 Bq/kg) were found to be lower than the safe limit value of 370 Bq/kg, prescribed by OECD (1979). The result obtained in this report shows that there is no radiological health hazards from the measured activity concentration of natural radionuclide.

- The rate at which radon escapes from a soil sample of unit mass, i.e. the radon mass exhalation rate was measured using a scintillation based radon detector, Smart RnDuo. The measured annual average values of radon mass exhalation for Kolasib district and Aizawl district of Mizoram were found to be quite comparable to the results obtained by Chhangte (2018) and Hmingchungnunga (2020), who used the same instrument and methods for measurement of radon mass exhalation rate in other districts of Mizoram. The seasonal variation of radon mass exhalation rate in both Kolasib and Aizawl districts shows that radon mass exhalation rate was highest during the summer season, followed by winter season, and the lowest rate of radon mass exhalation was observed during the monsoon season. This result can be explained from the effects of soil moisture content on the radon mass exhalation rate. The increase of moisture in soil at first increase the radon mass exhalation rate, but on further increasing the moisture content in soil, the rate eventually decreases (Owczarski *et al*, 1990; Stranden *et al*, 1984). During the summer season, there is small amount of moisture in soil due to light rainfall, so the radon mass exhalation increases. But in monsoon, there was heavy rainfall, resulting in increase of soil moisture, which in turn led to the decrease of radon mass exhalation rate compared to other seasons. While in winter, as no rainfall was observed, the soil was much drier and the radon mass exhalation rate therefore, was found to be lower than those observed during the summer season.

- Emanation factor is a parameter which characterizes the behaviour of radon in soils and rocks and is defined as the fraction of radon atoms generated, that escape the solid phase in which they are formed and become free to migrate through the bulk medium and was calculated using equation 2.6. The calculated values of radon emanation factor in Kolasib district (average value of 0.15 in the range of 0.04 to 0.27) and Aizawl district (average value of 0.13 in the range of 0.04 to 0.36) was found to be quite comparable to the usual range of 0.05 to 0.70 in typical rocks and soils, as mentioned by Nazaroff *et al.* (1988).
- Sieving of soil, using a mechanical sieve shaker was performed to indentify the soil type and grain size distribution of the collected soil samples. The grain size distribution obtained was triangular plotted and it was found that the soil type of most of the samples fall under "sand", while a very few of them are "sandy loam". The result obtained cannot be used to justify the variations observed in the radioactivity content and radon mass exhalation rate in soil, this is because the grain size distribution and soil type of all the soil samples collected falls more or less under the same category.
- Background gamma radiation at a height of 1 metre above the ground at the sampling sites was measured using a gamma survey meter PM 1405. The background gamma radiation level obtained in both Kolasib and Aizawl district were found to be higher than the values reported in UNSCEAR (2000) for different countries (mean of 59 nGy/h in the range of 18- 93 nGy/h). But, the results obtained were all within the values reported by Nambi *et al.* (1986) for India (89 nGy/h in the range of 27–3051 nGy/h). A very poor correlation between the background gamma level and radium equivalent activity in both studied district was obtained. The possible reason may be due to the fact that the background gamma level measured at each sampling sites measures both gamma radiations coming from cosmic and terrestrial origin, while the radium equivalent activity accounts only for the activity concentration measured from three terrestrial radionuclide, namely ^{238}U, ^{232}Th and ^{40}K. Also, other gamma-emitting terrestrial radionuclide which may contributes to the background gamma level was not taken into account while measuring the radium equivalent activity.

Certain drawbacks were faced during the research work. The NaI (Tl) detector used in this research work for gamma spectrometry provide low energy resolution, which could be replaced by an HPGe detector, to provide a higher gamma energy resolution and to distinguish close lying energy lines. Also, for future research work in measurement of seasonal concentration of available natural radionuclide in water, it is suggested that work starts during the winter season. This is because water source tends to dry up during the winter season and an incomplete seasonal data can be easily generated due to this shortcoming, which the author also faced while doing the research study.

The status of the radon monitoring in Mizoram is still at a budding stage. Most of the works done in the study of radon were in relation to indoor and outdoor air. This study is hoped to provide a new approach in the study of natural radioactivity in the state of Mizoram, especially with regards to water and soil.

Also, the result obtained in this work may be considered helpful in creating a baseline data for future works in analysis of natural radioactivity and its contribution to radiation dose assessment. Although the concentrations and effective doses of the measured natural radionuclide obtained in this study does not exceeds the recommended safety limit values proposed by certain organization worldwide, yet its effect on the health of human beings and carcinogenic nature cannot be ignored. This is because the areas under study in this research have one of the highest cancer incidences in India. A further in-depth study, covering a wider geographical area and a longer time span may be carried out to generate a larger variety of data for assessment of the effect of natural radiation on human health.

APPENDIX – I

Energy Calibration of NaI (Tl) Gamma Spectrometer using ^{137}Cs and ^{60}Co Standard Sources

APPARATUS REQUIRED:

NaI (Tl) detector coupled with GSPEC-SA, ^{137}Cs and ^{60}Co standard sources, Personal Computer.

THEORY:

Some detectors do not measure energy. Those which does are referred to as energy spectrometers. The performance of a detector used for energy measurement can be examined by its response to a monoenergetic source of radiation. The width measured at half of the maximum of the bell-shaped curve called the response function is indicated by FWHM (full width at half maximum). The resolution is a measured of detector's capability to distinguish between the closely spaced energies.

In the analyzer, the channel number vs energy calibration is representative of pulse height vs energy distribution. In an ideal multichannel analyzer (MCA), it is expected to be linear and is represented by

$$\text{Energy} = M*\text{Channel no.} + C$$

The calibration is done by using a spectrum containing known and well-separated energies. Most commonly, the spectrum of ^{137}Cs and ^{60}Co is used for this purpose. It is possible with the least squares program to compute the slope M (energy per channel) and intercept C (energy corresponding to channel no. zero) from the peak positions in channels and input energy in keV. It is also common to use second polynomial for energy calibration for analyzers of higher memories to account for the possible non-linearity in ADC (analog to digital converter).

PROCEDURE:

1. The NaI (Tl) detector, the GSPEC-SA multi-chhanel analyzer and computer are first inter-connected through a USB port.

2. After turning on the system, open the Spectrum Acquisition & Analysis software in the computer. Open the 'Set Parameter' from the drop-down 'Acquisition' and set the parameter as follow:

   SET HV – 607 V GAIN – 2 LLD – 1

   This parameter value came with the GSPEC-SA specification so that we get ^{137}Cs peak of energy 661.99 keV at about Channel number 210 - 220 and ^{60}Co 2nd peak of energy 1332.01 keV at Channel number ranging between 420 – 450.
3. Go to 'Control' and set the Preset Time to "500 s" in the 'Acquisition' drop down within the 'Control'. Click the 'Start Acquisition' to start acquiring the spectrum.
4. After acquisition time is over, go to the drop-down 'ROI' where the region of interest of each peak of the spectrum can be select. After this, click the 'ROI Analysis' from the 'ROI' drop down and 'SAVE/PRINT' the analysis report.
5. To calibrate the system, go to 'Math Functions' drop down and click the 'Calibration'. From 'Type' select '3 Point Calibration'. In the 'Data', enter the value of 'Centroid 1' and 'Energy' from the ROI analysis report and click 'Accept' from 'Valid Peaks'. Repeat this for Centroid 2 and Centroid 3. Click 'Calibrate Spectrum' and 'Close'. Calibration is completed at this point.

OBSERVATION:

Table 1: Photo-peak energy and Channel Number obtained for Energy calibration of ^{137}Cs and ^{60}Co Standard Sources.

Standard Source	Photo-peak Energy (keV)	Channel Number
^{137}Cs	661.99	210
^{60}Co	1173.009	365
^{60}Co	1332.01	429

The analysis of spectrum for ^{137}Cs give a photo-peak energy of 661.998 keV at Channel number 210. Also, the first photo-peak of ^{60}Co with energy 1173.009 keV occurs at Channel number 365 and the second photo-peak of ^{60}Co with energy 1332 keV occurs at Channel number 429.

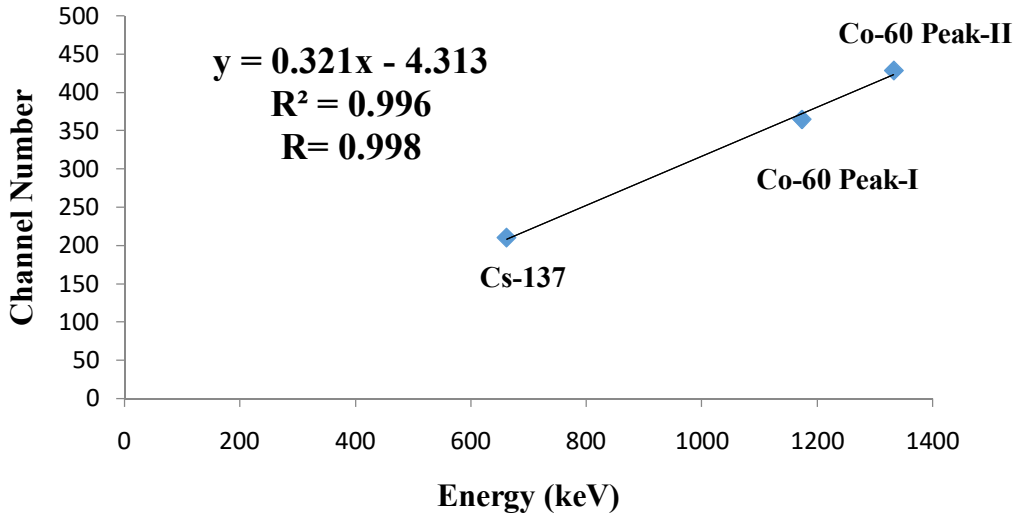

Figure 1: Energy calibration curve using standard source of ^{137}Cs and ^{60}Co.

The energy calibration curve in the figure 1 was obtained by plotting the known photo-peak energy of ^{137}Cs and ^{60}Co standard sources against the channel number at which they occur. As shown in the above figure, a good linear calibration energy curve is obtained, which shows that there is an ideal relationship between the channel number and the known photo-peak energy of the standard sources.

After the Calibration procedure is over, go to 'Math Functions' drop down and click 'Calibration', the result of the calibration will be displayed at the lower side of the display, m1 = 3.1423, m2 = 0 and c = -19.174.

PRECAUTIONS:

1. Good grounding system for mains is needed for the proper functioning of the instrument and to avoid Mains Noise feed-through through ground loops.
2. Care should be taken in setting the parameters SET HV, Gain and LLD that the ^{137}Cs and ^{60}Co peaks came at the right Channel number and energy.

APPENDIX – II

Efficiency Calibration using ^{40}K (RGK-1), ^{238}U (RGU-1) & ^{232}Th (RGTh-1) IAEA Standard Sources

APPARATUS REQUIRED:

IAEA standard sources of Potassium (^{40}K), Uranium (^{238}U) and Thorium (^{232}Th), NaI (Tl) detector, GSPEC-SA multichannel analyzer and Desktop Computer.

PROCEDURE:

1. The NaI (Tl) detector, the GSPEC-SA multi-chhanel analyzer and computer are first inter-connected through a USB port.
2. After turning on the system, open the Spectrum Acquisition & Analysis software in the computer. Open the 'Set Parameter' from the drop-down 'Acquisition' and set the parameter as follow:

   SET HV – 607 V

   GAIN – 2

   LLD – 1

   This parameter value came with the GSPEC-SA specification so that we get ^{137}Cs peak of energy 661.99 keV at about Channel number 230 and ^{60}Co 2^{nd} peak of energy 1332.01 keV at Channel number ranging between 420 – 450.
3. Set the Preset time to 10800 s so that photo peaks have sufficient counts for analysis by going to 'Acquisition' of the 'Control' drop down.
4. Start acquiring the spectrum either by going to 'Acquisition' drop-down and press 'Start' or by going to 'Control' and press 'Start Acquisition'.
5. After acquisition time is over, go to the drop-down 'ROI' where the region of interest (ROI) of each peak of the spectrum can be select. After this, click the 'ROI Analysis' from the 'ROI' drop down and 'SAVE/PRINT' the analysis report.
6. Taking ^{238}U source as an example, choose ^{214}Pb (which is a nuclide in ^{238}U decay series) as a nuclide for efficiency calibration.
7. Note down the 'Centroid (keV)' and 'Area' from the ROI analysis report.

8. Go to 'Utilities' drop down and click 'Gamma Library' and search for ^{214}Pb. Of all the isotope of ^{214}Pb, choose the one with energy closest to 'Centroid (keV)' and note down the branching intensity.
9. Calculate the efficiency of each source using the following equation

$$\eta(\%) = \frac{Area/s}{dps} \times \frac{100}{A\%} \times 100$$

where $\eta(\%)$ - Percentage Efficiency

$Area/s$ - Net Peak Area (background subtracted) per second

dps - Source strength in disintegration per second

$A\%$ - Gamma-ray abundance factor/branching intensity

OBSERVATION:

Table 1: Calculation of efficiency for ^{238}U, ^{232}Th and ^{40}K standard sources

Source	Count Time (s)	Activity of Source	Branching Intensity (%)	Area	Area/s	η%
^{238}U	10800	1636	19	297805	27.57	8.87
^{232}Th	10800	3854.21	29	663459	61.43	15.80
^{40}K	10800	4557.59	11	188600.33	17.46	3.48

Table 2: Photo-peak energy and Efficiency obtained for ^{238}U, ^{232}Th and ^{40}K standard sources.

Standard Source	Photo-peak energy (keV)	η%
^{238}U	301.261	8.87
^{232}Th	273.9	15.80
^{40}K	1381.772	3.48

For ^{238}U efficiency calibration, the Isotopes chosen is ^{214}Pb at channel number 115, with photopeak energy 295 keV (from gamma library) which is very close to 301.261 keV (from the acquired spectrum). For ^{232}Th efficiency calibration, the

isotope chosen is ^{228}Ac at channel number 110, with photopeak energy 270 keV (from gamma library) which is close to 273.9 keV (from the acquired spectrum).

The analysis of spectrum for ^{40}K give a photopeak at Channel number 444 with energy 1360.083 keV, but at a position with Channel number 504 with energy 1460 keV, there was no photopeak. which means that the ^{40}K photo peak shift to the left. Thus the efficiency for ^{40}K will not be the correct one.

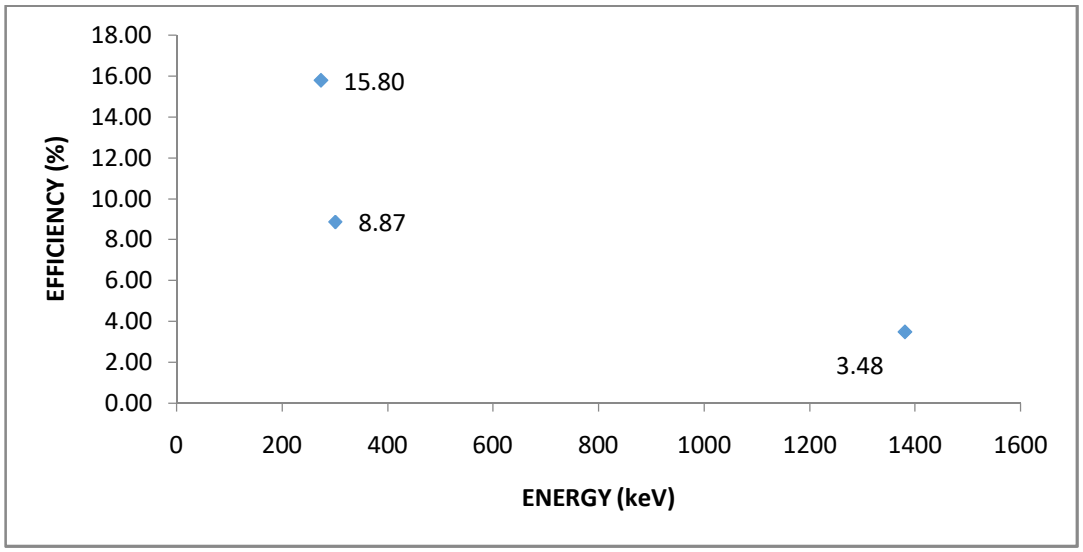

Figure 1: Energy (keV) vs Efficiency (%)

The efficiency calibration curve in figure 1 was obtained by plotting the photo-peak energy of ^{238}U, ^{232}Th and ^{40}K standard sources against the detector efficiency with respect to each element. Here, it was obtained that the efficiency decreases with an increase in photo-peak energy.

PRECAUTIONS:

1. Good grounding system for mains is needed for the proper functioning of the instrument and to avoid Mains Noise feed-through through ground loops.
2. Care should be taken in setting the parameters SET HV, Gain and LLD that the ^{137}Cs and ^{60}Co peaks came at the right Channel number and energy.

APPENDIX – III

Experiment to find the Radioactivity of soil sample

APPARATUS REQUIRED:

NaI (Tl) detector, GSPEC-SA, Desktop Computer and soil samples.

THEORY:

The fundamental approach in this type of analysis is to fit the response function of the detector for the sources of various energies of which the sample is composed of. This function is then used in the analysis of the spectral data. There are basically three methods commonly used for the analysis of gamma-ray spectra obtained from NaI(Tl) detectors.

1. **Method of spectral stripping**

This method is based on the principle that the gamma-ray spectra of multiple radionuclides are due to the linear sum of the spectrum of individual radionuclides. If the spectrum of single radionuclide is available, then after normalizing they can be subtracted from the composite spectrum one by one. This method is known as spectrum stripping. This method is simple but cannot be effectively used when more than three isotopes are present, because of the accumulation of error in the estimation of the peak areas.

2. **Simultaneous equation method**

It deploys a mathematical approach for removal of Compton interference from the photopeaks. The only requirement of this method is that

(i) all nuclides present in the sample must be identified

(ii) different photopeak be present for each nuclide

Let there be 'j' isotopes in the sample and C(1), C(2),…C(j) be the counts in the 'j' photopeak regions of various isotopes, and P(1), P(2),…P(j) are the photopeak counts of these isotopes to be determined and f(1,k), f(2,k),…f(j,k) is the Compton fractions of these isotopes P(k) in different regions. The simultaneous equation for j isotopes can be formed as

$$\begin{vmatrix} f(1,1) & f(1,2) & . & . & f(1,j) \\ f(2,1) & f(2,2) & . & . & f(2,j) \\ . & . & . & . & . \\ . & . & . & . & . \\ f(j,1) & f(j,2) & . & . & f(j,j) \end{vmatrix} \begin{vmatrix} P(1) \\ P(2) \\ . \\ . \\ P(j) \end{vmatrix} = \begin{vmatrix} C(1) \\ C(2) \\ . \\ . \\ C(j) \end{vmatrix}$$

$$|f||P| = |C|$$

Then the solution is

$$P = f^{-1}C$$

The inverted matrix f^{-1} is obtained by means of the computer when the order is more than two. This method can analyze a complex spectrum, but since it uses counts in the peak regions only, it is statistically less accurate than the method which uses all the channels.

3. **Least square method**

This is the most accurate method compared to earlier methods for unfolding the complex gamma-ray spectra from scintillation detectors. The principle of least squares requires that the sum of the squares of the random errors for the individual channel be a minimum. Initially, it is required to generate the response function corresponding to the monoenergetic photons for the nuclides under consideration. The net count after subtraction of background in any channel is the function of the activity of each nuclide present in the sample. In the given channel, the net counts can be represented as

$$C_i = P_1 f_{i,1} + P_2 f_{i,2} + ... P_m f_{i,\mathrm{m}}$$

where C_i is the net sample counts in the i^{th} channel. The P's are the unknown concentration of m nuclides contributing counts to the sample spectrum and the f's are the fraction of the photopeaks counts of the m^{th} isotope in the i^{th} channel, also called Compton fractions calculated from

$$f_{i,m} = N_{i,m} / P_m$$

where $N_{i,m}$ and P_m are the counts due to m^{th} isotope in channel 'i'. These fractions are determined by counting standards of each nuclide separately.

In a multilinear regression model, the C's (observed counts in each channel) are dependent variables and known f's are the independent variables. Even though

some of the 'm' nuclides may not contribute counts to all the channel, the model is valid because the channel efficiencies will merely be zero for those channels in which no counts appear from a particular nuclide.

Applying the theory of weightage least squares we can get a set of equations

$$P = \left(f^T W f\right)^{-1} \left(f^T W C\right)$$

where W is the weighing matrix. The variance of each value is calculated by the diagonal element of the inverted matrix. Unfolding of the NaI(Tl) spectrum is achieved in two steps. In the first step, the program generates the response functions for the individual isotopes from the separately counted spectral data of individual isotope standards. In the second step, the program calculates the energy and intensity of the individual gamma energies peaks based on the least squares method.

PROCEDURE:

1. Put the sample in the detector. Acquired the spectrum by setting the Preset time to 50000 seconds. The sample may not have high activity and must acquire the spectrum for a longer period of time so that the photopeaks have sufficient counts for the analysis.
2. After the acquisition period is over, select ROI from each photopeak and analyze the spectrum. Save the ROI analysis report.
3. From the Possible Isotopes obtain in the analysis report, select the one with which the system is previously efficiency calibrated (^{214}Pb for ^{238}U and ^{228}Ac for ^{232}Th).
4. Note down the 'Area' from ROI analysis report and calculate the activity using the following formula.

$$Activity(Bq/kg) = \frac{N}{T} \times \frac{100}{\gamma\%} \times \frac{100}{\eta\%} \times \frac{1}{W}$$

where

N - Background subtracted Net Peak Area counted in T second

$\gamma\%$ - Gamma-ray abundance factor/branching intensity

$\eta\%$ - Previously obtained percentage Efficiency of the standard source

W - Weight of the soil sample.

OBSERVATION:

Observation for one soil sample is given below

Nuclide	Weight (kg)	Counting time (s)	Branching Intensity	Net Area	η%	Activity (Bq/kg)
^{238}U	0.339	50000	19	6209	8.87	21.74
^{232}Th	0.339	50000	4	6209	15.80	57.95
^{40}K	0.339	50000	11	59827.833	3.48	909.18

RESULT:

Thus, the activity of potassium nuclide is highest followed by thorium nuclide and uranium nuclide have the lowest activity.

PRECAUTIONS:

1. Good grounding system for mains is needed for the proper functioning of the instrument and to avoid Mains Noise feed-through through ground loops.
2. Care should be taken in setting the parameters SET HV, Gain and LLD that the ^{137}Cs and ^{60}Co peaks came at the right Channel number and energy.

APPENDIX – IV

Calculated data of Emanation Factor for Kolasib District

The Emanation factor for soil samples collected from Kolasib district was calculated using equation 2.6 by taking into account the result of radium activity concentration (C_{Ra}) obtained using equation 2.8, and also the result of radon mass exhalation rate (J_m) calculated using equation 2.4.

Sample Code	C_{Ra} (Bq/kg)	C_{Ra} (mBq/kg)	J_m Annual Average (mBq/kg/hr)	Emanation Factor
K-1	43.39	43386.40	28.15	0.09
K-2	24.58	24578.34	28.95	0.16
K-3	20.28	20275.27	30.98	0.21
K-4	20.73	20728.21	14.26	0.09
K-5	30.97	30965.29	27.87	0.12
K-6	28.00	28003.76	33.09	0.16
K-7	24.83	24825.05	28.52	0.15
K-8	25.83	25829.95	27.06	0.14
K-9	25.83	25829.95	24.95	0.13
K-10	23.28	23284.73	14.64	0.08
K-11	31.13	31132.96	35.18	0.15
K-12	25.27	25272.67	30.37	0.16
K-13	36.60	36602.60	33.68	0.12
K-14	32.92	32920.78	35.28	0.14
K-15	12.90	12899.49	25.80	0.27
K-16	15.28	15275.39	25.12	0.22
K-17	20.10	20101.04	24.51	0.16
K-18	15.28	15280.87	20.25	0.18
K-19	32.54	32544.82	46.47	0.19
K-20	33.83	33833.31	26.68	0.11
K-21	38.23	38226.92	44.86	0.16
K-22	26.65	26647.15	23.82	0.12
K-23	17.87	17870.13	32.52	0.24
K-24	33.69	33687.68	21.11	0.08
K-25	21.82	21822.64	20.78	0.13
K-26	41.49	41491.89	12.66	0.04
K-27	21.28	21280.20	15.30	0.10

APPENDIX – V

Calculated data of Emanation Factor for Aizawl District

The Emanation factor for soil samples collected from Aizawl district was calculated using equation 2.6 by taking into account the result of radium activity concentration (C_{Ra}) obtained using equation 2.8, and also the result of radon mass exhalation rate (J_m) calculated using equation 2.4.

Sample Code	C_{Ra} (Bq/kg)	C_{Ra} (mBq/kg)	J_m Annual Average (mBq/kg/hr)	Emanation Factor
A-1	37.07	37068.30	38.48	0.14
A-2	21.74	21735.76	39.08	0.24
A-3	43.31	43313.12	23.90	0.07
A-4	32.38	32379.12	47.23	0.20
A-5	32.38	32379.12	47.23	0.20
A-6	29.29	29286.09	20.01	0.09
A-7	33.59	33588.79	32.89	0.13
A-8	39.05	39054.09	46.18	0.16
A-9	39.05	39054.09	46.18	0.16
A-10	50.81	50811.18	27.77	0.07
A-11	18.10	18104.76	48.30	0.36
A-12	18.10	18104.76	48.30	0.36
A-13	20.26	20257.70	19.55	0.13
A-14	37.87	37868.65	23.72	0.08
A-15	38.23	38234.50	26.66	0.09
A-16	58.69	58688.35	35.02	0.08
A-17	37.84	37838.99	46.72	0.17
A-18	38.30	38301.46	29.35	0.10
A-19	27.30	27299.67	20.39	0.10
A-20	27.30	27299.67	20.39	0.10
A-21	35.02	35015.63	29.10	0.11
A-22	40.09	40092.65	35.48	0.12
A-23	23.23	23231.94	13.58	0.08
A-24	38.23	38234.38	42.36	0.15
A-25	38.23	38234.38	42.36	0.15
A-26	28.43	28430.17	28.41	0.13

A-27	31.06	31059.46	24.18	0.10
A-28	21.20	21202.22	15.88	0.10
A-29	60.40	60400.47	24.03	0.05
A-30	47.95	47951.93	30.15	0.08
A-31	43.43	43433.90	13.80	0.04
A-32	35.90	35901.00	15.49	0.06
A-33	36.69	36694.31	33.38	0.12
A-34	20.13	20133.41	24.35	0.16
A-35	41.03	41032.27	48.06	0.16
A-36	40.99	40987.49	23.15	0.08
A-37	24.96	24963.96	26.61	0.14
A-38	20.52	20522.92	27.54	0.18
A-39	28.05	28054.47	12.09	0.06

References

Abdallaha MS, Rima RH, Rida YN, Malek Chatilac, Gabriel Katuld (2007). Radon measurements in well and springwater in Lebanon. *Radiation Measurements*, **42**, 298-303.

AERB (2004). Directive for Limit on Uranium in Drinking Water, India. Mumbai: Atomic Energy Regulatory Board.

Agarwal, Chhavi (2011). Nondestructive assay of nuclear materials by gamma ray spectrometry. (Doctoral dissertation, Homi Bhabha National Institute).

Ahmad Nisar, Jaafar MS, Khan SA (2014). Correlation of radon exhalation rate with grain size of soil collected from Kedah, Malaysia. *Sci. Int. (Lahore)*, **26 (2)**, 691-696.

Alaamer GAS (2008). Assessment of Human Exposures to Natural Sources of Radiation in Soil of Riyadh, Saudi Arabia. *Turkish Journal of Engineering & Environmental Sciences*, **32**, 229-234.

Amanjeet Kumar, Ajay KS (2018). Measurements of mass and surface exhalation rate from soil of eastern Haryana, India. *International Journal of Applied Engineering Research*, **13** (5), 2181-2186.

Bajwa BS, Sharma N, Walia V,Virk HS (2003). Measurements of natural radioactivity in some water and soil samples of Punjab state, India. *Indoor Built Environ*, **12**, 357-361.

Beretka J, Mathew PJ (1985). *Health Phys* **48(1)**, 87-95, DOI: 10.1097/00004032-198501000-00007.

Bureau International des Poids et Mesures Table of Radionuclides (2004). Monographie BIPM-5.

Chandrashekara MS (2017). Studies on uranium and radon concentration in bore well water of Kodagu District, India. *International Journal of Engineering Research and Development*, **13** (12), 1-5.

Chhangte LZ (2018). Analysis of Radon and Thoron in dwellings with special reference to Saiha and Lawngtlai Districts of Mizoram (Doctoral dissertation, Mizoram University).

Chikasawa K, Ishii T, Ugiyama H (2001). Terrestrial gamma radiation in Kochi Prefecture, Japan. *J Health Sci*, **47**, 361-372.

Cothern CR, Lappenbusch WL (1983). Occurrence of uranium in drinking water in the U.S. *Health Physics*, **45**, 89-99.

Darby S, et al. (2005). Radon in homes and risk of lung cancer: collaborative analysis of individual data from 13 European case-control studies. *BMJ*, **330 (7485)**, 223-227.

Darko EO, Adukpo OK, Fletcher JJ, Awudu AR Otoo (2009). Preliminary studies on ^{222}Rn concentration in ground water from selected areas of the Accra metropolis in Ghana. *J Radioanal Nucl Chem* DOI 10.1007/s10967-009-0378-y.

Diwan Vijita, Sar Santosh Kumar, Singh Shweta, Sahu Megha, Jindal Manoj Kumar, Arora Arun, Biswas Supriya (2018). Study of uranium contamination & its health effect in ground water of Balod District of Chhattisgarh State, India. *International Journal of Scientific Research in Science, Engineering and Technology*, **4 (4)**, 125-131.

Duggal V, Mehra R, Rani A (2013). Analysis of radon concentration in drinking water in Hanumangarh district of Rajasthan, India. *Radiat Prot Environ*, **36**, 65-70.

Duggal V, Mehra R, Rani A (2015). Study of radium and radon exhalation rate in soil samples from areas of northern Rajasthan, *J. Geol. Soc. Of India*, **86(3)**, 331-336.

European Commission. Commission recommendations of 20th December 2001 on the protection of the public against exposure to radon in drinking water. (2001), 2001/982/ Euratom, L344/85.

García-Gaines RA, Frankenstein Susan (2015). USCS and the USDA Soil Classification System: Development of a Mapping Scheme. ERDC/CRREL TR-15-4, 5-7.

Gusain GS, Prasad Ganesh, Prasad Yogesh, Ramola RC (2009). Comparison of indoor radon level with radon exhalation rate from soil in Garhwal Himalaya. *Radiation Measurements,* **44**, 1032-1035.

Hafeez AF, El-Khatib AM, Moharram BM, Kotb MA, and Abdel-Naby A (1991). Field Measurements of Radon Exhalation and Ra-226 Content in Soil using the Can-Technique. *Isotopenpraxis Isot. Env. and Health Studies*, **27(4)**,188-190.

Handbook an Radon Transport Models and Measurements Methods, Radiological Physics and Advisory Division (2016), Bhabha Atomic Research Centre, 27-28 (Unpublished).

Hassan Nabil M, Tokonami Shinji, Fukushi Masahiro (2011). A simple technique for studying the dependence of radon and thoron exhalation rate from building materials on absolute humidity. *J Radioanal Nucl Chem,* **287**, 185-191, DOI 10.1007/s10967-010-0665-7.

HDR (2009). National Resource Centre for Urban Poverty and All India Institute of Local Self Government. Human Development Report, Mumbai, India.

Hmingchungnunga (2020). Measurement of Radon and Uranium Concentration from drinking water sources and the surrounding soil in Mizoram: a case study of Champhai and Serchhip Districts (Doctoral dissertation, Mizoram University).

IAEA (2004). Application of the concepts of exclusion, exemption and clearance, Safety standards series No. RS-G-1.7.

IARC (1988). Man-made mineral fibres and radon. Lyon: International Agency for Research on Cancer. IARC Monographs on the Evaluation of Carcinogenic Risks to Humans, **43**

Ibrahim SA, Wrenn ME, Singh NP, Cohen N, Saccomano G (1983). Thorium concentrations in human tissues from two U.S. populations. *Health Physics*, **44 (1)**, 213-220.

ICRP, 1984, International Commission for Radiological Protection Publication No. 39, Principles of Limiting Exposure of the Public to Natural Sources of Radiation, Pergamon Press, Oxford.

International Standard, ISO 18589-3:2007(E), 7.3.1. Energy calibration.

Jacobi W (1993) The History of the Radon Problems in Mines and Homes, *Ann. ICRP,* **23**, 39-45.

Jaishi Hari Prasad, Singh Sanjay, Tiwari Raghavendra Prasad, Tiwari Ramesh Chandra (2015). Soil-gas Thoron Concentration Associated with Seismic Activity. *Chiang Mai J. Sci*., **41(4)**.

Kabir KA, Islam SMA, Rahman MM, (2009). Distribution of Radionuclides in Surface Soil and Bottom Sediment in the District of Jessore, Bangladesh and Evaluation of Radiation Hazard. *Journal of Bangladesh Academy of Sciences*, **33 (1)**, 117-130.

Kannan V, Rajan MP, Iyengar MAR, Ramesh R (2002). Distribution of natural and anthropogenic radionuclides in soil and beach sand samples of Kalpakkam (India) using HPGe gamma ray spectrometry. *Appl. Radiat. Isot.*, **57**, 109-119.

Kansal S, Mehra R (2015), Evaluation and analysis of ^{226}Ra, ^{232}Th and ^{40}K and radon exhalation rate in the soil samples for health risk assessment, *Int. J. Low Radiation*, **10 (1)**, 1-13.

Kaur Manpreet, Tripathi Pooja, Choudary Indu, Mehra Rohit, Kumar Ajay (2017), Assessment of Annual Effective Dose Due to Inhalation and Ingestion of Radon in

Water Samples from Some Regions of Punjab, India. *International Journal of Pure and Applied Physics*, **13 (2)**, 193-200.

Kumar Manish, Kaushal Anjali, Sahoo BK, Sarin. Amit, Mehra Rohit, Jakhu Rajan, Bhalla Atul, Sharma Navjeet (2017). Measurement of uranium and radon concentration in drinking water samples and assessment of ingestion dose to local population in Jalandhar district of Punjab, India. *Indoor and Built Environment*, **0(0)**, 1-8.

Kumar A, Kaur M, Sharma S, Mehra R (2016). A study of radon concentration in drinking water samples of Amritsar city of Punjab (India). *Radiat Prot Environ*, **39**,13-9.

Kutahyali C, Cobos J, Rondinella VV (2011). Comparison of fluorescence enhancing reagents and optimization of laser fluorimetric technique for the determination of dissolved uranium. *Journal of Radioanalytical and Nuclear Chemistry*, **287**, 1-5.

Lubin JH (1994). Lung Cancer and Exposure to Residential Radon. *Am. J. Epidemio.*, **140**, 323-332.

Lekshmi R, Arunima S, Jojo PJ (2018). Determination of Radon Exhalation Rates and Emanation Factor of Some Soil Samples Collected From Southern Seashore of Kerala, India. *JUSPS-A*, **30 (1)**, 80-85.

Mahur AK, Kumar Rajesh, Sonkawade RG, Sengupta D, Prasad Rajendra (2008). Measurement of natural radioactivity and radon exhalation rate from rock samples of Jaduguda uranium mines and its radiological implications. *Nuclear Instruments and Methods in Physics Research*, **266**, 1591-1597.

Majumdar D (2000). Radon in the Environment and Associated Health Problems. *Resonance*, July 2000, 44-55.

McDougall Ian, Harrison T Mark (1999). Geochronology and Thermochronology by the $^{40}Ar/^{39}Ar$ Method, 2nd Ed., Oxford.

Mujahid SA, Hussain S, Ramzan M (2010). Measurement of radon exhalation rate and soil gas radon concentration in areas of southern Punjab, Pakistan. *Radiation Protection Dosimetry*, 1-4. doi:10.1093/rpd/ncq119.

Nagaratnam A (1994), Radon: A Historical Overview, *Bull. of. Rad. Prot.,* **17**, 1-10.

Nambi KS, Bapat VN, David M, Sundaram VK, Santa CM, Soman SD, (1986). Natural Background Radiation and Population Dose Distribution in India. India: HPD, BARC.

Nazaroff WW, Nero AV (1988). Radon and its Decay Products in Indoor Air. John Wiley & Sons, New York. ISBN: 0-471-62810-7.

NCRP (National Council on Radiation Protection and Measurements) (1999). Biological Effects and Exposure Limits for 'Hot Particles'. NCRP-Report 130.

NRC (National Research Council) (1988), Health risks of radon and other internally deposited alpha-emitters. National Research Council,Washington, DC, National Academy Press.

OECD (Organisation for Economic Co-Operation and Development) (1979). Exposure to Radiation from the Natural Radioactivity in Building Materials, Report by a Group of Experts of the OECD Nuclear Energy Agency, Paris.

Owczarski PC, DJ Holford, HD Freeman, GW Gee (1990). Effects of changing water content and atmospheric pressure of radon flux from surface and fine soil samples. *Geophysical Research Letters*, **17**, 817-820.

Patra AC, Mohapatra S, Sahoo SK, Lenka P, Dubey JS, Tripathi RM, Puranik VD (2013). Age-dependent dose and health risk due to intake of uranium in drinking water from Jaduguda, India. *Radiation Protection Dosimetry*, **155 (2)**, 210–216.

Peterson John, MacDonell Margaret, Haroun Lynne, Monette Fred (2001). Radiological and Chemical Fact Sheets to Support Health Risk Analyses for Contaminated Areas, Argonne National Laboratory Environmental Science Division. 2007 Mar, 133.

Prasad Ganesh, Prasad Yogesh, Gusain GS, Badoni Manjari, Rana JMS, Ramola RC (2009). Variation of radon concentrations in soil and groundwater and its correlation with radon exhalation rate from soil in Budhakedar, Garhwal Himalaya. *Indian J. Phys.,* **83 (6)**, 887-892

Radenkovic MB, Alshikh SM, Andric VB, Miljanic SS (2009). Radioactivity of Sand from Several Renowned Public Beaches and Assessment of the Corresponding Environmental Risks. *Journal of the Serbian Chemical Society*, **74 (4)**, 461-470.

Ramachandran TV, Mayya YS, Sadashivan S, Nair RN, Eappen KP (2003). Radon-Thoron Levels and Inhalation Dose Distribution Patterns in Indian Dwellings. BARC Report, BARC/2003/E/026. Bhabha Atomic Research Centre, Mumbai, Government of India, 1-43.

Rajesh S, Kerur BR, Anilkumar S (2017). Radioactivity measurements of Soil samples from Devadurga and Lingasugur of Raichur District of Karnataka, India. *International Journal of Pure and Applied Physics*. **13 (1)**, 127-130.

Rathore D (2008). Advances in technologies for the measurement of uranium in diverse matrices. *Talanta*. **77**, 9-29.

Rohmingliana PC, Vanchhawng Lalmuanpuia, Thapa RK, Sahoo BK, Singh OP, Zoliana B, Mayya YS (2009). Measurement of Indoor Radon and Thoron Concentrations in Correlation to Geographical Location and Construction types of Buildings in Mizoram.(with special reference to Aizawl, Champhai and Kolasib districts). Proc. VIth Conference of Physics Academy of North East, Tripura University, April 3-4.

Ryan TP, Sequeira S, McKittrick L, Colgan PA (2003), Radon in drinking water in Co. Wicklow – a pilot study. Radiological Protection Institute of Ireland.

Sahoo BK, Nathwani Dipen, Eappen KP, Ramachandran TV, Gaware JJ, Mayya YS (2007). Estimation of radon emanation factor in Indian building materials. *Radiation Measurements,* **42**, 1422-1425.

Sahoo SK, Mohapatra S, Chakrabarty A, Sumesh CG, Jha VN, Tripathi RM, Puranik (2010). Determination of uranium at ultra trace level in packaged drinking water by laser fluorimeter and consequent ingestion dose. *Radioprotection*, **45 (1)**, 55-66.

Samiti JM, Stolwijk J, Rose SL (1991). Summary: International Workshop on Residential Radon Epidemiology, *Health Phys.*, **60**, 223-227.

Santawamaitre T, Malain D, Al-Sulaiti HA, Matthews M, Bradley DA, Regan PH (2010). Study of natural radioactivity in river bank soils along the Chao Phraya river basin in Thailand. *Nucl. Instr. and Meth. A*, doi:10.1016/j.nima.2010.10.057

Sarma HK, Deka PC, Sarkar S, Goswami TD, Sarma BK (2011). Radon activity and radon exhalation rates from some soil samples by using SSNTD. *In Proc. Of The Sevnt. Ntnl. Symp. On Sol. Stat. Nucl. Track Det. And Their Appl.: Abst. and Souv.*, **2(10)**, 5024-5029.

Singh B, Garg VK, Yadav P, Kishore N, Pulhani V (2014). Uranium in groundwater from Western Haryana, India. *J Radioanal Nucl Chem*, **301**, 427-433.

Singh Joga, Singh Harmanjit, Singh Surinder, Bajwa BS (2009). Estimation of uranium and radon concentration in some drinking water samples of Upper Siwaliks, India. *Environ Monit Assess*, **154**, 15-22.

Singh J, Singh H, Singh S, Bajwa BS (2008). Estimation of uranium and radon concentration in some drinking water samples. *Radiat Meas*, **43**, 523-526.

Singh Surinder, Sharma Dinesh Kumar, Dhar Sunil, Kumar Arvind, Kumar Ajay (2007). Uranium, Radium and Radon Measurements in the Environs of Nurpur Area, Himachal Himalayas, India. *Environ Monit Assess,* **128**, 301–309.

Smetanova I, Holy K, Mullerova M, Polaskova A (2010). The effect of meteorological parameters on radon concentration in borehole air and water. *Journal of Radioanalytical and Nuclear Chemistry*, **283**, 101-109.

Srivastava Alok, Lalramengzami R, Laldawngliana C, Sinha C, Ghosh S, Dwivedi KK, Saxena A, Ramachandran TV (1996). Measurement of Potential Alpha Energy Exposure (PAEE) of Radon and its Progenies in Dwellings in the North-Eastern Region of India. *Radiat. Meas.*, **26**, 291-295.

Stranden E, Kolstad A, Lind B (1984). Radon exhalation: Moisture and temperature dependence. *Health Physics*, **47(3)**, 480-484.

Tzortzis M, Tsertos H, Christofides S, Christodoulides G (2003). Gamma ray measurements of naturally occurring radioactive samples from Cyprus characteristic geological rocks. *Radiation Measurements*, **37**, 221-229.

UNSCEAR (2000), Source and effects of ionizing radiation, United Nations Scientific Committee on the Effects of Atomic Radiation, United Nations, New York, 2000.

UNSCEAR (2000) Annex A: Dose assessment methodologies; Annex B: Exposures from natural radiation sources. United Nations Scientific Committee on the Effects of Atomic Radiation, United States.

UNSCEAR (2000) Annex B: Exposures from natural radiation sources. United Nations Scientific Committee on the Effects of Atomic Radiation, United States.

UNSCEAR (United Nations Scientific Committee on the Effects of Atomic Radiation) (1993). Report to the General Assembly, New York.

UNSCEAR (2008). Exposure to the public and workers from various sources of radiation. Report to the General Assembly. New York, United Nations, **1**, Annexure B, 234.

UNSCEAR (1982). United Nations Scientific Committee on the effect of atomic radiations, ionizing radiation: Sources and biological effects, United Nations Press, New York.

USEPA (1991). National Primary Drinking Water Regulations for Radio Nuclides US, Government Printing Office EPA/570/9-91/700.

USEPA (2000a) United States Environmental Protection Agency, National Primary Drinking Water Regulations, Radionuclides Final Rule, 40 CFR Parts 9, 141, and 142, 76708–76712.

Vanchhawng Lalmuanpuia, Rohmingliana PC, Thapa RK, Sahoo BK, Singh OP, Zoliana B, Mayya YS (2009). To Correlate Radon and Thoron Concentrations with Gamma Background Radiation in Mizoram (Special reference to Aizawl, Champhai and Kolasib districts), Proc. VIth Conference of Physics Academy of North East, Tripura University, April 3-4.

Virk HS (2016). Measurement of concentration of natural uranium in ground waters of Bathinda District (S. Punjab) for the assessment of annual effective dose. *Global Journal of Human Social Science (B)*, **16 (5)**, 30-36.

Wentworth Chester K (1922). A scale of grade and class terms for clastic sediments. *The Journal of Geology*, **30 (5)**, 377-392.

WHO (2001). Depleted Uranium, Sources, Exposure and Health Effects. WHO, Geneva.

WHO, World Health Organization (1998). Guidelines for drinking-water quality, addendum to Vol. 1, recommendations. Geneva, Switzerland: WHO.

WHO, World Health Organization (2004). Guidelines for drinking-water quality (3rd ed.). Geneva, Switzerland:WHO.

WHO, World Health Organization (2011). Guidelines for drinking-water quality, (4th ed.) Geneva, Switzerland: WHO.

WHO, World Health Organization (2009). Handbook on Indoor Radon: A Public Health Perspective.Geneva: Switzerland: WHO.

Wrenn ME, Singh NP, Cohen N, Ibrahim SA, Saccomano G (1981). Thorium in Human Tissues. NUREG/CR-1227. Washington, DC: Nuclear Regulatory Commission.

LISTS OF RESEARCH PUBLICATIONS

(I) Journals:

1. **Vanramlawma**, Hmingchungnunga, B. Zoliana, LZ Chhangte, B. K. Sahoo, B. K. Sapra, Z. Pachuau (2020). Estimation of Radon mass exhalation rate and Radium content in soil samples collected from Kolasib District of Mizoram, India. *International Journal for Research in Applied Science & Engineering Technology,* **8 (6)**, 793-798, **ISSN: 2321-9653**.

2. LZ Chhangte, PC Rohmingliana, B.K. Sahoo, B.K. Sapra, Hmingchungnunga, **Vanramlawma**, Remlalsiama, Z. Pachuau, B. Zoliana (2019). Determination of Radon Mass Exhalation Rate in the region of highest lung cancer incidence in India. *Radiation Environment and Medicine*, 8 (2), 113-117. **ISSN: 2423-9097 (PRINT)**.

3. LZ Chhangte, PC Rohmingliana, B.K. Sahoo, B.K. Sapra, **Vanramlawma**, Hmingchungnunga, Remlalsiama, Z Pachuau, B. Zoliana (2018). Comparison of Twin Cup Dosimeter with Single and Double entry in measuring indoor Radon and Thoron Concentration in Mizoram, India. *Science Vision*, **15(1)**, 51-55. **ISSN: 0975-6175** (print)/**2229-6026** (online).

4. Hmingchungnunga, **Vanramlawma**, Z. Pachuau, B. Zoliana, L. Z. Chhangte, B. K. Sahoo, B. K. Sapra (2020). Seasonal variation of radon concentration in water sources using Smart RnDuo. *International Journal for Research in Applied Science & Engineering Technology,* **8 (7)**, 95-100, **ISSN: 2321-9653**.

5. **Vanramlawma**, Hmingchungnunga, Z. Pachuau, B. Zoliana, LZ Chhangte, Remlalsiama, Laldingngheta, B.K. Sahoo, B.K. Sapra. Estimation of ingestion and inhalation dose due to radon in water samples collected from the highest lung cancer incidence area of India. *Science and Technology Journal*, **ISSN: 2321–3388**. **(ACCEPTED FOR PUBLICATION)**

(II) Conference Proceedings:

(a) International:

1. **Vanramlawma**, Hmingchungnunga, Remlalsiama, Laldingngheta, LZ Chhangte, Z. Pachuau, B. Zoliana, Rosangliana, B.K. Sahoo, B.K. Sapra

(2018). Measurement of natural radioactivity using NaI (Tl) detector in soil samples collected from Aizawl, Mizoram, India, In *Perspective and Trends in the Development of Science Education and Research, Mizoram Science Congress 2018*, Atlantis Press, Paris, France, pp 201-211, **ISBN**:**978-94-6252-638-9**. **ISSN 2352-5401**.

2. LZ Chhangte**,** Hmingchungnunga, **Vanramlawma**, P.C. Rohmingliana, B.K. Sahoo, B.K. Sapra, B. Zoliana, Rosangliana, Z. Pachuau (2018). Measurement of promordial radionuclides in soil and building materials from Mizoram, India. In *Perspective and Trends in the Development of Science Education and Research, Mizoram Science Congress 2018*, Atlantis Press, Paris, France, pp 186-189. **ISBN**:**978-94-6252-638-9**. **ISSN 2352-5401**.

3. Hmingchungnunga, **Vanramlawma**, Remlalsiama, Laldingngheta, LZ Chhangte, Z Pachuau, B. Zoliana, Rosangliana, B.K. Sahoo, B.K Sapra (2018). Assessment of radon content in water using SMART RnDuo in Mizoram, Northeast India. In *Perspective and Trends in the Development of Science Education and Research, Mizoram Science Congress 2018*, Atlantis Press, Paris, France, pp 190-193. **ISBN:978-94-6252-638-9. ISSN 2352-5401.**

4. Laldingngheta, **Vanramlawma**, Hmingchungnunga, LZ Chhangte, R.C Tiwari, Rosangliana, B. Zoliana, B.K. Sahoo, T.K. Agarwal (2018). Measurement of radon exhalation from soil samples in various fault regions of Aizawl district, Mizoram, India. In *Perspective and Trends in the Development of Science Education and Research, Mizoram Science Congress 2018*, Atlantis Press, Paris, France, pp 198-201. **ISBN**:**978-94-6252-638-9**. **ISSN 2352-5401**.

(III) Conferences/Workshop Attended

(a) National:

1. **Vanramlawma,** Hmingchungnunga, Z. Pachuau, B. Zoliana, Remlalsiama, LZ Chhangte, B.K. Sahoo, B.K. Sapra (2017). Measurement of Natural Radioactivity using NaI (Tl) detector in soil samples from Aizawl, Mizoram. National Conference on *Solid State Nuclear Track Detectors and Their Applications* (SSNTDs-20), during October 26-28, 2017. Vidya Vikas Institute of Engineering and Technology, Mysuru. (**Poster Presentation**)

2. **Vanramlawma**, Hmingchungnunga, Remlalsiama, Laldingngheta, LZ Chhangte, Z. Pachuau, B. Zoliana, Rosangliana, B.K. Sahoo, B.K. Sapra (2018). Measurement of natural radioactivity using NaI (Tl) detector in soil samples collected from Aizawl, Mizoram, India. *Mizoram Science Congress 2018*, during October 4-5, 2018, Pachhunga University College, Aizawl. (**Oral Presentation**)

3. **Vanramlawma,** Hmingchungnunga, Remlalsiama, Laldingngheta, LZ Chhangte, Z. Pachuau, B. Zoliana, B.K. Sahoo, B.K. Sapra (2019). Estimation of ingestion and inhalation dose due to radon in water samples collected fom the highest lung cancer incidence area of India. *National Conference on Emerging Trends in Environmental Research*, during October 31- November 2, 2019, Pachhunga University College, Aizawl. (**Oral Presentation**)

(b) International:

1. **Vanramlawma,** Hmingchungnunga, Remlalsiama, Laldingngheta, LZ Chhangte, Z. Pachuau, B. Zoliana, B.K. Sahoo, B.K. Sapra, L. Hnamte (2018). Study of uranium and radon contents in water samples collected from Kolasib District of Mizoram, India. *The 12th Annual Convention of ABAP & International Conference on Biodiversity, Environment and human Health: Innovations and Emerging Trends* (*BEHIET-2018*), during November 12-14, 2018. Mizoram University, Mizoram. (**Poster Presentation**)

2. **Vanramlawma,** Hmingchungnunga, Remlalsiama, Laldingngheta, LZ Chhangte, Z. Pachuau, B. Zoliana, B.K. Sahoo, B.K. Sapra, (2019). Seasonal variation of radon concentration in water samples collected from Aizawl District of Mizoram, India. *International Conference on Chemistry and Environmental Sustainability (ICCES-2019)*, during February20-22, 2019. Mizoram University, Mizoram. (**Poster Presentation**)

BRIEF BIODATA OF VANRAMLAWMA

Name	:	Vanramlawma
Father's Name	:	C. Lalmawipuia
Date of Birth	:	11 - 04 - 1991
Address	:	House No. YB/08, Dawrkawn, Chaltlang, Aizawl, Mizoram, Pin- 796012.
Subject of Specialization	:	Advanced Electronics
Educational Qualification	:	

H.S.L.C	:	2006	Distinction	M.B.S.E.
H.S.S.L.C.	:	2008	Second Division	M.B.S.E.
B.Sc. (Physics)	:	2012	Second Division	M.Z.U.
M.Sc. (Physics)	:	2014	Distinction	M.Z.U.
Pre-Ph.D Course	:	2017	First Division	M.Z.U.

Working Experience:

- Completed M.Sc. Project work entitled "Study and analysis of signal distribution of AIR FM transmitter in Chaltlang Area of Aizawl City" at Department of Physics, Mizoram University, Mizoram (796004), 2014.
- Completed training course entitled "Science Academies' Refresher Course in Experimental Physics" at National Institute of Technology, Aizawl, Mizoram , during May 7-22, 2015.
- Completed training course on workshop entitled, "Measurement techniques for radon, thoron and their decay products", at Radiological Physics and Advisory Division, Bhabha Atomic Research Centre, Mumbai, during December 13-16, 2016.

- Completed research works on DAE-BRNS Sponsored Project entitled, "A comprehensive study of natural radio- nuclides like ^{238}U, ^{226}Ra, ^{222}Rn in various matrices available in Mizoram", from October 2016 - October 2018 under the supervision Prof. B Zoliana, Department of Physics, Govt. Zirtiri Residential Science College, Aizawl, Mizoram in collaboration with Radiological Physics and Advisory Division, Bhabha Atomic Research Centre, Mumbai, India.
- Started research work on "Concentrations of Natural Radionuclides in water sources and its surrounding soil in Aizawl and Kolasib districts of Mizoram" since April 2018 under the supervision of Prof. Zaithanzauva Pachuau, Department of Physics, Mizoram University, Aizawl, Mizoram and Joint Supervision of Prof. B Zoliana, Department of Physics, Govt. Zirtiri Residential Science College, Aizawl, Mizoram, in collaboration with Radiological Physics and Advisory Division, Bhabha Atomic Research Centre, Mumbai, India.

PARTICULARS OF THE CANDIDATE

NAME OF THE CANDIDATE	:	VANRAMLAWMA
DEGREE	:	DOCTOR OF PHILOSOPHY
DEPARTMENT	:	PHYSICS
TITLE OF THESIS	:	CONCENTRATIONS OF NATURAL RADIONUCLIDES IN WATER SOURCES AND ITS SURROUNDING SOIL IN AIZAWL AND KOLASIB DISTRICTS OF MIZORAM
DATE OF ADMISSION	:	11.08.2017

APPROVAL OF RESEARCH PROPOSAL

1.	BOS	:	11. 04.2018
2.	SCHOOL BOARD	:	24.04.2018
3.	MZU REGISTRATION No.	:	199 of 2008 to 2009
4.	Ph.D REGISTRATION No.	:	MZU/Ph.D./1102 of 24.05.2018
5.	EXTENSION (IF ANY)	:	NIL

(Prof. R.C. TIWARI)

Head,

Department of Physics